Indian Point Unit 2

Spent Fuel Pool

Increased Storage Capacity

Licensing Report

Consolidated Edison Company of New York, Inc.

Indian Point Unit 2
Docket No. 50-247

June 1989

TABLE OF CONTENTS

i

TABLE OF CONTENTS (continued)

TABLE OF CONTENTS (continued)

TABLE OF CONTENTS (continued)

LIST OF TABLES

LIST OF TABLES (continued)

LIST OF FIGURES

LIST OF FIGURES (continued)

1.0   INTRODUCTION AND NO SIGNIFICANT HAZARD CONSIDERATIONS

1.1   INTRODUCTION

Indian Point Unit No. 2 (IP2) is a pressurized water nuclear power reactor owned and operated by the Consolidated Edison Company of New York. IP2 received its Construction Permit from the AEC in October, 1966, and its Operating License in September 1973. The plant went into commercial operation in July, 1974. Table 1.1 provides the data on previous and projected fuel assembly discharge data in the IP2 spent fuel pool which currently contains 980 storage locations. Table 1.2, constructed from Table 1.1 data, indicates that IP2 will lose full core discharge (193 assemblies) capability after the discharge of the 12th batch into the pool during the outage anticipated to occur in 1995. This projected loss of full core discharge capability prompted the undertaking of steps to increase spent fuel storage capability in the spent fuel pool.

The existing spent fuel storage racks are free-standing and self supporting and are constructed of ASTM 240-Type 304 stainless steel. The poison material is borated stainless steel. These racks have 980 storage locations and are capable of storing fuel of up to 4.3 wt% U-235 initial enrichment.

The new spent fuel storage racks are also free-standing and self supporting. The principal construction materials for the new racks are ASTM 240-Type 304 stainless steel sheet and plate stock, and A564 (precipitation hardened stainless steel) for the adjustable support spindles. The only non-stainless material utilized in the rack is the neutron absorber material which is boron carbide impregnated silicone based polymer available under the patented product name "Boraflex".

The new racks are designed and analyzed in accordance with Section III, Division 1, Subsection NF of the ASME Boiler and Pressure Vessel Code. The material procurement and fabrication of the rack modules conforms to 10CFR 50 Appendix B requirements.

The proposed reracking effort will increase the number of storage locations to 1376, which, as indicated in Table 1.2, will extend the date of loss of full core discharge capability to the year 2007.

This Licensing Report documents the design and analyses performed to demonstrate that the new spent fuel racks satisfy all governing requirements of the applicable codes and standards, in particular, "OT Position for Review and Acceptance of Spent Fuel Storage and Handling Applications", USNRC (1978) and 1979 Addendum thereto.

The safety assessment of the proposed rack modules involved demonstration of its hydrothermal, criticality and structural adequacy. Hydrothermal adequacy requires that fuel cladding will not fail due to excessive thermal stress, and that the steady state pool bulk temperature will remain within the limits prescribed for the spent fuel pool. Demonstration of structural adequacy primarily involves analysis showing that the free-standing modules will not impact under the postulated SSE and OBE events, and that the primary stresses in the module structure will remain below the ASME Code allowables. The structural qualification also includes analytical demonstration that the subcriticality of the stored fuel will be maintained under accident scenarios such as fuel assembly drop, accidental misplacement of fuel outside a rack, etc.

The criticality safety analysis shows that the neutron multiplication factor for the stored fuel array is bounded by the USNRC limit of 0.95 under assumptions of 95% probability and 95% confidence. Consequences of the inadvertent placement of a fuel assembly are also evaluated as part of the criticality analysis. The criticality analysis also sets the requirements on the length of the B-10 screen and the areal B-10 density.

This Licensing Report contains documentation of the analyses performed to demonstrate the large margins of safety with respect to all USNRC specified criteria. This report also contains the results of the analysis performed to demonstrate the integrity of the fuel pool reinforced concrete structure, and an appraisal of radiological considerations.

The analyses presented herein clearly demonstrate that the rack module arrays possess wide margins of safety from all three — thermal-hydraulic, criticality, and structural — vantage points. The No Significant Hazard Consideration evaluation presented below is based on the descriptions and analyses synopsized in the subsequent sections of this report.

1.2   NO SIGNIFICANT HAZARDS CONSIDERATION

Consolidated Edison Company (Con Edison) has determined that the proposed amendment involves No Significant Hazards Consideration, focusing on the three criteria set forth in 10CFR 50.92(c) as quoted below:

The Commission may make a final determination, pursuant to the procedures in 50.91, that a proposed amendment to an operating license under 50.21(b) or 50.22 or for a testing facility involves no significant hazards considerations, if operation of the facility in accordance with the proposed amendment would not:

1. Involve a significant increase in the probability or consequences of an accident previously evaluated; or

2. Create the possibility of a new or different kind of accident from any accident previously evaluated; or

3. Involve a significant reduction in a margin of safety.

Con Edison has determined that the activities associated with this amendment request do not meet any of the Significant Hazards Consideration Criteria of 10CFR 50.92(c) and, accordingly, a No Significant Hazards Consideration finding is justified. In support of this determination, the following safety review is provided, followed by a discussion of each of the above three relevant criteria.

Safety Review

IP2 has a single spent fuel pool (SFP) which at the present time contains free-standing spent fuel storage racks with 980 total storage cells. The present racks provide adequate capacity for storage of spent fuel while maintaining reserve full core discharge capacity through Cycle 11. However, beginning with startup of Cycle 12 (anticipated to be in 1995), IP2 would lose full core reserve storage capability with existing racks. Therefore, to preclude this situation and to ensure that sufficient spent fuel storage capacity continues to exist at IP2,

Con Edison has contracted for high-density spent fuel storage racks whose design incorporates Boraflex as a neutron absorber in the cell walls thereby allowing for more dense storage of spent fuel. These racks have an ultimate storage capacity of 1376 fuel assemblies (including two locations for defective fuel containers), which is expected to extend the full core reserve storage capability until the year 2007.

The new free-standing high density spent fuel storage racks will store fuel in two discrete regions of the SFP. Region I includes three modules having a total of 269 storage cells. Each cell is designed for storage of unburned fuel assemblies with Uranium-235 initial enrichments up to 5.0 wt% while maintaining the required subcriticality ($k_{eff} \leq 0.95$). Region II includes nine modules having a total of 1105 storage cells, which are available for storage of spent fuel assemblies. This region is designed to store fuel which has experienced sufficient burnup such that storage in Region I is not required.

The high density spent fuel storage rack cells are fabricated from 0.075" thick type 304 stainless steel sheet material. In Region I, strips of Boraflex neutron absorber material are between the cell walls and a stainless steel coverplate, and the cells are separated by a specified water gap. In Region II, the Boraflex strips are between the checkerboard boxes and the sheathing without a water gap. The cells are welded together in a specified manner to become a free-standing structure which is seismically qualified without depending on neighboring modules or fuel pool walls for support. The nominal center-to-

center spacings of the cells within Region I are 10.545" and 10.765", respectively, in north-south and east-west directions. The nominal pitch in Region II is 9.04".

Since there is spent fuel presently in the IP2 SFP, special administrative controls and/or procedures will be developed to minimize radiation exposure during the installation of the new spent fuel racks. The evaluation of postulated accidents with respect to nuclear criticality and/or radioactivity release has shown acceptable results, in that k_{eff} does not exceed 0.95, including uncertainties, and postulated releases do not exceed 10 CFR 100 acceptance criteria.

Evaluation

The following evaluation demonstrates that the proposed amendment does not exceed any of the three significant hazards considerations criteria. The analysis of this proposed modification has been accomplished using currently accepted codes and standards. The three criteria are discussed below:

(1) Does the proposed amendment involve a significant increase in the probability or consequences of an accident previously evaluated:

In the course of the analysis, Con Edison has considered the following potential accident scenarios:

1. A spent fuel assembly drop in the spent fuel pool.

2. Loss of spent fuel pool cooling system flow.

3. A seismic event.

4. A spent fuel cask drop.

5. A construction accident.

The probability of any of the first four accidents is not affected by the racks themselves; thus the proposed modification cannot increase the probability of these accidents. The IP2 Technical Specifications prohibit movement of a spent fuel cask over the spent fuel pool at any time. Therefore, the drop of a spent fuel cask in the spent fuel pool is not possible. With regard to the construction accident, the IP2 Technical Specifications allow movement of a rack and its associated handling tool over the spent fuel pool but prohibit movement of a rack over fuel. All work in the spent fuel pool area will be controlled and performed in strict accordance with specific written procedures. Administrative controls will preclude the movement of a rack directly over any fuel. The maximum weight of a rack and its associated handling tool, as evaluated for purposes of applying Technical Specification 3.8.C.1, is 20 tons. The maximum weight of a rack and its associated handling tool to be carried over the spent fuel pool in connection with this proposed modification will be 19.4 tons. Therefore the probability of a construction accident previously evaluated is not significantly increased as a result of the proposed reracking.

In addition, Sections 5.1.1, 5.1.2 and 5.1.6 of NUREG-0612, entitled "Control of Heavy Loads at Nuclear Power Plants", provide guidance for heavy load handling operations pursuant to a spent fuel storage rack replacement. Section 5.1.2 provides four alternatives for assuring the safe handling of heavy loads during a fuel storage rack replacement. Alternative (1) of Section 5.1.2 provides that the control of heavy loads guidelines can be satisfied by establishing that the potential for a heavy load drop is extremely small, as demonstrated by satisfaction of the single-failure-proof crane guidelines. The provisions of alternative (1) will be met during implementation of the subject application.

NUREG-0554, entitled "Single-Failure-Proof Cranes for Nuclear Power Plants", provides guidance for the design, fabrication, installation and testing of new cranes that are of a high reliability design. For operating plants, NUREG-0612, Appendix C, entitled "Modification of Existing Cranes," provides guidelines on the implementation of NUREG-0554 at operating plants. An evaluation of storage rack movements

which will be accomplished by the IP2 Fuel Storage Building
crane to determine conformance with the NUREG-0612, Appendix
C guidelines demonstrated that alternative (1) above is
satisfied, i.e., the probability of a drop of a storage rack
is extremely small. The Fuel Storage Building crane has a
rated capacity of 40 tons, which incorporates a design safety
factor of five. The maximum weight of any existing or
replacement storage rack and its associated handling tool is
19.4 tons. Therefore, there is ample safety factor margin
for movements of the storage racks by the Fuel Storage
Building crane. This applies to non-redundant load-bearing
components. Redundant special lifting devices, which have a
rated capacity sufficient to maintain sufficient safety
factors, will be utilized in the movements of the storage
racks. As per NUREG-0612, Appendix B, the substantial safety
factor margin ensures that the probability of a load drop is
extremely low.

Accordingly, the proposed modification does not involve a
significant increase in the probability of an accident
previously evaluated.

Con Edison evaluated the consequences of a spent fuel
assembly drop in the spent fuel pool and found that the
criticality acceptance criterion, $k_{eff} \leq 0.95$, is not
violated. In addition, Con Edison found that there was no
significant change in the radiological consequences of a fuel
assembly drop from the previous analyses. Con Edison analyses
found that the calculated doses are well within 10 CFR Part
100 guidelines. The results of an analysis show that a
dropped spent fuel assembly on the racks will not distort the
racks such that they would not perform their safety function.
Thus, the consequences of this type of accident are not
significantly changed from the previously evaluated spent
fuel assembly drops which have been found acceptable by the
NRC.

The consequences of a loss of spent fuel pool cooling system
flow have been evaluated and it was found that sufficient
time is still available to provide an alternate means for
cooling in the event of a failure in the cooling system.
Thus, the consequences of this type accident are not
significantly increased from previously evaluated loss of
cooling system flow accidents.

The consequences of a seismic event, have been evaluated. The new racks will be designed and fabricated to meet the requirements of applicable portions of the NRC Regulatory Guides and published standards. The new free-standing racks are designed, as are the existing free-standing racks, so that the integrity of the racks is maintained during and after a seismic event. Thus, the consequences of a seismic event are not significantly increased from previously evaluated events.

The probability and consequences of a spent fuel cask drop will not be affected by the replacement of the racks. The IP2 Technical Specification prohibits spent fuel cask movements over any region of the spent fuel pool which contains irradiated fuel. This prohibition will remain effective during and after the storage rack replacement.

The consequences of a construction accident have been considered. A heavy load will not be carried in the spent fuel pool area until all fuel in the pool has decayed for a minimum of six months. This provides sufficient time for decay of gaseous radionuclides in the fuel (gap activity) such that an assumed accidental release of gases from damage to all stored fuel assemblies would result in a potential offsite dose less than 10% of 10 CFR 100 limits. In addition, there is no equipment which is essential to the safe shutdown of the reactor or employed to mitigate the consequences of an accident which is beneath, adjacent to or otherwise within the area of influence of any loads that will be handled during the expansion modification. Therefore, the consequences of a construction accident are not significantly increased from previously evaluated events.

Therefore, it is concluded that the proposed amendment to replace the spent fuel racks in the spent fuel pool does not involve a significant increase in the probability or consequences of an accident previously evaluated.

(2) <u>Does the proposed amendment create the possibility of a new</u>
<u>or different kind of accident from any accident previously</u>
<u>evaluated</u>:

Con Edison has evaluated the proposed modification in
accordance with the guidance of the NRC Position Paper
entitled, "OT Position for Review and Acceptance of Spent
Fuel Storage and Handling Applications," appropriate NRC
Regulatory Guides, appropriate NRC Standard Review Plans, and
appropriate industry codes and standards. In addition, Con
Edison has reviewed several previous NRC Safety Evaluation
Reports for rerack applications similar to our proposal.

No unproven technology will be utilized either in the
construction process or in the analytical techniques
necessary to justify the planned fuel storage expansion. In
fact, the basic reracking technology in this instance has
been developed and demonstrated in over 80 applications for
fuel pool capacity increases which have already received NRC
Staff approval.

The change to a two-region spent fuel pool requires the
performance of additional evaluations to ensure that the
criticality criterion is maintained. These include the
evaluation of the limiting criticality condition, i.e.,
misplacement of an unirradiated fuel assembly of 5.0%
enrichment into a Region II storage cell or outside and
adjacent to a Region II rack module. The evaluation for this
case shows that when the boron concentration meets the
proposed Technical Specifications requirement, the
criticality criterion is satisfied. Although this change
does pose the need to address additional aspects of a
previously analyzed accident, it does not create the
possibility of a previously unanalyzed accident.

Based upon the foregoing, Con Edison concludes that the
proposed reracking does not create the possibility of a new
or different of accident from any accident previously
evaluated.

(3) Does the proposed amendment involve a significant reduction in a margin of safety:

The NRC Staff Safety Evaluation Review process has established that the issue of margin of safety, when applied to a reracking modification, should address the following areas:

1.   Nuclear criticality considerations

2.   Thermal-hydraulic considerations

3.   Mechanical, material and structural considerations.

The established acceptance criterion for criticality is that the neutron multiplication factor in spent fuel pools shall be less than or equal to 0.95, including all uncertainties, under all conditions. This margin of safety has been adhered to in the criticality analysis methods for the new rack design.

The methods used in the criticality analysis conformed to the applicable portions of the appropriate NRC guidance and industry codes, standards, and specifications. In meeting the acceptance criteria for criticality in the spent fuel pool, such that k_{eff} is always less than 0.95, including uncertainties at a 95%/95% probability confidence level, the proposed amendment does not involve a significant reduction in the margin of safety for nuclear criticality.

Conservative methods were used to calculate the maximum fuel temperature and the increase in temperature of the water in the spent fuel pool. The thermal-hydraulic evaluation used the methods previously employed for evaluations of the present spent fuel racks to demonstrate that the temperature margins of safety are maintained. The proposed modification will increase the heat load in the spent fuel pool. The evaluation shows that the existing spent fuel cooling system will maintain the bulk pool water temperature at or below 180^0F. Thus a margin of safety exists such that the maximum allowable temperature for bulk boiling is not exceeded for the calculated increase in pool heat load. The evaluation also shows that maximum local water temperatures along the hottest fuel assembly are below the nucleate boiling

condition value. Thus, there is no significant reduction in the margin of safety for thermal-hydraulic or spent fuel cooling concerns.

The main safety function of the spent fuel pool and the racks is to maintain the spent fuel assemblies in a safe configuration through all normal or abnormal loadings. Abnormal loadings which have been considered are the effect of an earthquake, the impact due to a spent fuel cask drop, the drop of a spent fuel assembly, or the drop of any other heavy object. The mechanical, material, and structural design of the new spent fuel racks is in accordance with applicable portions of: "NRC Position for Review and Acceptance of Spent Fuel Storage and Handling Applications", dated April 14, 1978, as modified January 18, 1979; Standard Review Plan 3.8.4; and other applicable NRC guidance and industry codes. The rack materials used are compatible with the spent fuel pool and the spent fuel assemblies. The structural considerations of the new racks address margins of safety against tilting and deflection or movement, such that the racks do not impact each other during the postulated seismic events. In addition the spent fuel assemblies remain intact and no criticality concerns exist. Thus the margins of safety are not significantly reduced by the proposed rerack.

In summation, it has been shown that the proposed spent fuel storage facility modifications do not:

1. Involve a significant increase in the probability or consequences of an accident previously evaluated; or

2. Create the possibility of a new or different kind of accident from any accident previously evaluated; or

3. Involve a significant reduction in a margin of safety.

Thus, Con Edison has determined that the proposed amendments as described do not involve significant hazard considerations, and that the criteria of 10 CFR 50.92 have accordingly been met. Additionally, the proposed amendment most closely resembles example (X) of "Amendments That Are Considered Not Likely to

Involve Significant Hazards Considerations" as provided in the final NRC adoption of 10 CFR 50.92, 51 FR 7751 (March 6, 1986). This example indicates that an amendment is not likely to involve a significant hazards consideration as follows:

(X) An expansion of the storage capacity of a spent fuel pool when all of the following are satisfied:

1) The storage expansion method consists of either replacing existing racks with a design which allows closer spacing between stored spent fuel assemblies or placing additional racks of the original design on the pool floor if space permits.

The IP2 spent fuel pool rerack involves the replacement of the present low capacity racks with a design which, by incorporating a neutron absorber and requiring only burned fuel be stored in Region II, allows closer spacing of the stored spent fuel cells. Region I is designed for allowing safe storage of unburned fuel.

2) The storage expansion method does not involve rod consolidation or double tiering.

The IP2 racks are not double tiered and all racks will sit on the spent fuel pool floor. Additionally, the amendment application does not involve consolidation of spent fuel.

3) The k_{eff} of the pool is maintained less than or equal to 0.95.

The design of the spent fuel racks contains a neutron absorber, Boraflex, to allow closer storage of spent fuel assemblies while ensuring that the k_{eff} remains less than 0.95 under all conditions (with unborated water in the pool). Additionally, the water in the spent fuel pool contains at least 1500 ppm of boron, providing further assurance that k_{eff} remains less than 0.95.

4) No new technology or unproven technology is utilized in either the construction process or the analytical techniques necessary to justify the expansion.

The rack design has been licensed at least ten times. The construction processes and analytical techniques remain substantially the same as these other ten storage rack projects. Thus no new or unproven technology is utilized in the construction or analysis of the proposed IP2 spent fuel racks.

Thus, this submittal meets example (X) as presented in the supplementary information accompanying publication of the Final Rule as an example of situations which are considered not to involve significant hazards considerations.

Based on the foregoing, Con Edison has concluded that all criteria for issuance of a no-significant hazard statement are satisfied.

Table 1.1

FUEL ASSEMBLY DISCHARGE DATA

Batch	No. of Assemblies Discharged	Equivalent Operating Time (yrs)	Discharge[1] Date	Shutdown Time (yrs)	No. of Assemblies in Pool After Outage
1	72	1.50	03/30/76	30.78	72
2	60	2.50	02/13/78	28.90	132
3	61	3.50	06/16/79	27.57	
	2	2.00			195
4	49	3.00	10/17/80	26.23	
	4	2.00			
	1	1.00			249
5	16	4.20	09/18/82	24.31	
	43	3.20			
	16	2.20			324
6	10	4.40	06/02/84	22.60	
	40	3.40			
	8	3.20			
	7	2.40			
	7	2.20			396
7	61	3.60	01/13/86	20.98	
	3	2.30			
	4	2.00			464
8	57	3.50	09/01/87	19.35	
	11	2.30			532
9	57	3.31	03/18/89	17.80	
	15	2.22			604
10	72	4.00	01/01/91	16.01	676
11	72	4.75	01/01/93	14.01	748
12	72	4.75	01/01/95	12.01	820
13	72	4.75	01/01/97	10.01	892
14	72	4.75	01/01/99	8.01	964
15	72	4.75	01/01/2001	6.00	1036
16	72	4.75	01/01/2003	4.00	1108
17	72	4.75	01/01/2005	2.00	1180
18A	72	1.60	01/01/2007	174 hr	1252
18B	72	3.20		174 hr	1324
18C	49	4.75		174 hr	1373

(1) All dates from 1991 on are estimated dates.

TABLE 1.2

SPENT FUEL POOL STORAGE DATA

Discharge Batch No.	Year	Batch Size	Assemblies in the Pool After the Outage	No. of Available Locations	
				Current	After Proposed Reracking
1	1976	72	72	908	1302
2	1978	60	132	848	1242
3	1979	63	195	785	1179
4	1980	54	249	731	1125
5	1982	75	324	656	1050
6	1984	72	396	584	978
7	1986	68	464	516	910
8	1987	68	532	448	842
9	1989	72	604	376	770
10	1991	72	676	304	698
11	1993	72	748	232	626
12	1995	72	820	160*	554
13	1997	72	892	88**	482
14	1999	72	964	16	410
15	2001	72	1036		338
16	2003	72	1108		266
17	2005	72	1180		194
18A	2007	72	1252		122*
18B	2007	72	1324		50**
18C	2007	49	1373		1

Legend: *: Loss of full core discharge capacity
          **: Loss of normal batch discharge capacity

2.0 MODULE DATA

2.1 SYNOPSIS OF NEW MODULES

This section presents the proposed module layout in the IP2 spent fuel pool. It also contains a technical description of the neutron absorber material proposed for this project. The proposed increase in spent fuel pool storage capability entails removing, from the pool, the existing 12 modules containing 980 storage locations, and replacing them with 12 new high density rack modules containing 1374 storage locations. In addition, two special locations are provided to store failed fuel canisters. Figure 2.1 shows the module layout. The cell data for each module type may be found in Tables 2.1 and 2.2. Additional details are provided below.

2.1.1 Multi-Region Storage

The high density spent fuel storage racks will provide storage locations for up to 1376 fuel assemblies and will be designed to maintain the stored fuel, having an initial enrichment of up to 5.0 wt% U-235, in a safe, coolable, and subcritical configuration during normal and abnormal conditions.

All rack modules for IP2 fuel pool are of the "free-standing" type such that the modules are not attached to the pool floor nor do they require any lateral braces or restraints. These rack modules will be placed in the pool in their designated locations, and the support legs remotely leveled (using a telescopic removable handling tool) by an operator on the fuel handling bridge. No additional lifting equipment is needed to carry the weight of a rack while leveling is being performed.

The racks will be arranged in two regions in the spent fuel pool. Region I will have 269 locations capable of storing unirradiated fuel of up to 5.0 wt% U-235 initial enrichment. Region I has enough locations to store a full core discharge and one-third core of unirradiated fuel. Region II will have 1105 locations for storage of fuel which meets enrichment and burnup criteria developed as part of the rack design. Section 4 of this report addresses this in more detail. In addition, there are two locations for storage of failed fuel canisters. The total number of storage locations, as detailed above, is 1376.

Table 2.3 gives the essential storage cell data for all racks. As noted, the storage cells are 8.75" (internal dimension) for Region I and 8.80" for Region II which accommodates the standard Westinghouse fuel assembly or equivalent fuel.

The module's four support legs are remotely adjustable. Thus, the racks can be made vertical and the top of the racks can easily be made co-planar with each other. The rack module support legs are engineered to accommodate variations of the pool floor. The placement of the racks in the spent fuel pool has been designed to preclude any support legs from being located on the leak chase or liner welds. Support pads have been provided to bridge any obstructions which could potentially interfere with placement of a rack support leg.

2.1.2   Poison Material

Boraflex has been selected as the neutron absorber material for the new high density spent fuel storage racks.

Boraflex (dimethyl-polysiloxane polymer with powdered B_4C dispersion) has been used as the poison material in numerous plants in recent years. The B-10 loading for Region I is 0.028 gm/sq.cm. (min); the corresponding poison thickness is 0.095". In Region II, the B-10 loading is .022 gm/sq.cm and the corresponding Boraflex thickness is 0.075". Prior experience with Boraflex in spent fuel pool is quite extensive both in the U.S. and overseas. The U.S. experience list is presented in Table 2.4.

Published Boraflex test reports indicate the material was subjected in a reactor to an equivalent gamma dose of 2×10^{12} rads (including effects of neutron dose). This indicates a substantial margin of safety against material degradation. Numerous test programs dating to 1979 have confirmed the adequacy of Boraflex as a stable "poison" material in long term spent fuel pool environments.

2.2 EXISTING RACK MODULES AND PROPOSED RERACKING OPERATION

The Indian Point Unit No. 2 fuel pool currently has twelve free standing rack modules containing a total of 980 storage cells. At the time of the proposed reracking operation, 604 of these locations will be occupied with spent fuel. There is sufficient number of open (unoccupied) cells in the pool to permit relocation of all fuel to the east end of the pool to vacate the modules in the south-west end.

A remotely engagable lift rig, meeting NUREG-0612 stress criteria, will be used to lift the empty modules. The fuel storage

building crane will be used for this purpose. A module change-out scheme has been developed which ensures that all modules being handled are empty, and at least four to six feet laterally from a loaded module, when the module is more than six inches above the pool floor.

The fuel storage building crane is a gantry unit which rides on rails that traverse the entire Fuel Storage Building. This crane has a 40 ton main hoist, and an auxiliary 5 ton hoist. See Section 7.1.3 for further discussion of the crane.

Pursuant to the defense-in-depth approach of NUREG-0612, the following additional measures of safety will be undertaken for the reracking operation.

(i)   The crane and hoist will be given a preventive maintenance checkup and inspection within 3 months of the beginning of the reracking operation.

(ii)   The crane will be used to lift no more than 50% of its rated capacity of 40 tons at any time during the reracking operation. (The maximum weight of any existing module and its associated handling tool is 19.4 tons, and that of any "new" module and its associated handling tool is 13 tons).

(iii)   The old fuel racks will be lifted no more than 6 inches above the pool floor and held in that elevation for approximately 10 minutes before beginning the vertical lift.

(iv)   The rate of vertical lift will not exceed 4 feet per minute.

(v)   The rate of horizontal movement will not exceed 5 feet per minute.

(vi)   Safe load paths have been developed. The "old" or "new" racks will not be carried over any region of the pool containing fuel.

(vii)   The rack upending or laying down will be carried out in an area which is not proximate to any safety related component.

The fuel racks will be brought directly into the Fuel Storage Building through the access door, which is at ground level, without any maneuvering. This direct access to the building greatly facilitates the rack removal and installation effort.

The "old" racks will be "hydrolased" while in the pool, and approved for shipping per the requirements of 10 CFR71 and 49 CFR 171-178 before being brought to the Fuel Storage Building door. They will be housed in special shipping containers, and transported to a processing facility for volume reduction. Non-decontaminatable portions of the racks will be shipped to a licensed radioactive waste burial site.

All phases of the reracking activity will be conducted in accordance with written procedures which will be reviewed and approved by Con Edison.

Table 2.1

MODULE DATA

MODULE I.D.	NO. OF MODULE	REGION I.D.	NO. OF CELLS NORTH-SOUTH DIRECTION	EAST-WEST DIRECTION	PER MODULE	TOTAL CELL COUNT
A	1	I	10	8	80	80
B	1	I	12	9	108	108
C	1	I	9	9	81	81
D	1	II	13	11	143	143
E1-E3	3	II	11	11	121	363
F1-F2	2	II	12	10	120	240
G1-G2	2	II	12	11	132	264
H	1	II	11	10	95	95[*]
Total						1374

---

[*]   Plus 2 failed fuel containers

Table 2.2

MODULE DIMENSIONS AND WEIGHT DATA
(IP2 POOL)

NOMINAL DIMENSION

Module I.D.	North-South Direction	East-West Direction	Nominal Dry Weight (lb)
A	104"	84-1/2"	18,300
B	125"	95-1/4"	24,500
C	93-3/8"	95-1/4"	18,500
D	118"	100"	20,000
E1	100"	100"	17,000
E2	100"	100"	17,000
E3	100"	100"	17,000
F1	109"	91"	16,900
F2	109"	91"	16,900
G1	109"	100"	18,600
G2	109"	100"	18,600
H	100"	91"	13,800

Table 2.3

COMMON MODULE DATA

Storage cell inside dimension:	8.75" — Region I 8.80" — Region II
Storage cell height (above the baseplate):	166"
Baseplate thickness:	0.5"
Support leg height:	6" (nominal)
Support leg type:	Remotely adjustable legs
Number of support legs:	4 (minimum)
Remote lifting and handling provision:	Yes
Poison material:	Boraflex
Poison length:	Active fuel less axial leakage length plus five inches for axial shrinkage (144" in Region I and 150" in Region II)
Poison width:	7.5"

TABLE 2.4

BORAFLEX EXPERIENCE FOR HIGH DENSITY RACKS

SITE	PLANT TYPE	NRC DOCKET NO.
Point Beach 1 & 2	PWR	50-226 & 301
Nine Mile Point 1	BWR	50-220
Oconee 1 & 2	PWR	50-269 & 270
Prairie Island	PWR	50-282 & 306
Calvert Cliffs 2	PWR	50-318
Quad Cities 1 & 2	BWR	50-254 & 265
Watts Barr 1 & 2	PWR	50-390 & 391
Waterford 3	PWR	50-382
Fermi 2	BWR	50-341
H.B. Robinson 2	BWR	50-261
River Bend 1	BWR	50-458
Rancho Seco 1	PWR	50-312
Nine Mile Point	BWR	50-410
Shearon Harris 1	PWR	50-400
Millstone 3	PWR	50-423
Grand Gulf 1	BWR	50-416
Oyster Creek	BWR	50-219
V.C. Summer	PWR	50-359
Diablo Canyon 1 & 2	PWR	50-275 & 323
Byron Units 1 & 2	PWR	50-454 & 455
Turkey Point 3 & 4	PWR	50-250 & 251
St. Lucie Unit 1	PWR	50-335
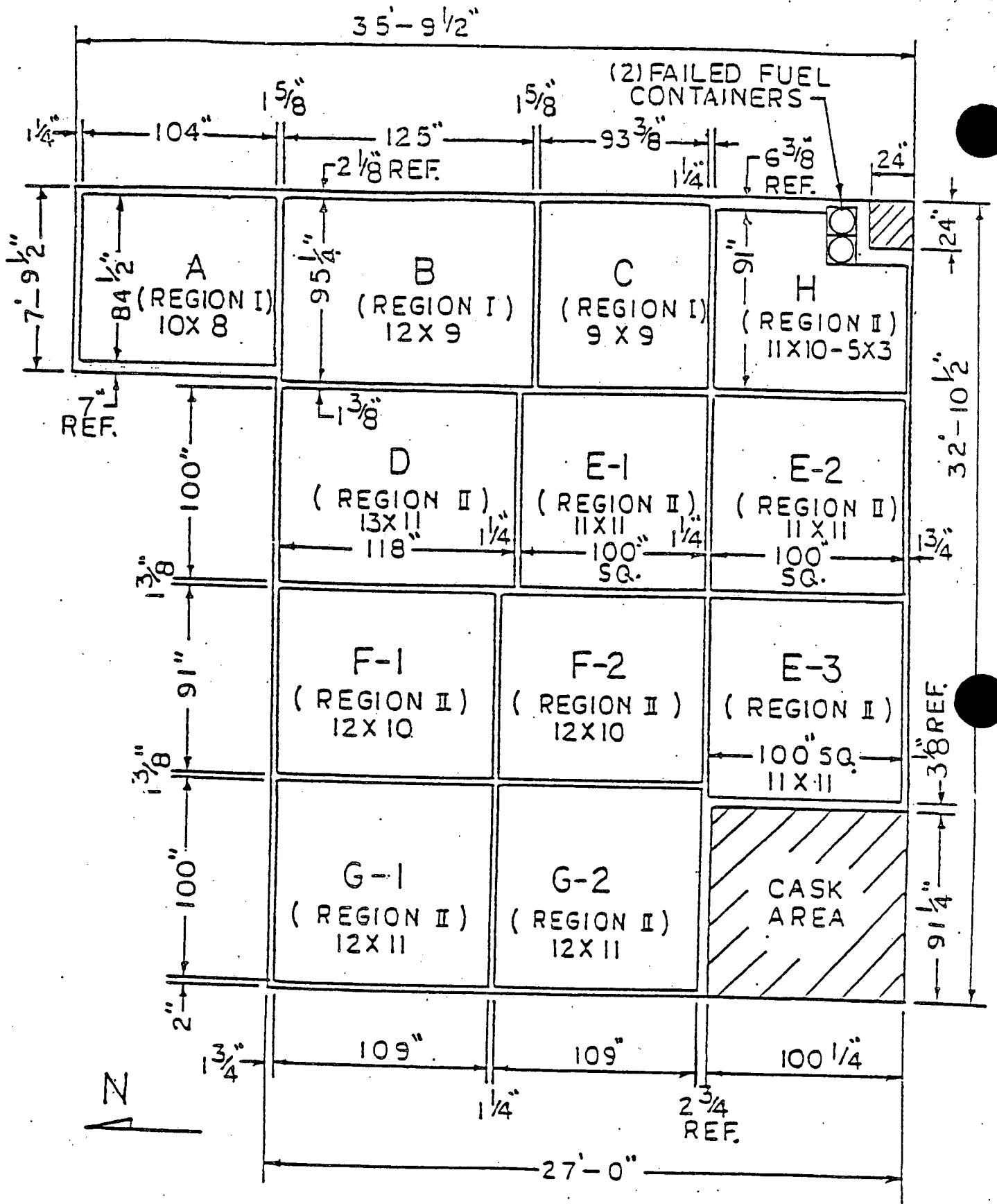
FIGURE 2.1   MODULE LAYOUT - IP2 POOL
(NOMINAL DIMENSIONS)

3.0   RACK FABRICATION AND APPLICABLE CODES

The object of this section is to provide a self-contained description of rack module construction to enable an independent appraisal of the adequacy of design. A list of applicable codes and standards is also presented.

3.1   FABRICATION OBJECTIVE

The requirements in manufacturing the high density storage racks for the IP2 fuel pool may be stated in four interrelated points:

(1)   The rack module will be fabricated in such a manner that there is <u>no</u> weld splatter on the storage cell surfaces which would come in contact with the fuel assembly.

(2)   The storage locations will be constructed so that redundant flow paths for the coolant are available.

(3)   The fabrication process involves operational sequences which permit immediate verification by the inspection staff.

(4)   The storage cells are connected to each other by austenitic stainless steel corner welds which leads to a honeycomb lattice construction. The extent of welding is selected to "detune" the racks from the ground motion (OBE and SSE).

3.2   RACK MODULE FOR REGION I

This section describes the constituent elements of the
IP2 Region I rack modules in the fabrication sequence.

The rack module manufacturing begins with fabrication of
the box.   The "boxes" are fabricated from two precision formed
channels by seam welding in a machine equipped with copper chill
bars and pneumatic clamps to minimize distortion due to welding
heat input.   Figure 3.1 shows the box.

The minimum weld penetration will be 80% of the box
metal gage which is 0.075" (14 gage).   The boxes are manufactured
to 8.75" I.D. (inside dimension) ± .032".

A die is used to flare out one end of the box to provide
the 30^0 tapered lead-in (Figure 3.2).   One inch diameter holes are
punched on two sides near the other end of the box to provide the
requisite auxiliary flow holes.

Each box constitutes a storage location. Each side of a
box facing another box is equipped with a narrow rectangular
cavity which houses one integral Boraflex sheet (poison material).

The design objective calls for installing Boraflex with
minimal surface loading. This is accomplished by die forming a
"picture frame sheathing" as shown in Figure 3.3.   This sheathing
is made to precise dimensions such that the offset is .010 to .005
inches greater than the poison material thickness.

The poison material is placed in the customized flat depression region of the sheathing, which is next laid on a side of the "box". The precision of the shape of the sheathing obtained by die forming guarantees that the poison sheet installed in it will not be subject to surface compression. The flanges of the sheathing (on all four sides) are attached to the box using skip welds. The sheathing serves to locate and position the poison sheet accurately, and to preclude its movement under seismic conditions.

Having fabricated the required number of the composite box assemblies, they are joined together in a fixture in the manner shown in Figure 3.4. The pitch between the box centerlines is p_x in one principal direction and p_y in the other principal direction. The values of p_x and p_y are given in Section 4 of this Licensing Report. The fabrication procedure in either direction is identical, since the channels are fillet welded to make the inter-box connection.

Joining the channel results in a well defined shear flow path, and essentially makes the box assemblage into a multi-flanged beam type structure.

In the next step of manufacture, the "base plate" is attached to the bottom edge of the boxes. The base plate is a 1/2" thick austenitic stainless steel plate stock which has a 6" hole burned out in a pitch identical to the box pitch. The base plate is attached to the cell assemblage by fillet welding the box edge to the plate.

In the final step, adjustable leg supports (shown in Figure 3.5) are welded to the underside of the base plate. The adjustable legs provide a ± 1/2" vertical height adjustment at each leg location. The manufacturing of the Region I rack modules culminates with appropriate NDE of welds, which includes visual examination of cell longitudinal seam welds and cell-to-cell connection welds and liquid dye penetrant examination of support welds, in accordance with the design drawings. Figure 3.6 shows an elevation view of two cells with a fuel assembly indicated in cross-section in one cell.

3.3   RACK MODULE FOR REGION II

Region II storage cell locations have a single poison panel between adjacent austenitic steel surfaces. The significant components (discussed below) of the Region II racks are: (1) the storage box subassembly (2) the base plate, (3) the neutron absorber material, (4) picture frame sheathing, and (5) support legs.

(1)   Storage cell box subassembly: As described for Region I, the "boxes" are fabricated from two precision formed channels by seam welding in a machine equipped with copper chill bars and pneumatic clamps to minimize distortion due to welding heat input. Figure 3.1 shows the "box".

The minimum weld penetration will be 80% of the box metal gage which is 0.075" (14 gage). The boxes are manufactured to 8.800" I.D. (inside dimension) ± .032".

As shown in Figure 3.7, each box has two lateral holes punched near its bottom edge to provide auxiliary flow holes. A "picture frame sheathing" similar to Region I rack construction is attached to each side of the box with the poison material installed in the sheathing cavity. Unlike Region I, the top of the sheathing extends to the top of the box. The edges of the sheathing and the box are welded together to form a smooth edge. The box, with integrally connected sheathing, is referred to as the "composite box".

The "composite boxes" are arranged in a checkerboard array to form an assemblage of storage cell locations (Figure 3.8). The inter-box welding and pitch adjustment are accomplished by small longitudinal connectors.

This assemblage of box assemblies is welded edge-to-edge as shown in Figure 3.8, resulting in a honeycomb structure with axial, flexural and torsional rigidity depending on the extent of intercell welding provided. It can be seen from Figure 3.8 that two edges of each interior box are connected to the contiguous boxes resulting in a well defined path for "shear flow".

(2) <u>Base Plate</u>: The base plate provides a continuous horizontal surface for supporting the fuel assemblies. The base plate has a concentric hole in each cell location as described in the preceding section.

The base plate is attached to the cell assemblage by fillet welds. The baseplate in each storage cell has a 6" diameter flow hole.

(3) <u>The neutron absorber material</u>: As mentioned in the preceding section, Boraflex is used as the neutron absorber material.

(4) <u>Picture Frame Sheathing</u>: As described earlier, the sheathing serves as the locator and retainer of the poison material. Figure 3.3 is a schematic of the sheathing.

(5) <u>Support Legs</u>: As stated earlier, all support legs are the adjustable type (Figure 3.5). The top position is made of austenitic steel material. The bottom part is made of 17:4 Ph series stainless steel to avoid galling problems.

Each support leg is equipped with a readily accessible socket to enable remote leveling of the rack after its placement in the pool. Lateral holes in the support leg provide the requisite coolant flow path.

3.4   <u>CODES, STANDARDS, AND PRACTICES FOR THE IP2 SPENT FUEL POOL RACKS</u>

The fabrication of the rack modules is performed under a strict quality assurance system suitable for ASME Section III, Class 1, 2 and 3 manufacturing and complies with the provisions of 10CFR50 Appendix B.

The following codes, standards and practices will be used as applicable for the design, construction, and assembly of the spent fuel storage racks. Additional specific references related to detailed analyses are given in each section.

a.   <u>Design Codes</u>

(1) AISC Manual of Steel Construction, 8th Edition, 1980.

(2) ANSI N210-1976, "Design Objectives for Light Water Reactor Spent Fuel Storage Facilities at Nuclear Power Stations."

(3) American Society of Mechanical Engineers (ASME), Boiler and Pressure Vessel Code, Section III, 1983 Edition up to and including Summer 1983 Addenda (Subsection NF).

(4) ASNT-TC-1A June, 1980 American Society for Nondestructive Testing (Recommended Practice for Personnel Qualifications).

b. **Material Codes**

(1) American Society for Testing and Materials (ASTM) Standards - A-240.

(2) American Society of Mechanical Engineers (ASME), Boiler and Pressure Vessel Code, Section II - Parts A and C, 1983 Edition, up to and including Summer 1983 Addenda.

c. **Welding Codes**

ASME Boiler and Pressure Vessel Code, Section IX- Welding and Brazing Qualifications, 1983 Edition up to and including Summer, 1983 Addenda.

d. **Quality Assurance, Cleanliness, Packaging, Shipping, Receiving, Storage, and Handling Requirements**

(1) ANSI N45.2.2 - Packaging, Shipping, Receiving, Storage and Handling of Items for Nuclear Power Plants.

(2) ANSI 45.2.1 - Cleaning of Fluid Systems and Associated Components during Construction Phase of Nuclear Power Plants.

(3) ASME Boiler and Pressure Vessel, Section V, Nondestructive Examination, 1983 Edition, including Summer and Winter 1983.

(4) ANSI - N16.1-75 Nuclear Criticality Safety Operations with Fissionable Materials Outside Reactors.

(5) ANSI - N16.9-75 Validation of Calculation Methods for Nuclear Criticality Safety.

(6) ANSI - N45.2.11, 1974 Quality Assurance Requirements for the Design of Nuclear Power Plants.

e. Other References

(1) NRC Regulatory Guides 1.13, Rev. 2 (proposed);
1.29, Rev. 3; 1.31, Rev. 3; 1.61, Rev. 0; 1.71,
Rev. 0; 1.85, Rev. 22; 1.92, Rev. 1; 1.124, Rev. 1;
and 3.41, Rev. 1.

(2) General Design Criteria for Nuclear Power Plants,
Code of Federal Regulations, Title 10, Part 50,
Appendix A (GDC Nos. 1, 2, 61, 62, and 63).

(3) NUREG-0800, Standard Review Plan, Sections 3.2.1,
3.2.2, 3.7.1, 3.7.2, 3.7.3, 3.8.4.

(4) "OT Position for Review and Acceptance of Spent
Fuel Storage and Handling Applications," dated
April 14, 1978, and the modifications to this
document of January 18, 1979.

3.5 MATERIALS OF CONSTRUCTION

Storage Cell:	SA240-304
Baseplate:	SA240-304
Support Leg:	SA351 Grade (casting) or SA240-304 (plate stock)
Support Leg (male):	Ferritic stainless (anti-galling material) SA564-630
Poison:	Boraflex

WELD SEAM

4.38

8.75

FIGURE 3.1

SEAM WELDING PRECISION FORMED CHANNELS
FOR REGION I OF IP2 POOL
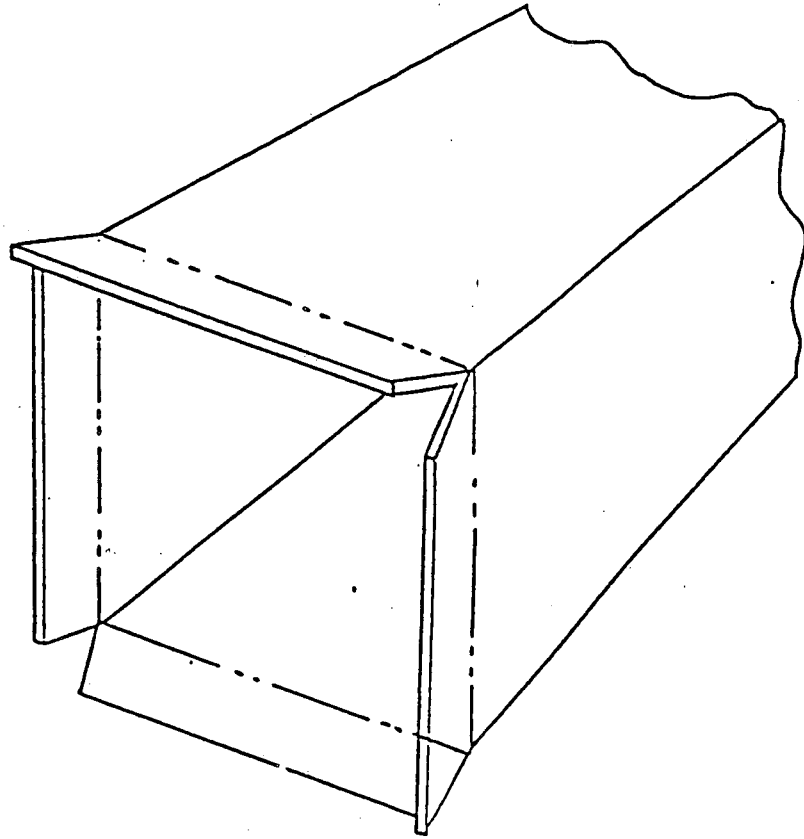
FIGURE 3.2   BOX LEAD-IN (REGION I)
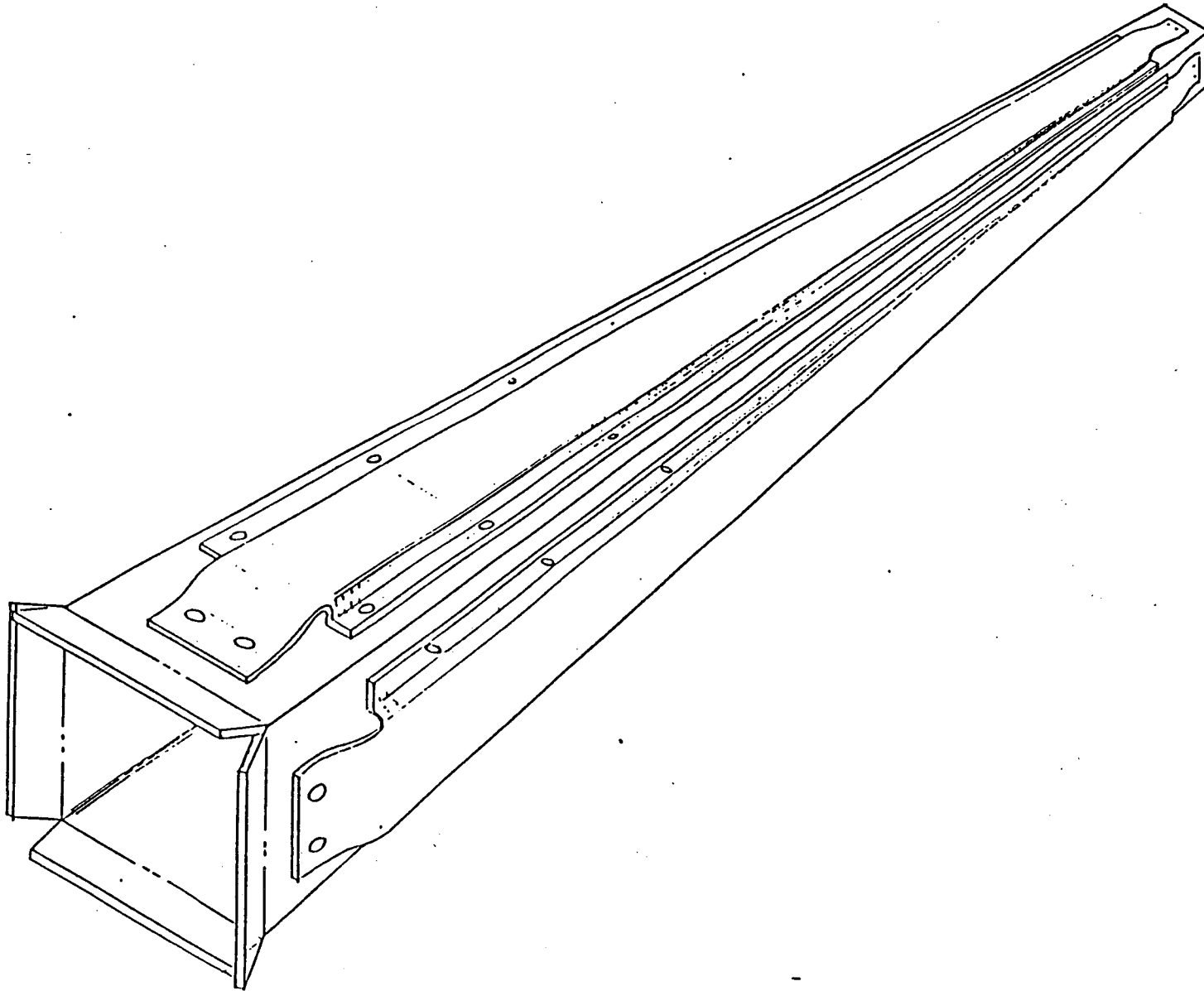
FIGURE 3.3   SHEATHING FOR REGION I

PRECISION FORMED SHEATHING

SEPARATOR CHANNEL

BOX WALL

POISON

BOX I.D.
(Closely Controlled)

FLUX
TRAP
GAP

P_y

LAYOUT PITCH

P_x
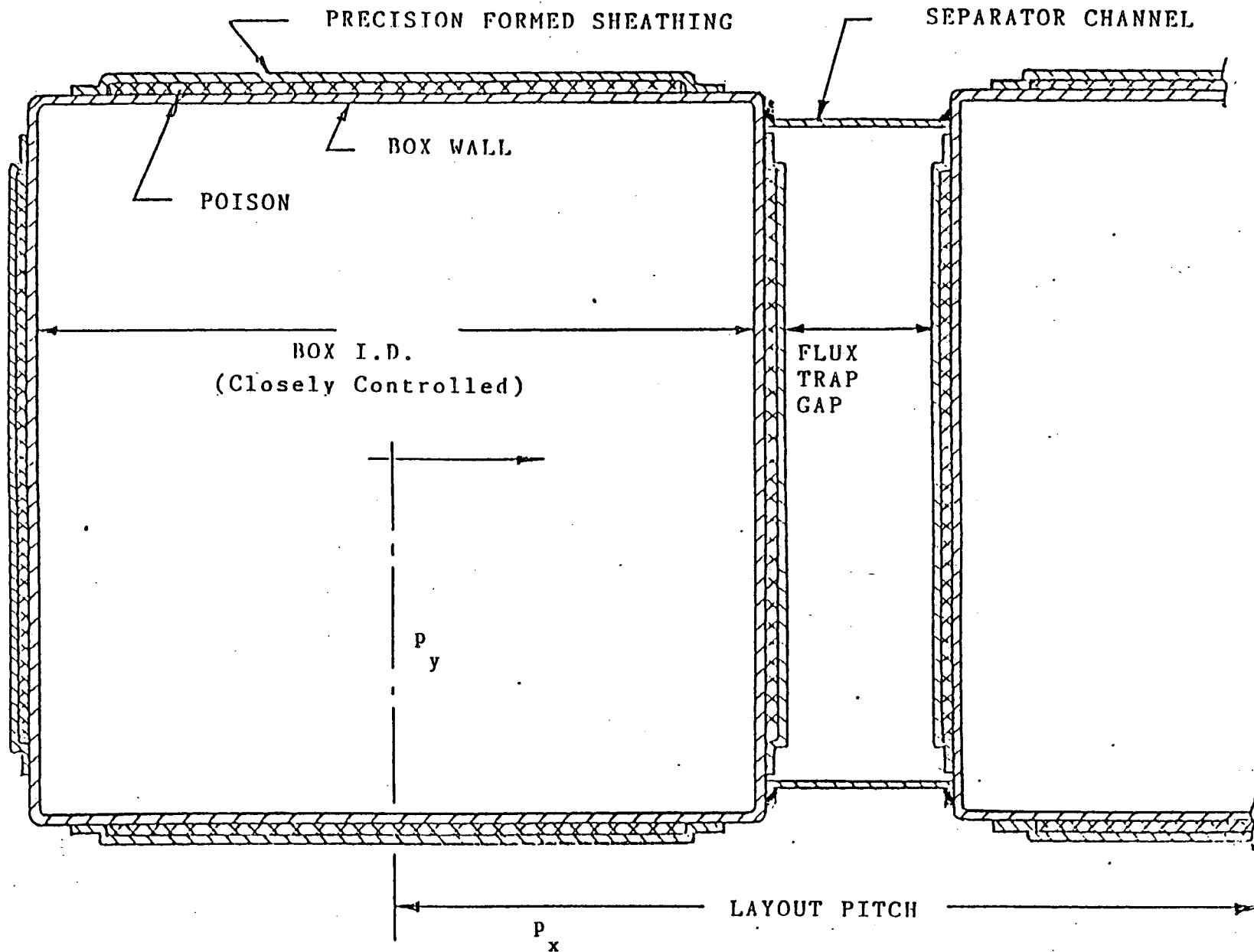
FIGURE 3.4   REGION I CELL   CROSS-SECTION

CELL

BASEPLATE

6" NOM.

6-1/2" MAX.

4-1/4"

1-3/4" NOM.

3-3/4"

4" 4UNC CLASS 1A

3/4" DIA. HOLE THRU

9" OD
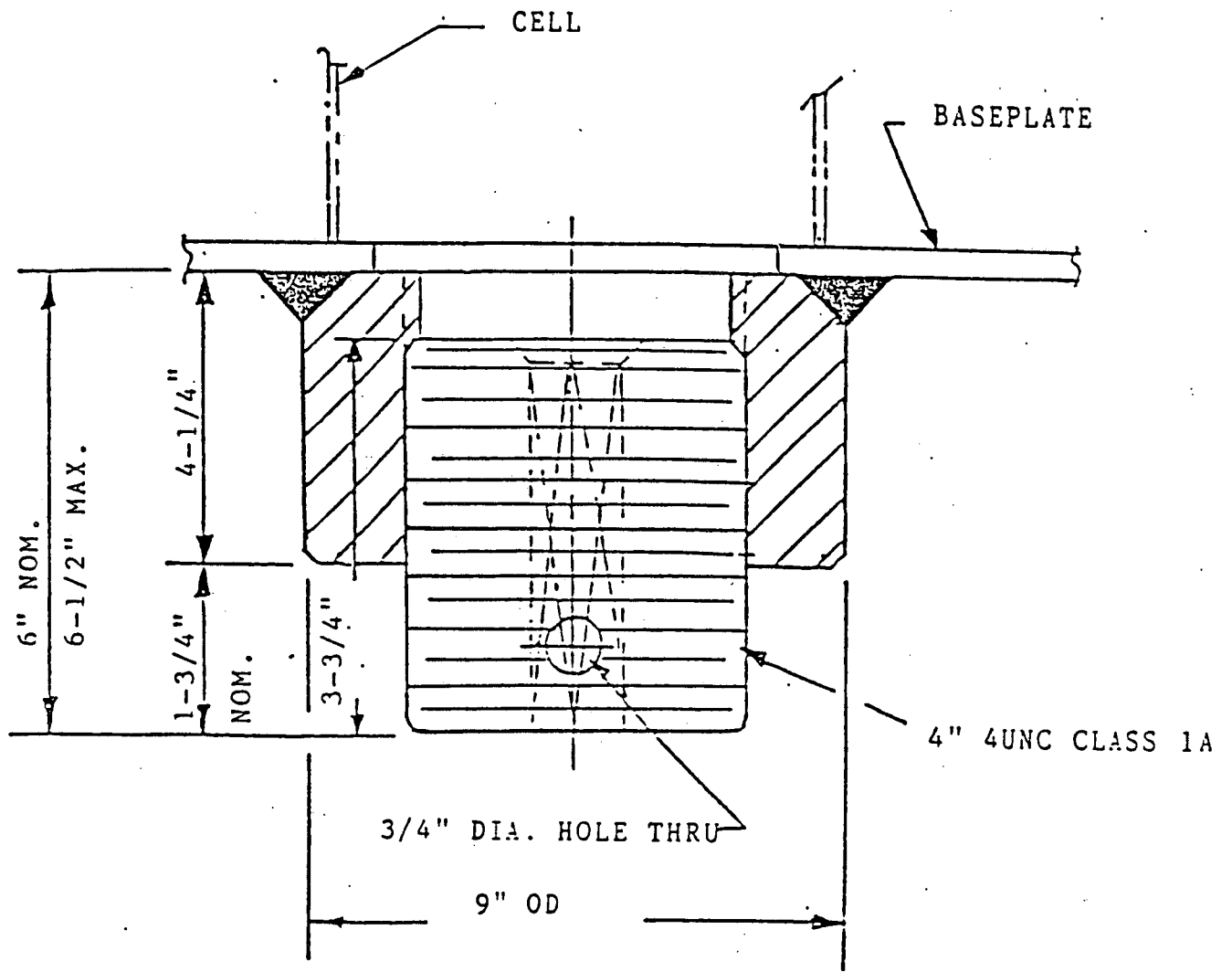
FIGURE 3.5   ADJUSTABLE SUPPORT
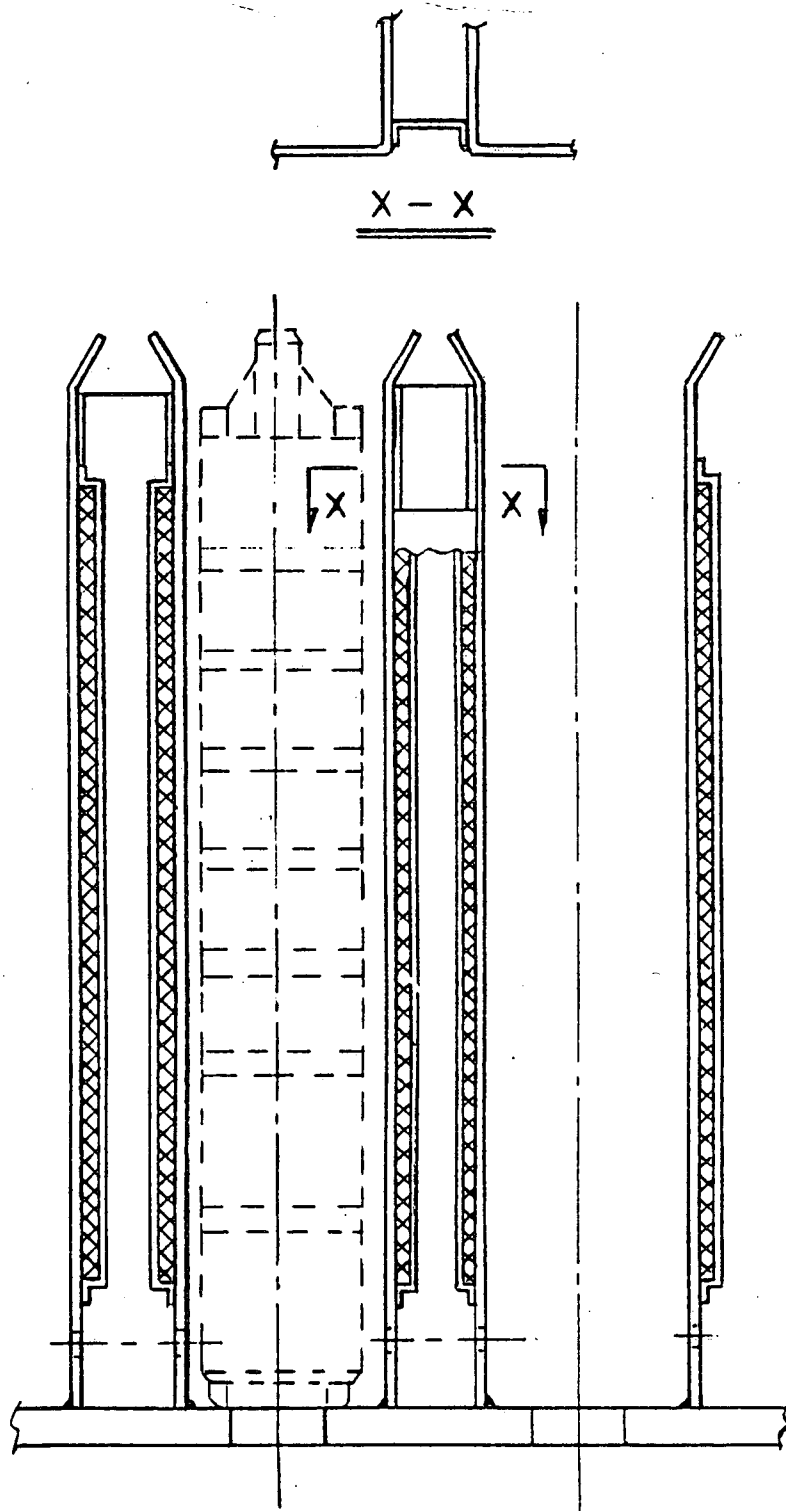
FIGURE 3.6

ELEVATION VIEW OF A REGION I RACK
SHOWING TWO STORAGE CELLS

CELL PITCH
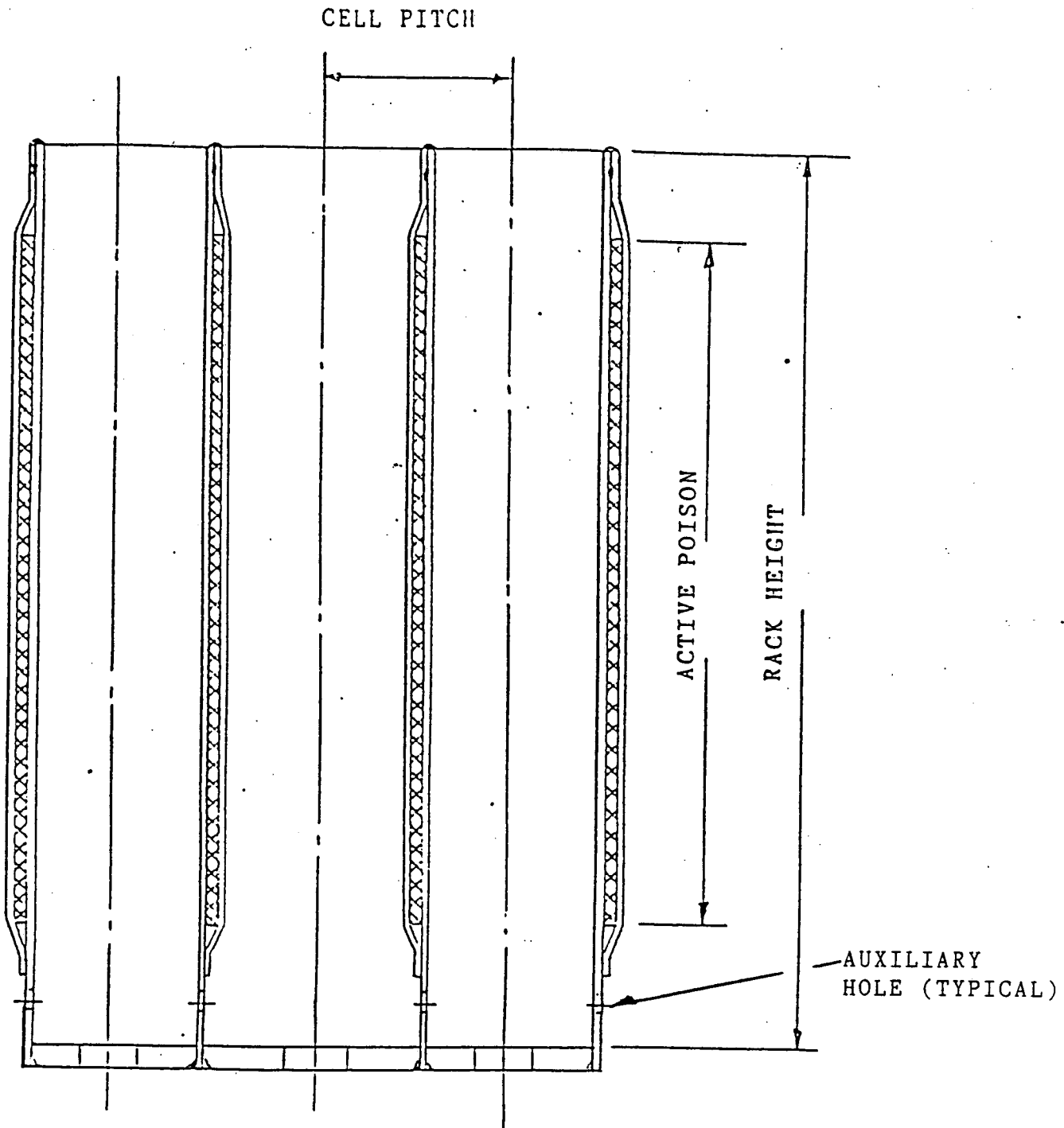
FIGURE 3.7   THREE CELLS OF REGION II
             IN ELEVATION VIEW
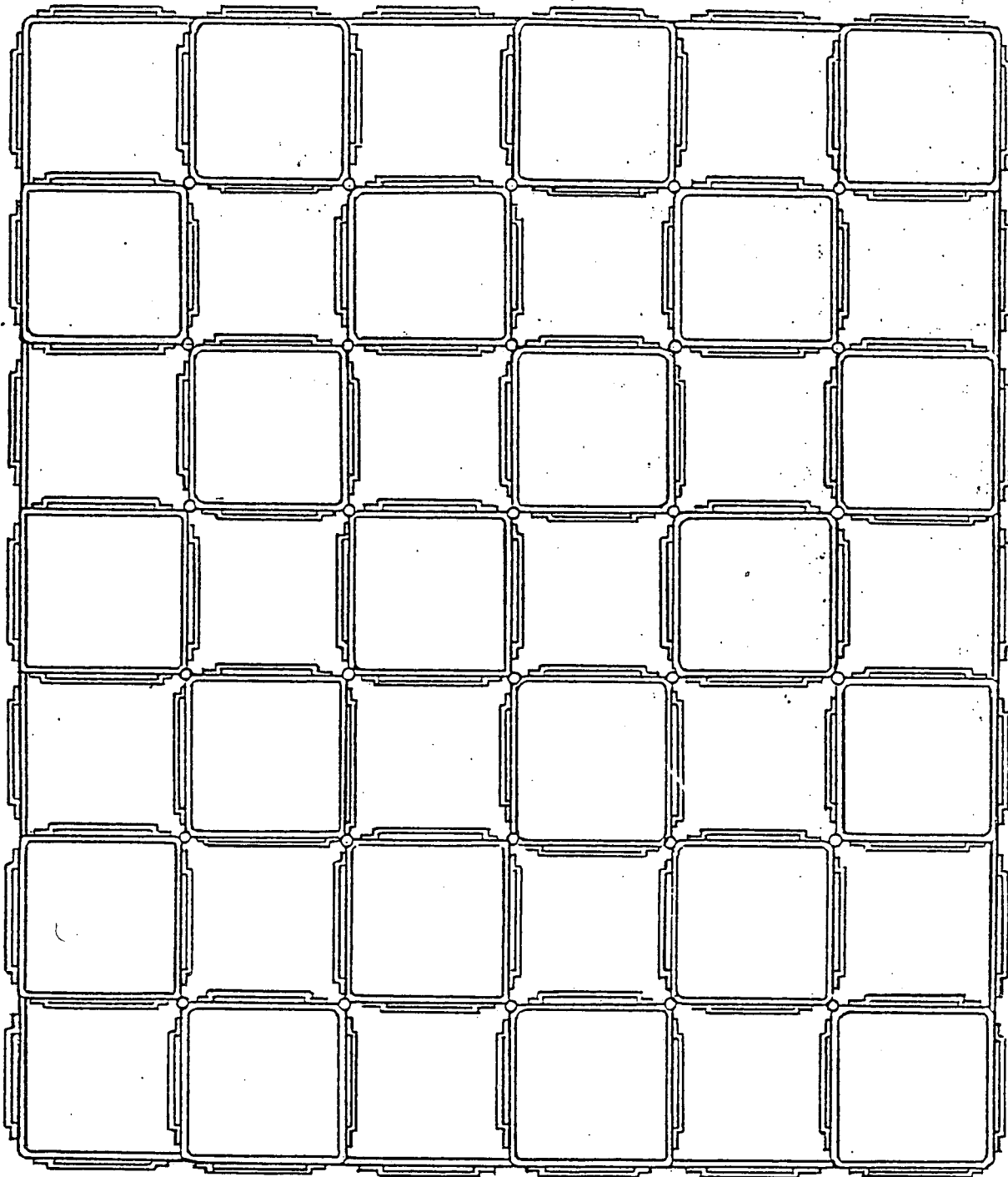
FIGURE   3.8   A CROSS SECTIONAL VIEW OF AN ARRAY
                OF STORAGE LOCATIONS

3-16

4.0 CRITICALITY SAFETY ANALYSES

4.1 DESIGN BASES

The high density spent fuel storage racks for Indian Point Unit 2 are designed to assure that the effective neutron multiplication factor (k_{eff}) is equal to or less than 0.95 with the racks fully loaded with fuel of the highest anticipated reactivity, and flooded with unborated water at a temperature corresponding to the highest reactivity (68°F). The maximum calculated reactivity includes a margin for uncertainty in reactivity calculations including mechanical tolerances. All uncertainties are statistically combined, such that the final k_{eff} will be equal to or less than 0.95 with a 95% probability at a 95% confidence level.

Applicable codes, standards, and regulations or pertinent sections thereof, include the following:

o   General Design Criteria 62, Prevention of Criticality in Fuel Storage and Handling.

o   USNRC Standard Review Plan, NUREG-0800, Section 9.1.2, Spent Fuel Storage, Rev. 3 - July 1981

o   USNRC letter of April 14, 1978, to all Power Reactor Licensees - OT Position for Review and Acceptance of Spent Fuel Storage and Handling Applications, including modification letter dated January 18, 1979.

o   USNRC Regulatory Guide 1.13, Spent Fuel Storage Facility Design Basis, Rev. 2 (proposed), December 1981.

o   USNRC Regulatory Guide 3.41, Validation of Calculational Methods for Nuclear Criticality Safety (and related ANSI N16.9-1975).

o   ANSI/ANS-57.2-1983, Design Requirements for Light
     Water Reactor Spent Fuel Storage Facilities at
     Nuclear Power Plants.

o   ANSI N210-1976, Design Objectives for Light Water
     Reactor Spent Fuel Storage Facilities at Nuclear
     Power Plants.

o   ANSI N18.2-1973, Nuclear Safety Criteria for the
     Design of Stationary Pressurized Water Reactor
     Plants.

USNRC guidelines and the applicable ANSI standards specify that the maximum _effective_ multiplication factor, "k_{eff}", including uncertainties, shall be less than or equal to 0.95. The _infinite_ multiplication factor, "k_∞", is calculated for an infinite array, neglecting neutron losses due to leakage from the actual storage rack, and therefore results in a higher and more conservative value. In the present evaluation of criticality safety in the Indian Point Unit 2 storage racks, the design basis criterion was assumed to be a "k_∞" of 0.95, which is more conservative than the limit specified in the regulatory guidelines. The word "reactivity" is a _qualitative_ term that may refer to either k_{eff} or k_∞ and is generally associated with another term such as "maximum", "highest", "lower", "calculated", or other appropriate descriptive and qualifying words.

To assure the true reactivity will always be less than the calculated reactivity, the following conservative assumptions were made:

o   Moderator is unborated water at a temperature that
     results in the highest reactivity (68°F).

4 - 2

o   In all cases (except for the assessment of peripheral
    effects and certain abnormal/accident conditions
    where neutron leakage is inherent), the infinite
    multiplication factor, k_∞, was used rather than the
    effective multiplication factor, k_{eff} (i.e., neutron
    loss from radial and axial leakage neglected).

o   Neutron absorption in minor structural members is
    neglected, i.e., spacer grids are analytically
    replaced by water and the results are applicable to
    HIPAR, LOPAR or OFA fuel.

The design basis fuel assembly is a 15 x 15 Westing-
house fuel assembly containing UO_2 at a maximum initial
enrichment of 5.0 wt% U-235   corresponding to 56.6
grams U-235 per axial centimeter of fuel assembly. Two
separate storage regions are provided in the spent fuel storage
pool, with independent criteria defining the highest potential
reactivity in each of the two regions as follows:

o   Region I is designed to accommodate new fuel with a
    maximum enrichment of 5.0 wt% U-235, or spent fuel
    regardless of the discharge fuel burnup.

o   Region II is designed to accommodate fuel of various
    initial enrichments which have accumulated minimum
    burnups within an acceptable bound as depicted in
    Figure 4.1.

The water in the spent fuel storage pool normally
contains soluble boron which would result in large subcriti-
cality margins under actual operating conditions. However, the
NRC guidelines, based upon the accident condition in which all
soluble poison is assumed to have been lost, specify that the
limiting k_{eff} of 0.95 be evaluated in the absence of soluble
boron. The double contingency principle of ANSI N-16.1-1975

and of the April 1978 NRC letter allows credit for soluble boron under other abnormal or accident conditions since only a single accident need be considered at one time. Consequences of abnormal and accident conditions have also been evaluated, where "abnormal" refers to conditions (such as higher water temperatures resulting from full-core discharge) which may reasonably be expected to occur during the lifetime of the plant and "accident" refers to conditions which are not expected to occur but nevertheless must be protected against.

4.2 SUMMARY OF CRITICALITY ANALYSES

4.2.1   Normal Operating Conditions

The criticality analyses of each of the two separate regions of the spent fuel storage pool are summarized in Table 4.1 for the design basis storage conditions which assumes the single accident condition of the loss of all soluble boron. The calculated maximum reactivity in Region II includes a burnup-dependent allowance for uncertainty in depletion calculations and, furthermore, provides an additional margin of approximately 1 % δk below the design basis infinite multiplication factor (k_∞) of 0.95. As cooling time increases in long-term storage, decay of Pu-241 results in a significant decrease in reactivity, which will provide an increasing subcriticality margin and tends to further compensate for any uncertainty in depletion calculations. An allowance is also included to allow for variations in spacing between two rack modules as installed in the spent fuel pool.

Data has shown that, under irradiation in a spent fuel pool, the Boraflex neutron absorber becomes a radiation-hardened ceramic-like material and shrinks ~2 to 2½ percent during long term storage. The Boraflex panels in both regions are initially 4% longer than required, as a conservative allowance to accommodate axial shrinkage, and the rack design provides for unrestrained shrinkage to preclude any mechanism that might cause gaps to form. The expected shrinkage in width (2½%) is included in the design basis criticality calculations. In the event the width shrinkage should approach 4% (a very conservative upper limit), the maximum k_∞, including uncertainties, could potentially increase to as much as 0.943 in either or both regions of the storage racks but would remain below the regulatory limit.

Region II can safely accommodate fuel of various initial enrichments and discharge fuel burnups, provided the combination falls within the acceptable domain illustrated by the solid line in Figure 4.1. For convenience, the minimum (limiting) burnup data in Figure 4.1 for unrestricted storage in Region II can be described as a function of the initial enrichment, E, in weight percent U-235 by a fitted polynomial expression as follows;

> For Region II Unrestricted Storage
>
> Minimum Burnup in MWD/MTU =
>
> $- 39,000 + 28,180 \ E - 3,960 \ E^2 + 304.8 \ E^3$
>
> (for initial enrichments up to 5 wt% U-235)

This polynomial fit is accurate to within 1% in burnup at the lower enrichments (2.5% enrichment or less), corresponding to a maximum error of less than 0.0006 δk in reactivity. At the higher enrichments, the polynomial fit slightly overpredicts the limiting burnup.

Because of large local neutron leakage, the peripheral cells in Region II facing non-fueled areas are capable of accommodating fuel assemblies of higher reactivity. The dashed curve in Figure 4.1 defines the acceptable domain for storage of fuel in these peripheral cells and has been fitted to the polynomial expression given below:

> For Peripheral Cells in Region II
>
> Minimum Burnup in MWD/MTU =
>
> $- 35,760 + 23,020 \ E - 2,712 \ E^2 + 197.1 \ E^3$
>
> (for initial enrichments up to 5 wt% U-235)

One assembly (No. F-65) had been prematurely discharged and does not satisfy either of the two criteria for storage in Region II. Assembly F-65, however, may be safely stored in one of the four outside corner cells facing non-fueled areas where leakage in two directions is adequate to reduce reactivity to below the acceptable limit.

The two burnup criteria identified above for acceptable storage in Region II can be implemented in appropriate administrative procedures to assure verified burnup as specified in the proposed Regulatory Guide 1.13, Revision 2. Administrative procedures will also be employed to confirm and assure the presence of soluble poison in the pool water during fuel handling operations, as a further margin of safety and as a precaution in the event of fuel misplacement during fuel handling operations. Soluble poison is only needed for accident conditions (where credit is permitted under the NRC guidelines by the double contingency principle) and 350 ppm soluble boron is adequate to protect against all accident conditions identified.

4.2.2   Abnormal and Accident Conditions

Although credit for the soluble poison normally present in the spent fuel pool water is permitted under abnormal or accident conditions, most abnormal or accident conditions will not result in exceeding the limiting reactivity (k_{eff} of 0.95) even in the absence of soluble poison. The effects on reactivity of credible abnormal and accident conditions are presented in detail in Section 4.7 and briefly summarized in Table 4.2. Of these abnormal/accident conditions, only one has the potential for a more than negligible positive reactivity effect.

4 - 7

The inadvertent misplacement of a fresh fuel assembly (either into a Region II storage cell or outside and adjacent to a rack module) has the potential for exceeding the limiting reactivity, should there be a concurrent and independent accident condition resulting in the loss of all soluble poison. Administrative procedures to assure the presence of soluble poison during fuel handling operations will preclude the possibility of the simultaneous occurrence of the two independent accident conditions. The largest reactivity increase (+0.0368 δk) would occur if a new fuel assembly were to be loaded into a Region II storage cell with all other cells fully loaded with fuel of the highest permissible reactivity. Under this accident condition, credit for the presence of soluble poison is permitted by NRC guidelines[*], although criticality would not be reached even in the absence of the soluble poison. A minimum boron concentration of only 350 ppm boron is adequate to assure that the regulatory limit (k_{eff} of 0.95) is not exceeded.

---

[*]Double contingency principle of ANSI N16.1-1975, as specified in the April 14, 1978 NRC letter (Section 1.2) and implied in the proposed revision to Reg. Guide 1.13 (Section 1.4, Appendix A).

4 - 8

4.3   REFERENCE FUEL STORAGE CELLS

4.3.1   Reference Fuel Assembly

The design basis fuel assembly, illustrated in Figures 4.2 and 4.3, is a 15 x 15 array of fuel rods with 21 rods replaced by 20 control rod guide tubes and 1 instrument thimble. Table 4.3 summarizes the design specifications and the expected range of significant variations. The fuel assembly grid spacers and miscellaneous hardware were conservatively neglected and the racks can therefore safely accommodate fuel of differing grid and guide tube designs, including HIPAR, LOPAR, and OFA fuel, since these assemblies have a lower reactivity than the design basis assembly used for the criticality analysis.

4.3.2   Region I Fuel Storage Cells

The nominal spent fuel storage cell used for the criticality analyses of Region I storage cells is shown in Figure 4.2. The rack is composed of Boraflex absorber material between an 8.75-inch I.D., 0.075-inch thick inner stainless steel box, and a 0.0235-inch outer stainless steel cover plate. Clearance is provided to allow unrestrained shrinkage of the Boraflex during irradiation. The fuel assemblies are centrally located in each storage cell on a nominal lattice spacing of 10.765 inches in the East-West direction and 10.545 inches in the North-South direction. Stainless steel gap channels connect one storage cell box to another in a rigid structure and define an outer water space between boxes. This outer water space constitutes a flux-trap between the two Boraflex absorber panels that are essentially opaque (black) to thermal neutrons. The Boraflex absorber has a thickness of 0.102 ± 0.007 inch and a nominal B-10 areal density of 0.0324 g/cm^2.

4.3.3 Region II Fuel Storage Cells

Region II storage cells are designed for fuel of 5.0 wt% U-235 initial enrichment burned to 40,900 MWD/MTU. In Region II, the storage cells are composed of a single Boraflex absorber panel between the 0.075-inch stainless steel walls of adjacent storage cells. These cells, shown in Figure 4.3, are located on a lattice spacing of 9.04 ± 0.05 inches. The Boraflex absorber has a thickness of 0.082 ± 0.007 inch and a nominal B-10 areal density of 0.0260 g/cm^2.

4.3.4 Boraflex Integrity

Under irradiation, Boraflex becomes a hard ceramic-like material of considerably increased tensile strength and with a maximum observed[1] shrinkage of 2 to 2-1/2 percent. In the Indian Point 2 racks, the Boraflex panels are installed in a space of sufficient size to allow unimpeded shrinkage and thereby preclude any mechanism that might cause gaps to develop. The initial Boraflex length in both regions is 6 inches (4%) longer than required as a conservative allowance for shrinkage in the axial direction. Width shrinkage (2½%) is included in the design basis calculations and the consequence of greater than expected shrinkage has also been evaluated (+0.0027 δk in Region I and +0.0021 in Region II for 4% width shrinkage). Estimates of the reactivity effect of width shrinkage do not take credit for the increase in B-10 concentration that accompanies the volume reduction.

4.4   ANALYTICAL METHODOLOGY

4.4.1   Reference Design Calculations

In the fuel rack analyses, the primary criticality analyses of the high density spent fuel storage racks were performed with a two-dimensional multi-group transport theory technique, using the CASMO-2E[2] computer code.   Independent verification calculations were made with a Monte Carlo technique utilizing the AMPX-KENO computer package[3], with the 27-group SCALE* cross-section library[4] and the NITAWL subroutine for U-238 resonance shielding effects (Nordheim integral treatment). Benchmark calculations, presented in Appendix A, indicate a bias of 0.0013 with an uncertainty of ± 0.0018 for CASMO-2E and 0.0106 ± 0.0048 (95%/95%) for NITAWL-KENO.

CASMO-2E was also used both for burnup calculations (with independent verification by NULIF[5] calculations) and for evaluating the small reactivity increments associated with manufacturing tolerances.   In tracking long-term (30-year) reactivity effects of spent fuel stored in Region II of the fuel storage rack, CASMO-2E calculations confirm a continuous reduction in reactivity with time (after Xe decay) due primarily to Pu-241 decay and Am-241 growth.

Two group diffusion theory constants, edited in the output of CASMO-2E, were used in PDQ07[6] for auxiliary calculations of the small incremental reactivity effect of eccentric fuel positioning.   These constants were also used in

---

*"SCALE" is an acronym for Standardized Computer Analysis for Licensing Evaluation, a standard cross-section set developed by ORNL for the USNRC.

a one dimensional diffusion theory routine (benchmarked against PDQ07) to evaluate reactivity effects of the Boraflex axial length.

In the geometric model used in the calculations, each fuel rod and its cladding were described explicitly and reflecting boundary conditions (zero neutron current) were used in the axial direction and at the centerline of the Boraflex and steel plates between storage cells. These boundary conditions have the effect of creating an infinite array of storage cells in all directions. However, limitations in the geometry options available in CASMO-2E required minor and generally insignificant approximations in the geometric description (e.g. in the use of an average water-gap thickness). The AMPX-KENO calculation (as well as other previous calculations) provided a verification of the validity of these approximations. AMPX-KENO Monte Carlo calculations inherently include a statistical uncertainty due to the random nature of neutron tracking. To minimize the statistical uncertainty of the KENO-calculated reactivity, a minimum of 50,000 neutron histories in 100 generations of 500 neutrons each, are accumulated in each calculation.

4.4.2   Fuel Burnup Calculations and Uncertainties

CASMO-2E was used for burnup calculations in the hot operating condition with an independent check calculation made with the NULIF code. NULIF gave k_∞ values consistently lower than CASMO-2E by as much as 0.03 δk at 40,900 MWD/MTU, suggesting that CASMO-2E could be conservative at high burnups.

CASMO-2E has been extensively benchmarked (Appendix A and Refs. 2 and 7) against cold, clean, critical experiments (including plutonium-bearing fuel), Monte Carlo calculations,

reactor operations, and heavy-element concentrations in irradiated fuel. In particular, the analyses[7] of 11 critical experiments with plutonium-bearing fuel gave an average k_{eff} of 1.002 ± 0.011 (95%/95%), showing adequate treatment of the plutonium nuclides. In addition, Johansson[8] has obtained very good agreement in calculations of close-packed, high-plutonium-content, experimental configurations.

Since critical experiment data with spent fuel is not available for determining the uncertainty in burnup-dependent reactivity calculations, an allowance for uncertainty in reactivity was assigned based upon other considerations. Over a considerable portion of the burnup history in PWRs, the reactivity loss rate is approximately 0.01 δk for each 1000 MWD/MTU burnup, becoming smaller at the higher burnups. Assuming the uncertainty in depletion calculations is less than 5% of the total reactivity decrement, an uncertainty in reactivity* equal to 0.0005 δk for each 1000 MWD/MTU in burnup may be assigned. For the Indian Point Unit 2 storage racks at the design basis burnup of 40,900 MWD/MTU, the reactivity allowance for uncertainty is 0.0205 δk. Table 4.4 summarizes results of the burnup analyses and allowances for uncertainties at other burnups. At the higher burnups, this assumption results in an uncertainty greater than 5% of the reactivity decrement which provides an extra margin to allow for the existence of a small positive reactivity increment from the axial distribution in burnup (see Section 4.4.3). In addition, although the reactivity uncertainty due to burnup may be either positive or negative, it is treated as an additive term rather than being combined statistically with other uncertainties. Thus, the allowance for uncertainty in burnup calculations is believed to

---

*Only that portion of the uncertainty due to burnup. Other uncertainties are accounted for elsewhere.

be a conservative estimate, particularly in view of the substantial reactivity decrease with aged fuel as discussed in Section 4.4.4.

4.4.3   Effect of Axial Burnup Distribution

Initially, fuel loaded into the reactor will burn with a slightly skewed cosine power distribution. As burnup progresses, the burnup distribution will tend to flatten, becoming more highly burned in the central regions than in the upper and lower ends. This effect may be clearly seen in the curves compiled in Ref. 9. At high burnup, the more reactive fuel near the ends of the fuel assembly (less than average burnup) occurs in regions of lower reactivity worth due to neutron leakage. Consequently, it would be expected that over most of the burnup history, distributed burnup fuel assemblies would exhibit a slightly lower reactivity than that calculated for the average burnup. As burnup progresses, the distribution, to some extent, tends to be self-regulating as controlled by the axial power distribution, precluding the existence of large regions of significantly reduced burnup.

Among others, Turner[10] has provided generic analytic results of the axial burnup effect based upon calculated and measured axial burnup distributions. These analyses confirm the minor and generally negative reactivity effect of the axially distributed burnup. The trends observed, however, suggest the possibility of a small positive reactivity effect at the high burnup values (estimated to be less than 0.008 δk at 40,900 MWD/MTU) and the uncertainty in k_∞ due to burnup, assigned at the higher burnups (Section 4.4.2) is considered adequate to encompass the potential for a small positive reactivity effect of axial burnup distributions. Furthermore,

4 - 14

reactivity significantly decreases with time in storage (Section 4.4.4 below) providing a continuously increasing margin below the 0.95 limit.

4.4.4   Long-term Changes in Reactivity

Since the fuel racks in Region II are intended to contain spent fuel for long periods of time, calculations were made using CASMO-2E to follow the long-term changes in reactivity of spent fuel over a 30-year period. Early in the decay period, Xenon grows from Iodine decay (reducing reactivity) and subsequently decays, with the reactivity reaching a maximum at 100-200 hours. The decay of Pu-241 (13-year half-life) and growth of Am-241 substantially reduce reactivity during long term storage, as indicated in Table 4.5. The reference design criticality calculations do not directly take credit for this long-term reduction in reactivity, other than to indicate an increasing subcriticality margin in Region II of the spent fuel storage pool.

4.5   REGION I CRITICALITY ANALYSES AND TOLERANCES

4.5.1   Nominal Design

For the nominal storage cell design in Region I, the CASMO-2E calculation resulted in a bias-corrected k_∞ of 0.9323 ± 0.0018, which, when combined with all known uncertainties, results in a maximum k_∞ of 0.9401. Independent calculations with AMPX-KENO gave a k_∞ of 0.9148 ± 0.0066, including a one-sided tolerance factor[11] for 95% probability at a 95% confidence level. Correcting for a 0.0106 ± 0.0048 δk bias and combining all known uncertainty factors, the calculated k_∞ becomes 0.925 ± 0.010 or a maximum k_∞ value of 0.935. This agreement confirms the reference CASMO-2E calculations.

4.5.2   Uncertainties Due to Tolerances

4.5.2.1   Boron Loading Tolerances

The Boraflex absorber panels used in the storage cells are nominally 0.1022-inch thick, 7.50-inch wide and 144-inch long, with a nominal B-10 areal density of 0.0324 g/cm^2. Independent manufacturing tolerance limits are ± 0.007 inch in thickness and ±0.0090 g/cm^3 in B-10 content. This assures that at any point where the minimum boron concentration (0.1158 g B-10/cm^3) and minimum Boraflex thickness (0.0952 inch) may coincide, the B-10 areal density will not be less than 0.028 g /cm^2. Differential CASMO-2E calculations indicate that these tolerance limits result in incremental reactivity uncertainties of ±0.0025 δk for boron concentration and ± 0.0034 for the Boraflex thickness tolerance.

4.5.2.2   Boraflex Width Tolerance

The reference storage cell design uses a Boraflex panel with an initial width of 7.500 ± 0.063 inches. The calculations, however, assumed a 2½ % shrinkage in Boraflex width, to 7.312 ± 0.063 inches. A positive increment in reactivity occurs for a decrease in Boraflex absorber width. For the maximum tolerance of 0.063 inch, the calculated reactivity uncertainty is +0.0015 δk.

4.5.2.3   Tolerances in Cell Lattice Spacing

The design storage cell lattice spacing between fuel assemblies is 10.545 ± 0.035 in one direction and 10.765 ± 0.035 inches in the other direction. A decrease in storage cell lattice spacing may or may not increase reactivity depending upon other dimensional changes that may be associated with the decrease in lattice spacing. Decreasing the water spacing between the fuel and the inner stainless steel box results in a small decrease in reactivity. However, decreasing the flux-trap water spacing increases reactivity and both of these effects have been evaluated for their independent design tolerances.

The inner stainless steel box dimension, 8.75 ± 0.03 inches, defines the inner water thickness between the fuel and the inside box. For the tolerance limit of ± 0.03 inches, the uncertainty in reactivity is ±0.0012 δk as determined by differential CASMO-2E calculations, with k_∞ increasing as the inner stainless steel box dimension (and derivative lattice spacing) increases.

The design flux-trap water thickness is 1.371 ± 0.016 inches in one direction and 1.591 ± 0.016 inches in the other direction, which results in an uncertainty of ±0.0013 δk due to the ± 0.016 inch tolerance in flux-trap water thickness, assuming the water thickness is simultaneously reduced on all four sides. Since the manufacturing tolerances on each of the four sides are statistically independent, the actual reactivity uncertainties would be less than ± 0.0013 δk, although the more conservative value has been used in the criticality evaluation.

4.5.2.4   Stainless Steel Thickness Tolerances

The nominal stainless steel thickness is 0.075 ± 0.005 inch for the inner stainless steel box and 0.0235 ± 0.0030 inch for the Boraflex cover plate. The maximum positive reactivity effect of the expected stainless steel thickness tolerance variations, was calculated (CASMO-2E) to be ±0.0005 δk.

4.5.2.5   Fuel Enrichment and Density Tolerances

The design maximum enrichment is 5.00 ± 0.05 wt% U-235. Calculations of the sensitivity to small enrichment variations by CASMO-2E yielded a coefficient of 0.0032 δk per 0.1 wt% U-235 at the design enrichment. For the assumed tolerance on U-235 enrichment of ± 0.05 wt%, the uncertainty on k_∞ is ±0.0016 δk.

Calculations were also made with the UO_2 fuel density increased to the maximum expected value of 10.52 g/cm^3 (smeared density). For the reference design calculations, the uncertainty in reactivity is ± 0.0021 δk over the maximum expected range of UO_2 densities.

4 - 18

4.5.3   Eccentric Fuel Positioning

The fuel assembly is assumed to be normally located in the center of the storage rack cell. Calculations were also made with the fuel assemblies assumed to be in the corner of the storage rack cell (four-assembly cluster at closest approach). These calculations indicated that, in Region I, the reactivity remains essentially the same (+0.0001 δk), as determined by differential PDQ07 calculations with diffusion coefficients generated by CASMO-2E. This uncertainty is included in the evaluation of the highest potential reactivity of the Region I storage cells.

4.5.4   Reactivity Effects of Boraflex Length

Based upon diffusion theory constants edited in the CASMO-2E output (reference design and a special case with water replacing the Boraflex), one-dimensional axial calculations were made to evaluate the reactivity effect of reduced Boraflex axial lengths. Reduced length of the Boraflex leaves small regions of active fuel without poison at each end of the fuel assembly. The unpoisoned region at each end is referred to as "cutback".

The axial calculations used a thick (30 cm.) water reflector, neglecting the higher absorption of the stainless-steel structural material at the ends of the fuel assembly. Results of the calculations showed that the k_{eff} remains less than the reference k_∞ of the storage cells until the axial reduction in Boraflex length substantially exceeds the design 3 inch cutback top and bottom, corresponding to an overall Boraflex length of 138 inches. Thus, the axial neutron leakage

more than compensates for the 3-inch design cutback and the reference k_∞ remains a conservative over-estimate of the true k_{eff}.

In manufacturing the racks, a 3-inch cutback is used at the bottom of the rack. However, an initial Boraflex length of 144 inch is used which provides an allowance of 6 inches at the top of the racks to more than accommodate radiation-induced shrinkage of the Boraflex without exceeding the design cutback.

4.6 REGION II CRITICALITY ANALYSES

4.6.1 Nominal Design Case

The principal method of analysis in Region II was the CASMO-2E code, using the restart option in CASMO-2E to transfer fuel of a specified burnup into the storage rack configuration at a reference temperature of 20°C (68°F). Calculations were made for fuel of several different initial enrichments and, at each enrichment, a limiting k_∞ value was established which included an additional factor for uncertainty in the burnup analyses and for the axial burnup distribution. The restart CASMO-2E calculations (cold, no-Xenon, rack geometry) were then interpolated to define the burnup value yielding the limiting k_∞ value for each enrichment, as indicated in Table 4.6. These converged burnup values define the boundary of the acceptable domain shown in Figure 4.1. Burnup values calculated with the polynomial function given below are shown in Table 4.6 and on Figure 4.1.

For Region II Unrestricted Storage

Minimum Burnup in MWD/MTU =

$- 39,000 + 28,180 \ E - 3,960 \ E^2 + 304.8 \ E^3$

(for initial enrichments up to 5 wt% U-235)

At a burnup of 40,900 MWD/MTU, the sensitivity to burnup is calculated to be 0.007 δk per 1000 MWD/MTU. During long-term storage, the k_∞ values of the Region II fuel rack will decrease continuously as indicated in Section 4.4.4.

An independent AMPX-KENO calculation was used to provide additional confidence in the reference Region II criticality analyses. Fuel of 1.764 wt% initial enrichment (equivalent to the reference rack design for burned fuel) was analyzed by AMPX-KENO and by the CASMO-2E model used for the Region II rack analysis. For this case, the CASMO-2E k_∞ (0.9305) at 1.764 wt% enrichment was within the statistical uncertainty of the bias-corrected value (0.9311 ± 0.0068, 95%/95%) obtained in the AMPX-KENO calculations, thereby confirming the validity of the primary CASMO-2E calculations.

4.6.2 Uncertainties Due to Tolerances

4.6.2.1 Boron Loading Tolerances

The Boraflex absorber panels used in the Region II storage cells are also 0.082 inch thick with a nominal B-10 areal density of 0.026 g/cm^2. Independent manufacturing limits are ±0.007 inch in thickness and ±0.0094 g/cm^3 in B-10 content. This assures that at any point where the minimum boron concentration (0.1154 g B-10/cm^3) and the minimum Boraflex thickness (0.075 inch) may coincide, the boron-10 areal density will not be less than 0.022 g/cm^2). Differential CASMO-2E calculations indicate that these tolerance limits result in an incremental reactivity uncertainty of ± 0.0038 δk for boron content and ± 0.0046 δk for Boraflex thickness.

4.6.2.2 Boraflex Width Tolerance

The reference storage cell design for Region II (Figure 4.3) uses a Boraflex absorber width of 7.500 ± 0.063 inches which, for calculational purposes including the 2½ % width shrinkage, was taken as 7.313 inches. With an additional

4 - 22

reduction in width of the 0.063 inch tolerance, the calculated positive reactivity increment is $\pm$ 0.0012 δk.

4.6.2.3   Tolerance in Cell Lattice Spacing

The manufacturing tolerance on storage cell lattice spacing between fuel assemblies in Region II is $\pm$ 0.05 inches, corresponding to an uncertainty in reactivity of $\pm$ 0.0012 δk.

4.6.2.4   Stainless Steel Thickness Tolerance

The nominal thickness of the stainless steel box wall is 0.075 inch with a tolerance of $\pm$0.005 inch, resulting in an uncertainty in reactivity of $\pm$0.0001 δk.

4.6.2.5   Fuel Enrichment and Density Tolerances

Uncertainties in reactivity due to tolerances on fuel enrichment and UO_2 density in Region II are assumed to be the same as those determined for Region I.

4.6.3   Eccentric Fuel Positioning

The fuel assembly is assumed to be normally located in the center of the storage rack cell. Calculations were also made with the fuel assemblies assumed to be in the corner of the storage rack cell (four-assembly cluster at closest approach). These calculations indicated that eccentric fuel positioning results in a decrease in reactivity by about 0.010 δk, as determined by PDQ07 calculations with diffusion coefficients generated by CASMO-2E. The highest reactivity, therefore, corresponds to the reference design with the fuel assemblies positioned in the center of the storage cells.

4 - 23

4.6.4   Reactivity Effect of Boraflex Length

Because the ends of the fuel assemblies in Region II have less burnup than the average, and hence are more reactive, an axial cutback is not used in this region. The initial length of the Boraflex panel, as installed, is 150 inches which conservatively allows for a 6 inch shrinkage (4%) without uncovering any of the fuel. The rack design provides sufficient space for unrestrained shrinkage of the Boraflex panel to assure that gaps will not be formed.

4.7   ABNORMAL AND ACCIDENT CONDITIONS

4.7.1   Temperature and Water Density Effects

The moderator temperature coefficient of reactivity is negative; a moderator temperature of 20°C (68°F) was assumed for the reference designs, which assures that the true reactivity will always be lower over the expected range of water temperatures. Temperature effects on reactivity have been calculated and the results are shown in Table 4.7. Introducing voids in the water internal to the storage cell (to simulate boiling) decreased reactivity, as shown in the table. Since, at saturation temperature, there is no significant thermal driving force, voids due to boiling will not occur in the outer (flux-trap) water region of Region I.

With soluble poison present, the temperature coefficients of reactivity would differ from those inferred from the data in Table 4.7. However, the reactivities would also be substantially lower at all temperatures with soluble boron present, and the data in Table 4.7 is pertinent to the higher-reactivity unborated case.

4.7.2   Dropped Fuel Assembly

For a drop on top of the rack, the fuel assembly will come to rest horizontally on top of the rack with a minimum separation distance from the fuel in the rack of more than 12 inches which is sufficient to preclude neutron coupling. Maximum calculated deformation under seismic or accident conditions (<1 inch) will not reduce the minimum spacing (~19 inches) between the dropped assembly and the stored fuel assemblies to less than 12 inches. Consequently, fuel assembly drop accidents will not result in a significant

increase in reactivity (<0.0001 δk) due to the separation distance. Furthermore, soluble boron in the pool water would substantially reduce the reactivity and assure that the true reactivity is always less than the limiting value for any conceivable dropped fuel accident.

4.7.3   Lateral Rack Movement

Lateral motion of the rack modules under seismic conditions could potentially alter the spacing between rack modules. However, the maximum rack movement has been determined to be less than 0.35 inches under the design basis seismic event (See Table 6.6, Section 6). In Region I, the water gap between rack modules (north - south direction) is nominally 1 $^5/_8$ inches, which, if reduced by 0.35 inches, would be only slightly smaller (1.275") than the corresponding design water-gap spacing (1.371") internal to the rack modules. To compensate, an estimated allowance of 0.0020 δk has been included as an additive term in the criticality analysis (Table 4.1) in determining the maximum reactivity. Region II storage cells do not use a flux-trap and the reactivity is therefore insensitive to the spacing between modules. The spacing between Region I and Region II modules is sufficiently large to preclude adverse interaction even with the maximum seismically-induced reduction in spacing. Furthermore, soluble poison would assure that a reactivity less than the design limitation is maintained under all accident or abnormal conditions.

4.7.4   Abnormal Location of a Fuel Assembly

The abnormal location of a fresh unirradiated fuel assembly of 5.0 wt% enrichment could, in the absence of soluble poison, result in exceeding the design reactivity limitation (k_∞ of 0.95). This could occur if a fresh fuel assembly of the

4 - 26

highest permissible enrichment were to be either positioned
outside and adjacent to a storage rack module or inadvertently
loaded into a Region II storage cell, with the latter condition
producing the larger positive reactivity increment. Although
criticality would not be attained even in the absence of
soluble poison (maximum k_∞ of 0.978, including uncertainties),
soluble boron actually present in the spent fuel pool water,
for which credit is permitted under these conditions, would
assure that the reactivity is maintained substantially less
than the design limitation. Calculations show that a soluble
poison concentration of 350 ppm boron is sufficient to maintain
a k_∞ less than 0.946 (including uncertainties) under the
maximum postulated accident condition.

4.8 EXISTING SPENT FUEL ASSEMBLIES

Of the 604 fuel assemblies now in storage, 595 are acceptable for unrestricted storage in Region II of the racks. Nine (9) assemblies fall below the acceptable burnup line and these assemblies, listed in Table 4.8, require storage in Region I or in a specially designated area of Region II. Figure 4.4 reproduces the minimum acceptable burnup curve (Figure 4.1) with the burnup ranges of existing spent fuel superimposed. The data points in the acceptable domain indicate ranges of burnups in the various batches of fuel. These data are also shown in Table 4.9.

Of the 9 assemblies with burnups unacceptable for unrestricted storage in Region II, 8 have burnups very close to the acceptable limit. These 8 assemblies (all except assembly F-65 in Table 4.8) may be safely stored in the outer peripheral cells of Region II facing non-fueled areas where the locally high neutron leakage compensates for the slightly higher reactivity of these assemblies. These high-leakage cells are the outer north, west and south boundaries of the storage rack facing the pool walls or the cask pit area. Calculations (diffusion theory with CASMO-2E generated constants) confirm that this configuration results in a negligible increase in reactivity (<0.0002 δk) above the reference design value.

Calculations were also made for various initial enrichments to define the minimum burnup for acceptable storage of fuel in the peripheral or boundary cells. These burnup values define the dashed curve in Figure 4.1 as the acceptable

4 - 28

domain for storage of fuel in these peripheral cells. These
data have been fitted to a polynomial expression as follows:

$$\boxed{\begin{array}{c} \text{For Peripheral Cells in Region II} \\[2mm] \text{Minimum Burnup in MWD/MTU} = \\[2mm] -35{,}760 + 23{,}020\,E - 2{,}712\,E^2 + 197.1\,E^3 \\[2mm] \text{(for initial enrichments up to 5 wt\% U-235)} \end{array}}$$

One assembly (No. F-65) was prematurely discharged
and, solely on the basis of the criteria described above, would
not be acceptable for storage in either the unrestricted or
peripheral areas of Region II. This assembly, however, may be
safely stored in one of the four outside corner cells facing
two non-fueled areas. In this case, leakage in two directions
is more than adequate to maintain the reactivity below the
acceptable limit with F-65 present in the corner cell (con-
firmed by 2-dimensional PDQ07 calculations). Assembly F-65
could also be safely stored in the unrestricted area of Region
II (provided only that it be stored well away from any periphe-
ral cells) with only a small local increase in the maximum k_∞
from 0.9408 to 0.9417, which would still be well below the
acceptable limit.

4.9 REFERENCES

1. S. E. Turner, "Irradiation Study of Boraflex Neutron Absorber Material, Interim Test Data", Brand Industrial Services, Inc., Park Ridge, Il., NS-1-050, Rev 1, November 25, 1987

2. A. Ahlin, M. Edenius, H. Haggblom, "CASMO - A Fuel Assembly Burnup Program," AE-RF-76-4158, Studsvik report (proprietary).

   A. Ahlin and M. Edenius, "CASMO - A Fast Transport Theory Depletion Code for LWR Analysis," ANS Transactions, Vol. 26, p. 604, 1977.

   M. Edenius et al., "CASMO Benchmark Report," Studsvik/ RF-78-6293, Aktiebolaget Atomenergi, March 1978.

3. Green, Lucious, Petrie, Ford, White, Wright, "PSR-63/AMPX-1 (code package), AMPX Modular Code System for Generating Coupled Multigroup Neutron-Gamma Libraries from ENDF/B," ORNL-TM-3706, Oak Ridge National Laboratory, March 1976.

4. R.M. Westfall et al., "SCALE: A Modular Code System for performing Standardized Computer Analyses for Licensing Evaluation," NUREG/CR-0200, 1979.

5. W.A. Wittkopf, et. al., "NULIF - Neutron Spectrum Generator, Few-Group Constant Calculator, and Fuel Depletion Code", Babcock & Wilcox Co., BAW 426, Rev. 11, July 1988.

6. W.R. Cadwell, PDQ07 Reference Manual, WAPD-TM-678, Bettis Atomic Power Laboratory, January 1967.

7. E.E. Pilat, "Methods for the Analysis of Boiling Water Reactors (Lattice Physics)," YAEC-1232, Yankee Atomic Electric Co., December 1980.

REFERENCES (Continued)

8.   E. Johansson, "Reactor Physics Calculations on Close-Packed Pressurized Water Reactor Lattices," <u>Nuclear Technology</u>, Vol. 68, pp. 263-268, February 1985.

9.   H. Richings, Some Notes on PWR (<u>W</u>) Power Distribution Probabilities for LOCA Probabilistic Analyses, NRC Memorandum to P.S. Check, dated July 5, 1977.

10. S. E. Turner, "Uncertainty Analysis - Burnup Distributions", presented at the DOE/SANDIA Technical Meeting on Fuel Burnup Credit, Special Session, ANS/ENS Conference, Washington, D.C.,November 2, 1988

11. M.G. Natrella, Experimental Statistics National Bureau of Standards, Handbook 91, August 1963.

Table 4.1

SUMMARY OF CRITICALITY SAFETY ANALYSES

	Region I	Region II
Design Basis burnup at 5.0% initial enrichment	0	40,900 MWD/MTU
Temperature for analysis	20°C (68°F)	20°C (68°F)
Reference k_∞ (CASMO-2E) (Includes 2½% width shrinkage of the Boraflex)	0.9310	0.9100
Calculational bias, δk	0.0013	0.0013
Uncertainties		
Bias	± 0.0018	± 0.0018
B-10 concentration	± 0.0025	± 0.0038
Boraflex thickness	± 0.0034	± 0.0046
Boraflex width	± 0.0015	± 0.0012
Inner box dimension	± 0.0012	± 0.0012
Water gap thickness	± 0.0013	NA
SS thickness	± 0.0005	± 0.0001
Fuel enrichment	± 0.0016	± 0.0016[1]
Fuel density	± 0.0021	± 0.0021[1]
Eccentric position	± 0.0001	Negative
Statistical combination of uncertainties[2]	± 0.0058	± 0.0070
Allowance for Burnup Uncertainty	NA	+ 0.0205
Allowance for Module Interfaces	+0.0020	+ 0.0020
Total	0.9343 ± 0.0058	0.9338 ± 0.0070
Maximum Reactivity (k_∞)	0.9401	0.9408

[1] For fuel tolerances, uncertainties in Region II assumed to be the same as those for Region I.
[2] Square root of sum of squares.

Table 4.2

REACTIVITY EFFECTS OF ABNORMAL AND ACCIDENT CONDITIONS

Accident/Abnormal Conditions	Reactivity Effect
Temperature increase (above 68°F)	Negative (Table 4.7)
Void (boiling)	Negative (Table 4.7)
Assembly dropped on top of rack	Negligible (<0.0001 δk)
Lateral rack module movement	Negligible (<0.0001 δk)
Misplacement of a fuel assembly	Positive (0.037 Max δk)

Table 4.3
DESIGN BASIS FUEL ASSEMBLY SPECIFICATIONS

FUEL ROD DATA

Outside diameter, in.	0.422
Cladding thickness, in.	0.0243
Cladding inside diameter, in.	0.3734
Cladding material	Zr-4
Pellet density, % T.D.	95
Pellet diameter, in.	0.3659
Maximum enrichment, wt % U-235	5.00 ± 0.05
Maximum stack density, g UO_2/cc	10.31 ± 0.21

FUEL ASSEMBLY DATA

Fuel rod array	15x15
Number of fuel rods	204
Fuel rod pitch, in.	0.563
Number of control rod guide and instrument thimbles	21
Thimble O.D., in. (nominal)	0.546
Thimble I.D., in. (nominal)	0.512

Table 4.4

ALLOWANCE FOR UNCERTAINTIES IN REACTIVITY
DUE TO DEPLETION CALCULATIONS

Initial Enrichment	Design Burnup MWD/MTU	Uncertainty due to Burnup, δk	Design k_∞(1)	Total Reactivity Loss, δk (2)
1.764	0	0	0.9305	0
2.5	11,520	0.0058	0.9247	0.1115
3.0	18,000	0.0090	0.9215	0.1662
3.5	24,050	0.0120	0.9185	0.2094
4.0	29,870	0.0149	0.9156	0.2450
4.5	35,350	0.0177	0.9128	0.2752
5.0	40,900	0.0205	0.9100	0.3004

(1) The design k_∞ is determined by subtracting the burnup-dependent allowance for uncertainty (Column 3) from the design basis k_∞ (0.9305) for unburned fuel of 1.764% enrichment. With all uncertainties added (Table 4.1), the maximum k_∞ is 0.9408 in all cases.

(2) Total reactivity decrement, calculated for the cold, Xe-free condition in the fuel storage rack, from the beginning-of-life to the design burnup.

Table 4.5

LONG-TERM CHANGES IN REACTIVITY IN STORAGE RACK
CALCULATED BY CASMO-2E

Storage Time, years	δk from Shutdown (Xenon-free) at 5 wt% E and 40,000 MWD/MTU
0.5	-0.0008
1.0	-0.0075
10.0	-0.0216
20.0	-0.0389
30.0	-0.0495

Table 4.6

FUEL BURNUP VALUES FOR REQUIRED REACTIVITIES (k_∞) WITH FUEL OF VARIOUS INITIAL ENRICHMENTS

Calculated Initial Enrichment	Uncertainty [1] in Burnup, δk	Design Limit k_∞	Burnup limit MWD/MTU [2]	
1.764	0	0.9305	0.	(60)
2.5	0.0058	0.9248	11,520	(11,460)
3.0	0.0090	0.9216	18,000	(18,130)
3.5	0.0120	0.9186	24,050	(24,190)
4.0	0.0149	0.9157	29,870	(29,870)
4.5	0.0177	0.9129	35,350	(35,390)
5.0	0.0205	0.9100	40,900	(41,000)

[1] See Section 4.4.2
[2] Parenthetical values are calculated from the polynomial fit for unrestricted storage in Region II.

Table 4.7

EFFECT OF TEMPERATURE AND VOID ON CALCULATED REACTIVITY OF STORAGE RACK

Case	Incremental Reactivity Change, δk	
	Region I	Region II
20°C (68°F)	Reference	Reference
40°C (104°F)	-0.003	-0.002
60°C (140°F)	-0.007	-0.005
90°C (194°F)	-0.014	-0.010
120°C (248°F)	-0.022	-0.016
120°C (248°F) + 20% void	-0.087	-0.061

Table 4.8

EXISTING SPENT FUEL ASSEMBLIES
WITH LOW DISCHARGE BURNUPS

| Fuel Assembly | Initial Enrichment | Burnup, MWD/MTU | Acceptable Burnup* | |
			Unrestricted	Periphery
E-56	3.195	19,190	20,650	16,530
E-15	3.195	19,200	20,650	16,530
F-65	3.346	12,030	22,370	18,285
F-36	3.346	19,770	22,370	18,285
F-21	3.346	19,900	22,370	18,285
F-61	3.346	20,690	22,370	18,285
F-01	3.346	21,090	22,370	18,285
F-50	3.350	19,650	22,420	18,330
F-40	3.459	19,990	23,700	19,575

* Calculated from the polynomial fits to the limiting burnup for unrestricted storage and for storage in the peripheral cells. In the vicinity of 20,000 MWD/MTU , the reactivity worth of burnup is 0.008 δk per 1000 MWD/MTU.

4 - 39

Table 4.9

STORAGE OF EXISTING SPENT FUEL ASSEMBLIES
IN THE ACCEPTABLE BURNUP DOMAIN

Fuel ID	No. Assem.	Initial Enrichment	Burnup Range, MWD/MTU Lowest	Highest	Acceptable Burnup*
A	65	2.212	15,040	18,620	7255
B	64	2.804	18,610	35,970	15,600
D	68	3.105	24,720	39,480	19,445
D	4	3.112	35,190	39,070	19,530
E	58	3.195	24,250	41,810	20,550
G	1	3.200	34,270	34,270	20,615
H	56	3.210	29,000	43,200	20,735
G	62	3.289	29,890	41,380	21,690
G	9	3.290	33,250	39,960	21,705
C	64	3.307	28,340	37,300	21,905
F	61	3.346	22,700	37,590	22,375
J	68	3.436-3.447	30,690	42,143	23,570
K	15	3.188-3.208	29,366	30,303	20,710

* Calculated from the polynomial fit to the limiting burnup for unrestricted storage, rounded to nearest 5 MWD/MTU
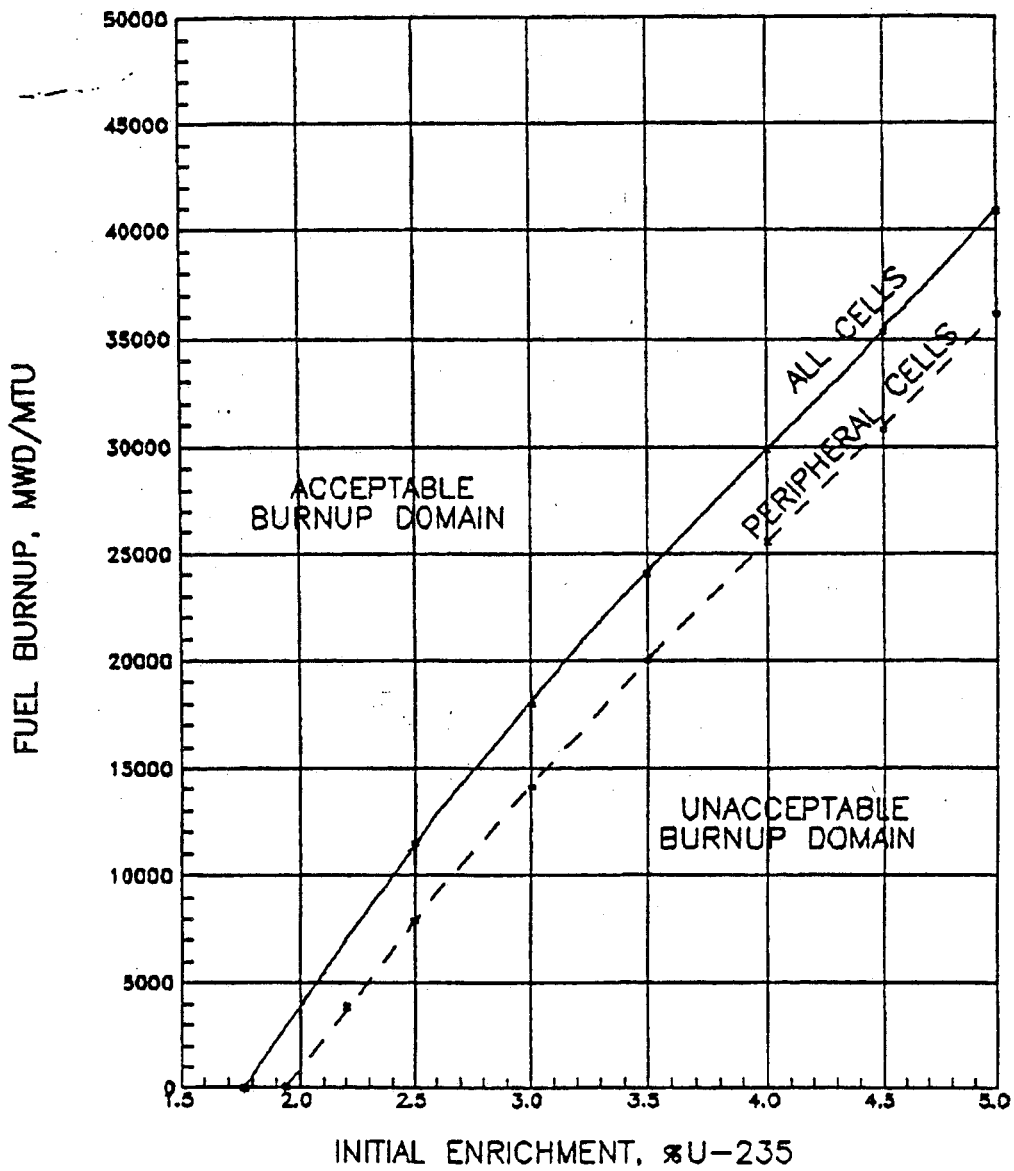
Fig. 4.1   ACCEPTABLE BURNUP DOMAIN IN REGION II
FOR FUEL OF VARIOUS INITIAL ENRICHMENTS

7.500" ± 0.063" BORAFLEX
IN 0.1137" ± 0.0035" GAP
0.1022" ± 0.007" THK 0.0323 g B-10/cm^2

0.075" ANGLE

FUEL OD   0.3659 IN.
DENSITY   10.31 g/cc
NUMBER   204 (15 X 15)
CLAD ID   0.3734 IN.
ROD OD   0.422 IN.
PITCH   0.563 IN.

THIMBLES OD   0.546 IN.
          ID   0.512 IN.
          NO. 21

0.0235" ± 0.003" SS SHEATHING

0.2122"

WATER GAP
1.591 ± 0.016" E-W
1.371 ± 0.016" N-S

8.75 ± 0.03" BOX I.D.

0.075" ± 0.005" SS BOX

10.765 ± 0.035" E-W DIRECTION
10.545 ± 0.035" N-S DIRECTION

NOT TO SCALE
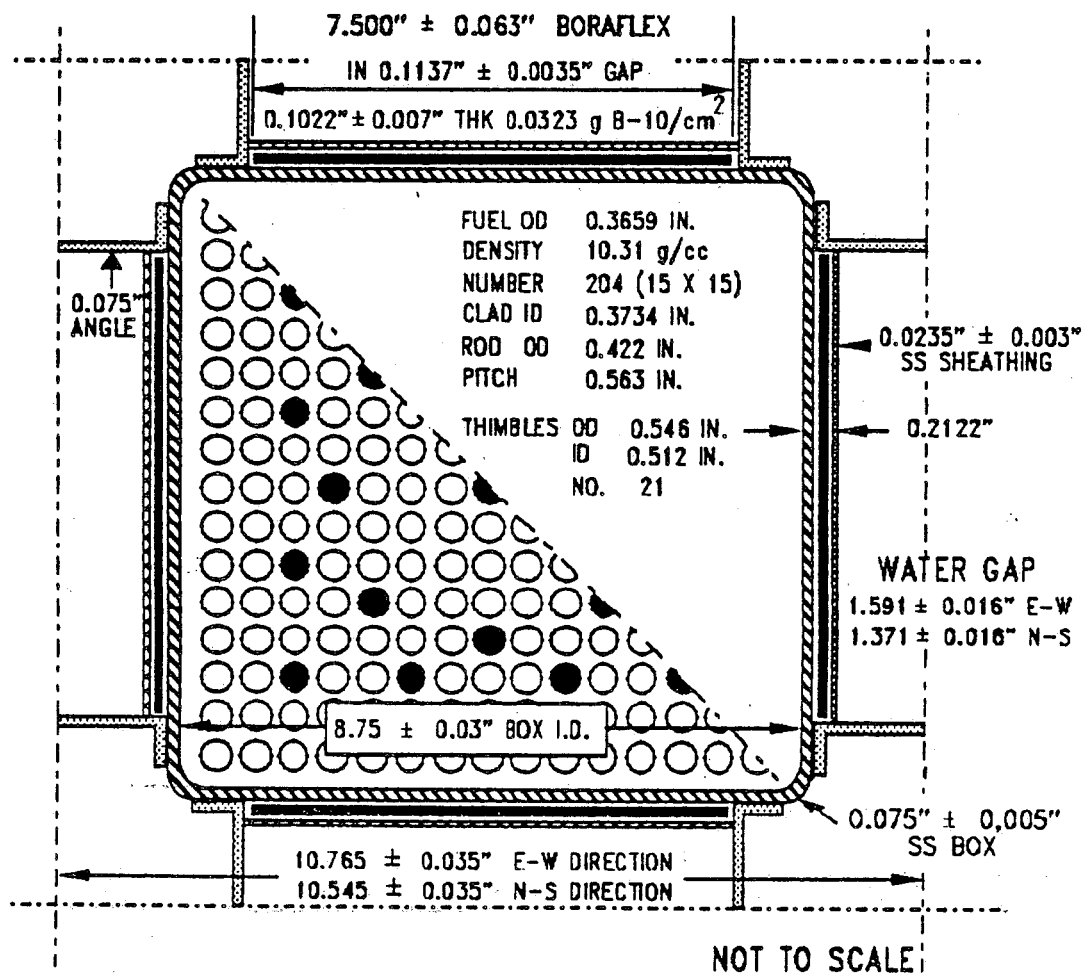
Fig. 4.2 CROSSECTION OF REGION I STORAGE CELL

4 - 42

7.500" ± 0.063" BORAFLEX
IN 0.0935" ± 0.0035" GAP

0.082" ± 0.007" THK   0.0260 g B-10/cm^2

FUEL OD   0.3659 IN.
DENSITY   10.31 g/cc
NUMBER   204 (15 X 15)
CLAD ID   0.3734 IN.
ROD OD   0.422 IN.
PITCH   0.563 IN.

THIMBLES OD   0.546 IN.
         ID   0.512 IN.
         NO. 21

0.2035"

8.80 ± 0.03" BOX I.D.

0.036" ± 0.002"
SHEATHING

NOT TO SCALE

0.075" ± 0.005"
SS BOX

LATTICE SPACING
9.04 ± 0.05"
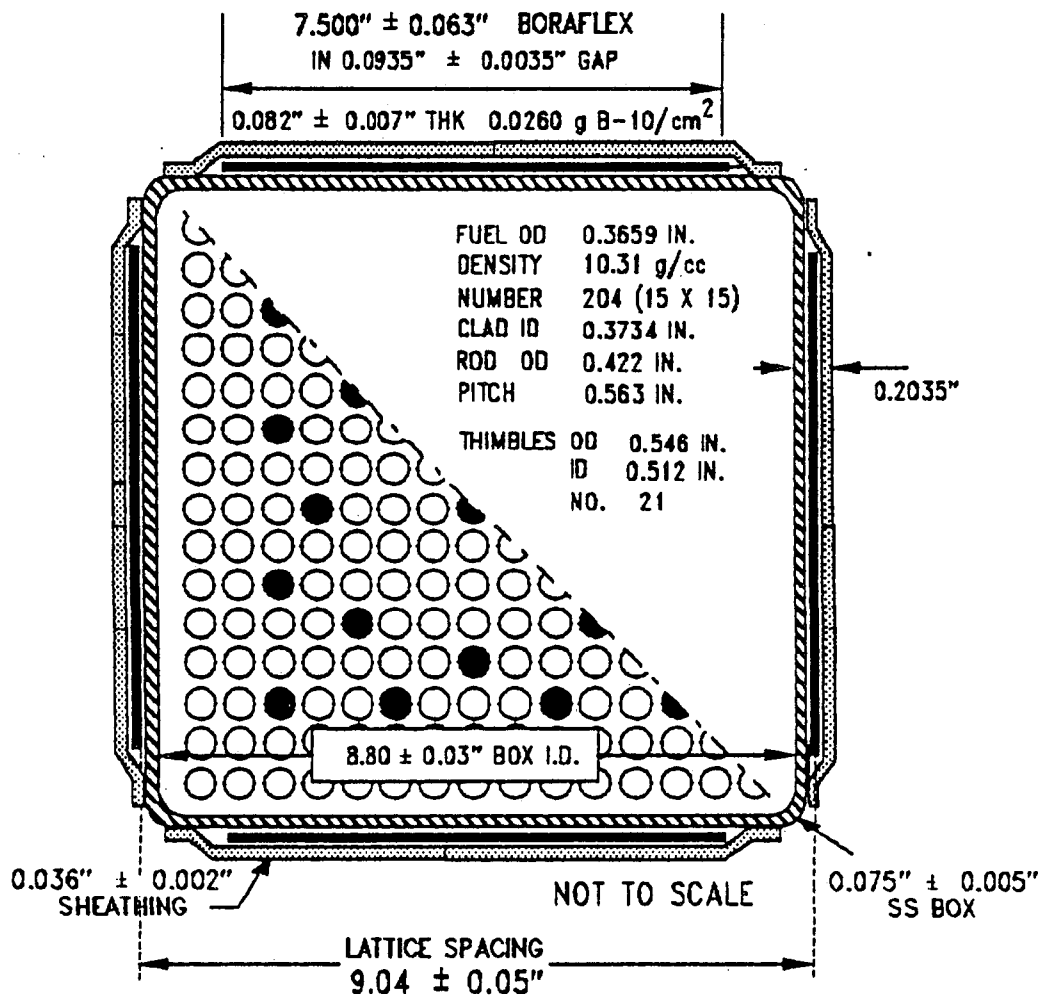
Fig. 4.3 CROSSECTION OF REGION II STORAGE CELL

4 - 43

⊙ : Range of fuel now in storage

⊕ : Acceptable for storage in corner cell

+ : Assemblies acceptable for storage in peripheral cells
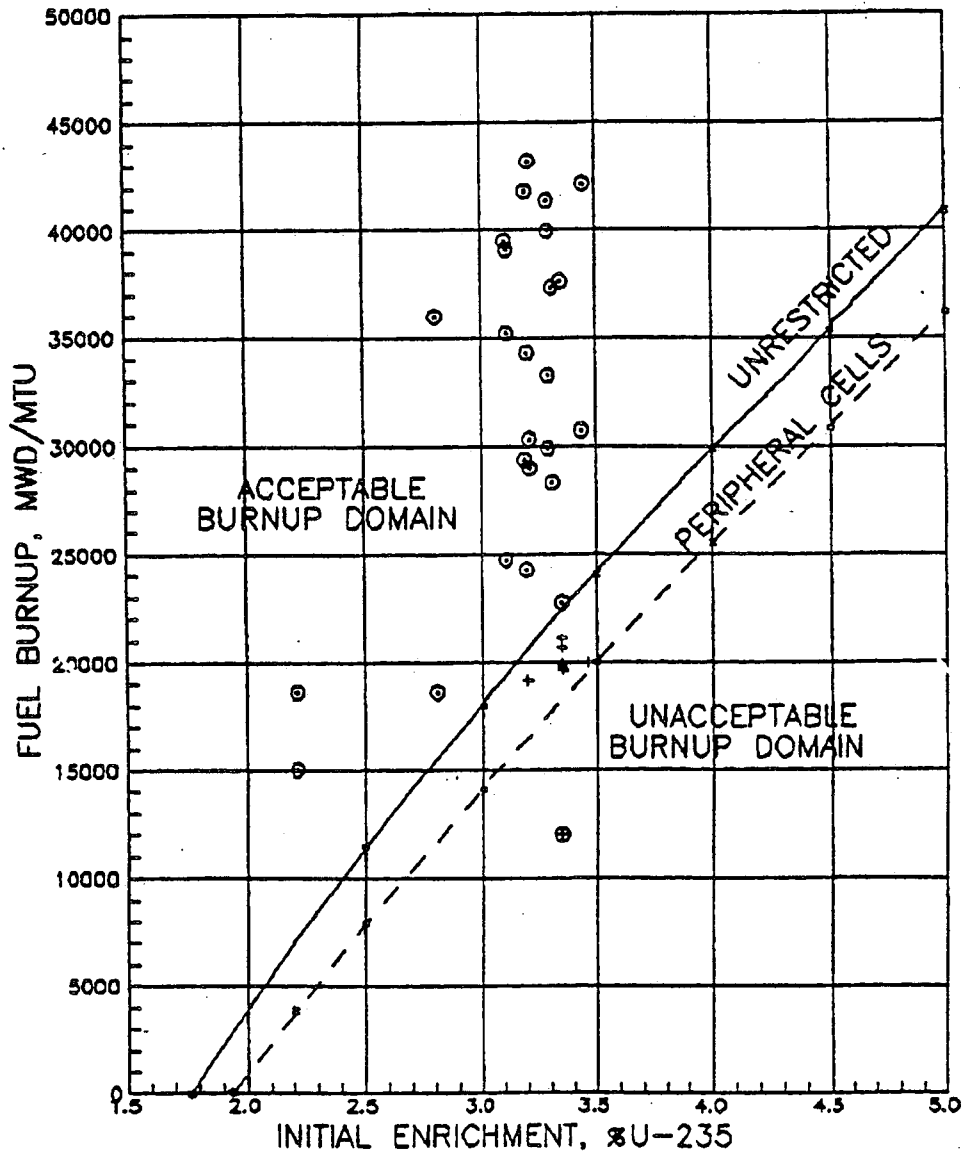
Fig. 4.4   ACCEPTABLE BURNUP DOMAIN IN REGION II
SHOWING EXISTING SPENT FUEL ASSEMBLIES

APPENDIX 4A

BENCHMARK CALCULATIONS

1.0 <u>INTRODUCTION AND SUMMARY</u>

The objective of this benchmarking study is to verify both the AMPX (NITAWL)-KENO IV (Refs. 1 and 2) methodology with the 27-group SCALE cross-section library (Ref. 3 and 4) and the CASMO-2E code (refs. 5,6,7, and 8) for use in criticality safety calculations of high density spent fuel storage racks. Both calculational methods are based upon transport theory and have been benchmarked against critical experiments that simulate typical spent fuel storage rack designs as realistically as possible. Results of these benchmark calculations with both methodologies are consistent with corresponding calculations reported in the literature.

Results of these benchmark calculations show that the 27-group (SCALE) AMPX-KENO calculations consistently under-predict the critical eigenvalue by 0.0106 ± 0.0048 δk (with a 95% probability at a 95% confidence level) for critical experiments (Ref. 9) selected to be representative of realistic spent fuel storage rack configurations and poison worths. Similar calculations by Westinghouse (Ref. 11) suggest a bias of 0.0120 ± 0.0023, and the results of ORNL analyses of 54 relatively "clean" critical experiments (Ref. 12) show a bias of 0.0100 ± 0.0013.

Similar calculations with CASMO-2E for clean critical experiments resulted in a bias of 0.0013 with an uncertainty of ± 0.0018 (95%/95%). CASMO-2E and AMPX-KENO intercomparison calculations of infinite arrays of poisoned cell configurations show very good agreement and suggest that a bias of 0.0013 ± 0.0018 is the reasonably expected bias and uncertainty for CASMO-2E calculations.

The benchmark calculations reported here indicate that either the 27-group (SCALE) AMPX-KENO or CASMO-2E calculations are acceptable for criticality analysis of high-density spent fuel storage racks. Reference calculations for the rack designs should be performed with both code packages to provide independent verification.

Analysis of a series of Babcock & Wilcox critical experiments (Ref. 9), which include some with absorber panels typical of a poisoned spent fuel rack, is summarized in Table 1, as calculated with AMPX-KENO using the 27-group SCALE cross-section library and the Nordheim resonance integral treatment in NITAWL. The mean for these calculations is 0.9894 ± 0.0019, conservatively assuming the larger standard deviation calculated from the k_{eff} values. With a one-sided tolerance factor corresponding to 95% probability at a 95% confidence level (Ref. 10), the calculational bias is + 0.0106 with an uncertainty of ± 0.0048.

Similar calculational deviations reported by Westinghouse (Ref. 11) are also shown in Table 1 and suggest a bias of 0.0120 ± 0.0023 (95%/95%). In addition, ORNL (Ref. 12) has analyzed some 54 critical experiments using the same methodology, obtaining a mean bias of 0.0100 ± 0.0013 (95%/95%). These published results are in good agreement with the results obtained in the present analysis and lend further credence to the validity of the 27-group AMPX-KENO calculational model for use in criticality analysis of high density spent fuel storage racks. Variance analysis of the data in Table 1 suggest the possibility that an unknown factor may be causing a slightly larger variance than might be expected from Monte Carlo statistics alone. However, such a factor, if one truly exists, is too small to be resolved on the basis of the critical experiment data presently available. No trends in k_{eff} with intra-assembly water gap, with absorber panel reactivity worth, or with poison concentration were identified.[*]

---

[*]Significantly large trends in k_{eff} with water gap and with absorber panel reactivity worth have been reported[8] for AMPX-KENO calculations with the 123-group GAM-THERMOS library.

3. CASMO-2E BENCHMARK CALCULATIONS

3.1 GENERAL

The CASMO-2E code is a multigroup transport theory code utilizing transmission probabilities to accomplish two-dimensional calculations of reactivity and depletion for BWR and PWR fuel assemblies. As such, CASMO-2E is well-suited to the criticality analysis of spent fuel storage racks, since general practice is to treat the racks as an infinite medium of storage cells, neglecting leakage effects.

CASMO-2E is closely analogous to the EPRI-CPM code (ref. 13) and has been extensively benchmarked against hot and cold critical experiments by Studsvik Energiteknik (Refs. 5, 6, 7 and 8). Reported analyses of 26 critical experiments indicate a mean k_{eff} of 1.0000 ± 0.0037 (1σ). Yankee Atomic (Ref. 14) has also reported results of extensive benchmark calculations with CASMO-2E. Their analyses of 54 Strawbridge and Barry critical experiments (Ref. 15) using the reported bucklings indicate a mean of 0.9987 ± 0.0009 (1σ), or a bias of 0.0013 ± 0.0018 (with 95% probability at a 95% confidence level). Calculations were repeated for seven of the Strawbridge and Barry experiments selected at random, yielding a mean k_{eff} of 0.9987 ± 0.0021 (1σ), thereby confirming that the cross-section library and analytical methodology being used for the present calculations are the same as those used in the Yankee analyses. Thus, the expected bias for CASMO-2E in the analysis of "clean" critical experiments is 0.0013 ± 0.0018 (95%/95%).

3.2 BENCHMARK CALCULATIONS

CASMO-2E benchmark calculations have also been made for the B&W series of critical experiments with absorber panels simulating high density spent fuel storage racks. However, CASMO-2E, as an assembly code, cannot directly represent an entire core configuration* without introducing uncertainty due to reflector constants and the appropriateness of their spectral weighting. For this reason, the poisoned cell configurations of the central assembly, as calculated by CASMO-2E, were benchmarked against corresponding calculations with the 27-group (SCALE) AMPX-KENO IV code package. Results of this comparison are shown in Table 2. Since the differences are well within the normal KENO statistical variation, these calculations confirm the validity of CASMO-2E calculations for the typical high density poisoned spent fuel rack configurations. The differences shown in Table 2 are also consistent with a bias of 0.0013 ± 0.0018, determined in Section 3.1 as the expected bias and uncertainty of CASMO-2E calculations.

---

*Yankee has attempted such calculations[10] using CASMO-2E generated constants in a two-dimensional, four-group PDQ model, obtaining a mean k_{eff} of 1.005 for 11 poisoned cases and 1.009 for 5 unpoisoned cases. Thus, Yankee benchmark calculations suggest that CASMO-2E tends to slightly overpredict reactivity.

REFERENCES TO APPENDIX A

1. Green, Lucious, Petrie, Ford, White, and Wright, "PSR-63-/AMPX-1 (code package) AMPX Modular Code System For Generating Coupled Multigroup Neutron-GAmma Libraries from ENDF/B", ORNL-TM-3706, Oak Ridge National Laboratory, November 1975.

2. L.M. Petrie and N.F. Cross, "Keno-IV. An Improved Monte Carlo Criticality Program", ORNL-4938, Oak Ridge National Laboratory, November 1975.

3. R.M. Westfall et. al., "SCALE: A Modular System for Performing Standardized Computer Analysis for Licensing Evaluation", NUREG/CR-0200, 1979.

4. W. E. Ford, III, et al., "A 218-Neutron Group Master Cross-section Library for Criticality Safety Studies", ORNL/TM-4, 1976

5. A. Ahlin, M. Edenius, and H. Haggblom, "CASMO - A Fuel Assembly Burnup Program", AE-RF-76-4158, Studsvik report.

6. A. Ahlin and M. Edenius, "CASMO - A Fast Transport Theory Depletion Code for LWR Analysis", ANS Transactions, Vol. 26, p. 604, 1977.

7. M. Edenius et al., "CASMO Benchmark Report", Studsvik/RF-78/6293, Aktiebolaget Atomenergi, March 1978

8. "CASMO-2E Nuclear Fuel Assembly Analysis, Applications Users Manual", Rev. A, Control Data Corporation, 1982

9. M.N. Baldwin et al., "Critical Experiments Supporting Close Proximity Water Storage of Power Reactor Fuel", BAW-1484-7, The Babcock & Wilcox Co., July 1979.

10. M.G. Natrella, Experimental Statistics, National Bureau of Standards, Handbook 91, August 1963.

11. B.F. Cooney et al., "Comparisons of Experiments and Calculations for LWR Storage Geometries", Westinghouse NES, ANS Transactions, Vol. 39, p. 531, November 1981.

REFERENCES TO APPENDIX A (Continued)

12. R.W. Westfall and J. h. Knight, "SCALE System Cross-section Validation with Shipping-cask Critical Experiments", _ANS Transactions_, Vol. 33, p. 368, November 1979

13. "The EPRI-CPM Data Library", _ARMP Computer Code Manuals_, Part II, Chapter 4, CCM3, Electric Power Research Institute, November 1975

14. E.E. Pilat, "Methods for the Analysis of Boiling Water Reactors (Lattice Physics), YAEC-1232, Yankee Atomic Electric Co., December 1980.

15. L.E. Strawbridge and R.F. Barry, "Criticality Calculations for Uniform, Water-moderated Lattices", _Nuclear Science and Engineering_, Vol. 23, p. 58. September 1965.

16. S.E. Turner and M.K. Gurley, "Evaluation of AMPX-KENO Benchmark Calculations for High Density Spent Fuel Storage Racks", _Nuclear Science and Engineering_, 80(2):230-237, February 1982.

Table 1

RESULTS OF 27-GROUP (SCALE) AMPX-KENO IV CALCULATIONS
OF B&W CRITICAL EXPERIMENTS

Experiment Number	Calculated k_{eff}	σ	Westinghouse $\delta\ k_{eff}$
I	0.9889	± 0.0049	-0.008
II	1.0040	± 0.0037	-0.012
III	0.9985	± 0.0046	-0.008
IX	0.9924	± 0.0046	-0.016
X	0.9907	± 0.0039	-0.008
XI	0.9989	± 0.0044	-0.002
XII	0.9932	± 0.0046	-0.013
XIII	0.9890	± 0.0054	-0.007
XIV	0.9830	± 0.0038	-0.013
XV	0.9852	± 0.0044	-0.016
XVI	0.9875	± 0.0042	-0.015
XVII	0.9811	± 0.0041	-0.015
XVIII	0.9784	± 0.0050	-0.015
XIX	0.9888	± 0.0033	-0.016
XX	0.9922	± 0.0048	-0.011
XXI	0.9783	± 0.0039	-0.017
Mean	0.9894	± 0.0011[1]	-0.0120 ± 0.0010
Bias	0.0106	± 0.0019[2]	0.0120 ± 0.0010
Bias (95%/95%)	0.0106	± 0.0048	0.0120 ± 0.0023

[1] Calculated from individual standard deviations.
[2] Calculated from k_{eff} values and used as reference.

Table 2

RESULTS OF CASMO-2E BENCHMARK (INTERCOMPARISON) CALCULATIONS

B&W Experiment[1]	k_∞[1] AMPX-KENO IV[2]	CASMO-2E	δk
XIX	1.1203 ± 0.0032	1.1193	0.0010
XVII	1.1149 ± 0.0039	1.1129	0.0020
XV	1.1059 ± 0.0038	1.1052	0.0007
Interpolated[3]	1.1024 ± 0.0042	1.1011	0.0013
XIV	1.0983 ± 0.0041	1.0979	0.0004
XIII	1.0992 ± 0.0034	1.0979	0.0013
Mean	± 0.0038		0.0011
Uncertainty			± 0.0006
Typical BWR fuel rack	0.9212 ± 0.0027	0.9218	− 0.0006

[1] Infinite array of central assemblies of the 9-assembly V&W critical configuration (Ref. 9).

[2] k_∞ from AMPX-KENO corrected for bias of 0.0106 δk.

[3] Interpolated from Fig. 28 of Ref. 9 for soluble boron concentration at the critical condition.

5.0　THERMAL-HYDRAULIC CONSIDERATIONS

5.1　ANALYSES FOR THE SPENT FUEL POOL (Bulk)

The purpose of the bulk fuel pool thermal-hydraulic analyses is to demonstrate the adequacy of the existing spent fuel pool cooling system for utilization of the increased number of storage cells.

5.1.1　Spent Fuel Pool Cooling System Design

The spent fuel pool cooling system consists of two pumps (main and standby), a heat exchanger, a filter, a demineralizer, piping and associated valves and instrumentation. The operating pump draws water from the pool, circulates it through the heat exchanger and returns it to the pool.

The spent fuel pool heat exchanger is of the shell and U-tube type with the tubes welded to the tubesheet. Component cooling water circulates through the shell, and spent fuel pool water circulates through the tubes. The tubes are austenitic stainless steel and the shell is carbon steel.

The clarity and purity of the spent fuel pool water are maintained by using a second pumping system to pass approximately 5 percent of the cooling system flow through a filter and demineralizer. The spent fuel pool pump suction line, which is used to draw water from the pool, penetrates the spent fuel pool wall above the fuel assemblies. The penetration location prevents fuel uncovery as a result of a possible suction line rupture.

The primary source of makeup water to the spent fuel pool is the Primary Water Storage Tank, which is a seismic Class I component. The pumps and most of the piping associated with this tank are also seismic Class I. The makeup water to the spent fuel pool is seismic Class II, as is the spent fuel pool cooling and cleanup loop. Additional backup can be provided through a temporary connection from the Fire Protection System.

In addition to the second spent fuel pool cooling system pump to provide standby pool cooling capacity, there is also a provision for adding a portable cooling pump.

5.1.2   Basis

Fuel storage racks have been designed to increase the present fuel storage capacity of the Indian Point 2 spent fuel storage pool to a total of 1376 assemblies.

The Indian Point 2 reactor is currently licensed for a core power level of 2758 megawatts thermal (MWt). A proposed increase to 3071.4 MWt has been submitted to the NRC (Ref. 1). The thermal hydraulic analyses for the replacement fuel storage racks have been done for the proposed core power level of 3071.4 MWt.

The heat sink for the spent fuel pool is the component cooling water system. The ultimate heat sink for the component cooling water system is the river water. It is expected that, for a short duration during the summer months, a maximum of approximately 95°F river water temperature may be experienced at

Indian Point 2. This time of year is the least likely period for Indian Point 2 to be shutdown for refueling due to peak power requirements in the Consolidated Edison system. In order to account for the variations in river water temperature, analyses have been done for the spent fuel pool over a range of river water temperatures to a maximum of 95^0F. These analyses include the lower river water temperature more likely to be seen at the preferred times during a year for refueling IP2. These analyses have been done for the full core discharge case. In addition, limited analysis has been done for the refueling load case in accordance with SRP 9.1.3 section III.1.h[3]. The results are presented as a curve of river water temperature versus discharge time. Discharge time is defined as the period of time from reactor shutdown to movement of fuel asssemblies from the core to the spent fuel pool.

The maximum heat loads resulting from the expanded spent fuel storage capacity, have been calculated. The assumptions used are:

o   Refueling load discharge: 72 assemblies

o   Full core discharge: 193 assemblies

o   Power level of 3071.4 beginning in
     Cycle 10 (next cycle of operation)

o   24 month fuel cycles beginning in Cycle 11, 22
     months of operation at 90% capacity factor and 2
     months refueling outage

o   All fuel pool rack locations are filled at the end
     of full core discharge

5.1.3   Model Description

Decay heat generation is calculated according to Branch Technical Position ASB 9-2 (Ref. 2). For cooling times greater than 10^7 seconds an uncertainty factor of 0.1 is used, as recommended in Standard Review Plan 9.1.3 (Ref. 3). The computations and results reported here are based on the discharge taking place when the inventory of fuel in the pool will be at its maximum, resulting in an upper bound on the decay heat rate.

Having determined the decay heat generation rate, the time-dependent temperature of the pool water was evaluated. The initial pool temperature in these calculations is that value that balances energy removal and decay power, due to prior cycles spent fuel. Table 5-1 identifies the assumed heat transfer data for the Spent Fuel Pool Heat Exchanger at $180^0 F$ and $95^0 F$ for the spent fuel pool and river water respectively.

The energy removal calculations are based on the spent fuel pool and component cooling heat exchangers, with minimum flows and maximum heat loads. The major parameter affecting the energy removal capability is the river water temperature discussed above.

The thermal inertia is calculated based on the volume and heat capacity of the pool water but conservatively ignores the contained racks and fuel heat capacity, pool liner and concrete, piping and contained water external to the pool boundaries, and pool water in the transfer canal. A number of additional simplifying assumptions are made which render the analysis conservative, including:

o   Additions of fuel to the spent fuel pool at the end of the in-reactor cooldown period are assumed to occur instantaneously.

o   No credit is taken for heat loss by evaporation and natural convection of the pool water to the air.

o   No credit is taken for heat loss to pool walls and pool floor slab.

Following the above calculations, the increase of the bulk pool temperature as a function of time was determined assuming a complete loss of spent fuel cooling capability. Maximum bulk pool water temperature was assumed. The heatup rates and times to reach boiling temperature of 212^0F were based on complete mixing of the pool water.

5.1.4   Bulk Pool Temperature and Pool Heat-Up Results

The results of the analysis for variations in river water temperature are presented in Figure 5-1. This curve shows the required discharge time at different river water temperatures for the limiting case of a full core discharge, and is based on a maximum bulk pool temperature as follows:

Full Core Discharge Case: 180^0F

In addition, an analysis was done without credit for the pool thermal inertia for a refueling load and a full core discharge. This analysis used the same discharge schedule assumed in the prior full core discharge case. In all cases the maximized decay power, which is at the end of cycle, was used. For the full core discharge case in this analysis, one additional refueling load

with 36 days cooling time and 4 3/4 years operating time was added to the total pool heat load (this is consistent with SRP 9.1.3). The analysis results are as follows:

Refueling Load Discharge Case: 138.4^0F
Full Core Discharge Case: 205.2^0F

This calculation (for one refueling load and full core discharge consistent with SRP 9.1.3) was performed using similar or more conservative methods than those used in the full core discharge analysis leading to Figure 5-1. Namely, instantaneous discharge of the fuel and 5% heat exchanger plugging, as shown in Table 5.1. This calculation assumes the discharge times versus river water temperatures given in Figure 5-1. The discharge time for IP2 has been limited to a minimum of 174 hours as shown in Figure 5-1. The pool thermal inertia has been conservatively neglected in this calculation. In addition, this calculation was done for a maximum river water temperature of 95^0F, which correlates to a discharge time of approximately 393 hours as shown in Figure 5-1. The guidance in SRP 9.13 Section III.1.h, maximum bulk pool temperature of 140^0F for the refueling load case and no bulk pool boiling for the full core discharge case, has been met.

Based on the conservatisms in the Branch Technical Position ASB 9-2 decay heat methodology, the pool temperature modelling assumptions and the worst case extreme assumptions, these results are considered acceptable.

For the worst case assumptions, resulting pool heat-up rates, times until pool boiling begins, and resulting boil-off rates for a complete loss of pool cooling are as follows:

River Water Temperature	Pool Heat-Up Rate – ^{0}F/hr	Time Until Pool Boiling Begins, Hr	Pool Boil-Off Rate, gpm
95^0F or less	17.8	1.8 or more	62

These results and Figure 5-1 are based on a conservatively low value of the pool water mass ($2.05\% \times 10^6$ lbs) and no credit for the additional energy absorbing material.

The temperature and level indicators for the spent fuel pool would warn the operator of a loss of cooling. Thus, there is sufficient time to take any necessary action to provide adequate cooling and makeup while the cooling capability of the spent fuel pool cooling system is being restored.

The total increase in heat rejected to the environment through the cooling systems due to the increased spent fuel storage over the current rejected heat load is 1.48 MBTU/hr. This represents an increase of less than 0.03 percent of the total heat rejected to the environment during normal plant operation. This increase in rejected heat will have negligible impact on the environment.

5.2   ANALYSES FOR THE SPENT FUEL POOL (Localized)

The primary purpose of the localized thermal-hydraulic analysis is to determine the maximum fuel clad temperatures which may occur as a result of using the spent fuel racks in the Indian Point 2 spent fuel pool. In addition, maximum water temperatures

due to gamma heating of rack walls, poison material, and Region I flux traps are determined.

5.2.1   Criteria

The criteria used to determine the acceptability of the design from a thermal-hydraulic viewpoint are summarized as follows:

1. The design must allow adequate cooling by natural circulation and by flow provided by the spent fuel pool cooling system. The coolant should remain subcooled at all points within the pool.

2. the rack design must not allow trapped air or steam. Direct gamma heating of the storage cell walls must not result in boiling of the adjacent water or in the region of Boraflex.

5.2.2   Key Assumptions

o   A conservatively hot assembly is assumed based on a time after reactor shutdown of 174 hours and a peak to average radial assembly peaking factor of 1.3.

o   All decay energy is assumed to be absorbed in the fuel and surrounding coolant for the hot assembly natural circulation analysis.   In reality, some gamma radiation will be absorbed in the adjacent regions (stainless steel, Boraflex and within the flux trap region).

o   For the gamma heating of rack walls, poison, and the Region I flux traps, the decay heat absorbed is taken to be proportional to the mass fractions of the materials in the spent fuel pool. (In reality, most of the gamma radiation never leaves the fuel assembly due to strong uranium attenuation). Gamma heating proportional to the mass fraction is roughly equivalent to the assumption of uniform gamma flux in the repeating unit cell.

o   A circulation flow path between the rack and the wall is assumed for a row composed of the hottest assemblies. This derates the flow to the hottest assembly since there will also be flow down the other rack to wall clearances.

5.2.3   Description of Analytical Method and Calculations Performed

The adequacy of natural circulation flow throughout the fuel racks to cool the fuel assemblies was verified. The natural circulation flow was calculated by establishing a thermal-hydraulic balance for the highest power row of assemblies (9 assemblies) in a Region I rack module with the associated downcomer (adjacent to the row of hot assemblies). Coolant from the cask handling area and rack-to-rack gaps was conservatively neglected. All fuel assemblies were assumed to have been freshly discharged with a radial assembly peaking factor of 1.3. A maximum bulk pool temperature of 180^0F was assumed.

The calculation is a momentum (and energy) balance between the skin friction and form losses and the buoyancy due to heating of the fluid in the assemblies. In addition no energy deposition in the flux trap region is assumed for the assembly natural circulation calculation. The results show that the assembly fluid outlet condition is subcooled (below the local boiling point at the assembly outlet of 240.5^0F).

This analysis methodology is extremely conservative since flow through any and all downcomer regions (including the much lower power assemblies) is available subject to the

constraints of the momentum balance(s). However, in order to perform a simple analytic solution, this conservative model was used.

For the flux trap region, a natural circulation calculation was also performed which demonstrated that the fluid temperature remains below the local saturation temperature (as was the case for the assemblies).

The natural circulation analysis, discussed above, was solved analytically. In order to achieve this:

1)   The assembly power and pool temperature were used to obtain the assembly flow and outlet temperature and elevation (and frictional) pressure change.

2)   The pressure change (a boundary condition) was used to obtain the flow and outlet temperature in:

   a)   The fuel cell locations with the adjustable support legs, and

   b)   The flux trap regions

3)   The cell and flux trap region outlet temperatures and flows were used to obtain the Boraflex temperatures, including the effect of heat generation (gamma deposition) in the Boraflex and stainless steel.

The flow conditions in the assembly are laminar and the fuel surface temperature is about 10°F above the local cell outlet fluid temperature. The temperature variation from the surface to the fuel centerline will be small (the heat flux is on the order

of 1/300 of the normal operating conditions) and thus only a few degrees above the surface temperature. The void fraction in the assembly is zero (subcooled conditions prevail).

5.2.4   Gamma Heating of Rack Walls, Poison and Region I Flux Trap

The flux trap region is available to receive coolant via 2 one inch diameter holes at the bottom of the region. These holes allow a portion of the coolant entering two neighboring cells to flow into and up the flux trap region. The basic flow mechanism is identical to the fuel assembly calculations except that the pressure drop across this region is imposed by the analysis completed for the assemblies and coupled downcomer and pool floor-to-rack clearance (since the fraction of the power released in this region is small and the flow rate in this region is small).

The analysis has been done and shows that boiling does not occur in this region; the fluid remains subcooled. In addition, a heat transfer (laminar flow convection/conduction) calculation results in the maximum Boraflex region temperature-which is also subcooled.

5.3   <u>REFERENCES</u>

1.   Consolidated Edison letter to NRC dated September 30,
          1988, Application for License Amendment to Increase
          Authorized Power Level.

2.   NUREG-0800 U.S. Nuclear Regulatory Commission, Standard
          Review Plan, Branch Technical Position ASB 9-2, Rev. 2,
          July 1981.

3.   NUREG-0800 U.S., Nuclear Regulatory Commission, Standard
          Review Plan, Section 9.1.3, Spent Fuel Pool Cooling and
          Cleanup System Rev. 1, July 1981.

Table 5-1

Heat Transfer Data for the Spent Fuel Pool Heat Exchanger*

Type:	Shell and U-Tube
Tube Side (Spent Fuel Pool Water) Flow Rate, lb/hr:	1.1×10^6
Shell Side (Component Cooling Water) Flow Rate, lb/hr:	9.5×10^5
Heat Transfer Rate, Btu/hr:	26.79×10^6
Overall Heat Transfer Coefficient, Btu/hr/ft^2/^{0}F	300
Area Used, ft^2	0.95×2000**
Component Cooling Water Inlet Temperature, ^{0}F	104.28
Component Cooling Water Outlet Temperature, ^{0}F:	132.48
Spent Fuel Pool Water Inlet Temperature, ^{0}F:	180
Spent Fuel Pool Water Outlet Temperature, ^{0}F:	155.64

---

* For river water temperature of 95^{0}F and bulk pool temperature of 180^{0}F

** 5% tube plugging assumed

REQUIRED MINIMUM DISCHARGE TIME
versus
RIVER WATER TEMPERATURE

Basis: 180°F Bulk Pool Temperature
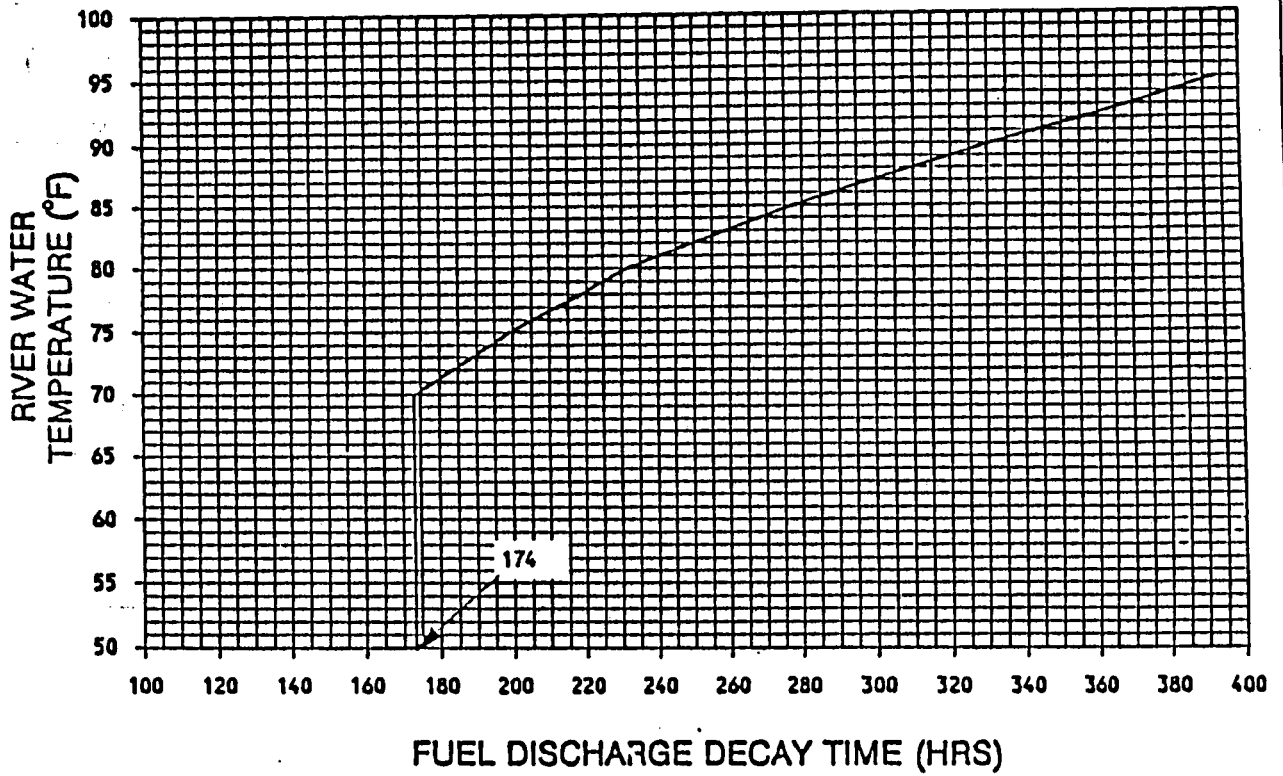
FIGURE 5-1

6.0   RACK STRUCTURAL CONSIDERATIONS

The purpose of this section is to demonstrate the structural adequacy of the Indian Point 2 spent fuel pool rack design under normal and accident loading conditions following the guidelines of the USNRC OT Position Paper. The method of analysis presented herein uses a time-history integration method similar to that previously used in the licensing reports on high density spent fuel racks for Fermi 2 (USNRC Docket No. 50-341), Quad Cities 1 and 2 (USNRC Docket Nos. 50-254 and 50-265), Rancho Seco (USNRC Docket No. 50-312), Grand Gulf Unit 1 (USNRC Docket No. 50-416), Oyster Creek (USNRC Docket No. 50-219), V.C. Summer (USNRC Docket No. 50-395), Diablo Canyon Units 1 and 2 (USNRC Docket Nos. 50-275 and 50-323), Millstone Unit 1 (Docket No. 50-245), Vogtle Unit 2 (Docket No. 50-425), and Kuosheng Nuclear Power Station of Taiwan Power Company. The results show that the high density spent fuel racks are structurally adequate to resist the postulated stress combinations associated with level A, B, C, and D conditions as defined in References 1 and 2.

6.1   ANALYSIS OUTLINE (FOR NEW PROPOSED RACK MODULES)

The spent fuel storage racks are Seismic Category I equipment. Thus, they are required to remain functional during and after a Safe Shutdown Earthquake (Ref. 3). As noted previously, these racks are neither anchored to the pool floor nor attached to the sidewalls. The individual rack modules are not

interconnected. Furthermore, a particular rack may be completely
loaded with fuel assemblies (which corresponds to the greatest
rack inertia), or it may be completely empty. The coefficient of
friction, μ, between the supports and pool floor is another
varying factor. According to Rabinowicz (Ref. 4), the results of
199 tests performed on austenitic stainless steel plates submerged
in water show a mean value of μ to be 0.503 with a standard
deviation of 0.125. The upper and lower bounds (based on twice
the standard deviation) are thus 0.753 and 0.253, respectively.
Two separate analyses are performed for single rack simulations
with values of the coefficient of friction equal to 0.2 (lower
limit) and 0.8 (upper limit), respectively. Analyses performed for
the geometrically limiting rack modules focus on limiting values
of the coefficient of friction, and the number of fuel assemblies
stored. In summary, the following analyses are performed for each
rack studied.

O   Fully loaded rack (all storage locations occupied),
     μ = 0.8; 0.2 (μ = coefficient of friction)

O   Nearly empty rack

The seismic analyses were performed utilizing the time-
history method. Pool slab acceleration data in three orthogonal
directions was developed and verified to be statistically
independent.

The objective of the seismic analysis of single racks is to
determine the structural response (stresses, deformation, rigid
body motion, etc.) due to simultaneous application of the three
statistically independent, orthogonal excitations. Thus, recourse

to approximate statistical summation techniques (Ref. 5) is avoided. For nonlinear analysis, the only practical method is simultaneous application of the seismic loading to a nonlinear model of the structure.

Pool slab acceleration data are developed from specified response spectra for the IP-2 site. Figure 6.1 shows the response spectra governing the pool. This response spectrum is taken from the IP-2 FSAR. Figures 6.2 - 6.7 show the time-histories corresponding to the SSE response spectra, and a comparison of the spectra corresponding to the synthetic time histories with the respective target design spectra. The target design spectra are enveloped by the spectra corresponding to the generated seismic events.

The seismic analysis is performed in three steps, namely:

1. Development of a nonlinear dynamic model consisting of inertial mass elements, spring, gap, and friction elements.

2. Generation of the equations of motion and inertial coupling and solution of the equations using the "component element time integration scheme" (Refs. 6 and 7) to determine nodal forces and displacements.

3. Computation of the detailed stress field in the rack (at the critical location) and in the support legs using the nodal forces calculated in the previous step. These stresses are checked against the design limits given in Section 6.5.

A brief description of the dynamic model follows.

6.2   FUEL RACK - DYNAMIC MODEL

Since the racks are not anchored to the pool slab or attached to the pool walls or to each other, they can execute a wide variety of motions. For example, a rack may slide on the pool floor ("sliding condition"); one or more legs may momentarily lose contact with the liner ("tipping condition"); or a rack may experience a combination of sliding and tipping conditions. The structural model permits simulation of these kinematic events with inherent built-in conservatisms. Since the modules are designed to preclude the incidence of inter-rack impact, it is also necessary to include the potential for inter-rack impact phenomena in the analysis to demonstrate that such impacts do not occur. Lift off of the support legs and subsequent liner impacts are modelled using appropriate impact (gap) elements, and Coulomb friction between the rack and the pool liner is simulated by appropriate piecewise linear springs. The elasticity of the rack structure, relative to the base, is also included in the model even though the rack may be nearly rigid. These special attributes of the rack dynamics require a strong emphasis on the modelling of the linear and nonlinear springs, dampers, and stop elements. The model outline in the remainder of this section, and the model description in the following section, describe the detailed modelling technique to simulate these effects, with emphasis placed on the nonlinearity of the rack seismic response.

6.2.1   Outline of Model for Computer Code DYNARACK

a. The fuel rack structure is a folded metal plate assemblage welded to a baseplate and supported on four legs. An odd-shaped module may have more than four legs. The rack structure itself is a very rigid structure. Dynamic analysis of typical multicell racks has shown that the motion of the structure is captured almost completely by modelling the rack as a twelve degree-of-freedom structure, where the movement of the rack cross-section at any height is described in terms of six degrees-of-freedom of the rack base and six degrees of freedom defined at the rack top. The rattling fuel is modelled by five lumped masses located at H, .75H, .5H, .25H, and at the rack base, where H is the rack height as measured from the base.

b. The seismic motion of a fuel rack is characterized by random rattling of fuel assemblies in their individual storage locations. Assuming a certain statistical coherence in the vibration of the fuel assemblies exaggerates the computed dynamic loading on the rack structure. This assumption, however, greatly reduces the required degrees-of-freedom needed to model the fuel assemblies which are represented by five lumped masses located at different levels of the rack. The centroid of each fuel assembly mass can be located, relative to the rack structure centroid at that level, so as to simulate a partially loaded rack.

c. The local flexibility of the rack-support interface is modelled conservatively in the analysis.

d. The rack base support may slide or lift off the pool floor.

e. The pool floor has a specified time-history of seismic accelerations along the three orthogonal directions.

f. Fluid coupling between rack and assemblies, and between rack and adjacent racks, is simulated by introducing appropriate inertial coupling into the system kinetic energy. Inclusion of these effects uses the methods of References 6 and 9 for rack/assembly coupling and for rack/rack coupling (see Section 6.2.3 of this report).

g. Potential impacts between rack and assemblies are accounted
    for by appropriate "compression only" gap elements between
    masses involved.

h. Fluid damping due to viscous effects between rack and
    assemblies, and between rack and adjacent rack, is
    conservatively neglected; form drag has also been
    conservatively neglected.

i. The supports are modelled as "compression only" elements for
    the vertical direction and as "rigid links" for transferring
    horizontal stress. The bottom of a support leg is attached
    to a frictional spring as described in Section 6.3. The
    cross-section inertial properties of the support legs are
    computed and used in the final computations to determine
    support leg stresses.

j. Because of the aspect ratio of the IP2 pool, the effect of
    sloshing is negligible at the bottom of the pool and is hence
    neglected.

k. The possible incidence of inter-rack impact is simulated by
    gap elements at the top and bottom of the rack in the two
    horizontal directions.   The most conservative case of
    adjacent rack movement is assumed; each adjacent rack is
    assumed to move completely out of phase with the rack being
    analyzed. This maximizes the potential for impact.

l. Rattling of fuel assemblies inside the storage locations
    causes the "gap" between the fuel assemblies and the cell
    wall to change from a maximum of twice the nominal gap to a
    theoretical zero gap. Fluid coupling coefficients are based
    on the nominal gap.

m. The cross coupling effects due to the movement of fluid from
    one interstitial (inter-rack) space to the adjacent one is
    modelled using potential flow and Kelvin's circulation
    theorem. This formulation has been reviewed and approved by
    the Nuclear Regulatory Commission, during the post-licensing
    multi-rack analysis for Diablo Canyon Unit I and II reracking

project in 1987 and for several dockets since that time. The
coupling coefficients are based on a consistent modelling of
the fluid flow and are based on the gaps between rack faces.
Updating of the coefficients may be made for each time step
of integration to reflect the changing gaps; in these
analyses, in the interest of added conservatism, no updating
is used and the hydrodynamic effect is based on the nominal
starting gaps.

Figure 6.8 shows a schematic of the model. Twelve degrees-of-
freedom are used to track the motion of the rack structure.
Figures 6.9 and 6.10, respectively, show the inter-rack impact
springs (to track the potential for impact between racks) and fuel
assembly/storage cell impact springs at a particular level.

As shown in Figure 6.8, the model for simulating fuel
assembly motion incorporates five rattling lumped masses. The five
rattling masses are located at the baseplate, at quarter height,
at half height, at three quarter height, and at the top of the
rack. Two degrees-of-freedom are used to track the motion of each
rattling mass in the horizontal plane. The vertical motion of each
rattling mass is assumed to be the same as the rack base. Figures
6.11, 6.12 and 6.13 show the modelling scheme for including rack
elasticity and the degrees of freedom associated with rack
elasticity. In each plane of bending a shear and a bending spring
are used to simulate elastic effects in accordance with Reference
6.

6.2.2   Model Description

The absolute degrees-of-freedom associated with each of the mass locations are identified in Figure 6.8 and in Table 6.1. The rattling masses (nodes 1^*, 2^*, 3^*, 4^*, 5^*) are described by translational degrees-of-freedom q_7-q_{16}.

$U_i(t)$ is the pool floor slab displacement seismic time-history. Thus, there are twenty-two degrees-of-freedom in the system. Not shown in Fig. 6.8 are the gap elements used to model the support legs and the impacts with adjacent racks.

6.2.3   Fluid Coupling

An effect of some significance requiring careful modelling is the so-called "fluid coupling effect". If one body of mass (m_1) vibrates adjacent to another body (mass m_2), and both bodies are submerged in a frictionless fluid medium, then Newton's equations of motion for the two bodies have the form:

$$(m_1 + M_{11}) X_1{''} - M_{12} X_2{''} = \text{applied forces on mass } m_1 + 0 (x_1{'}^2)$$

$$-M_{21} X_1{''} + (m_2 + M_{22}) X_2{''} = \text{applied forces on mass } m_2 + 0 (x_2{'}^2)$$

$X_1{''}$, $X_2{''}$ denote absolute accelerations of mass m_1 and m_2, respectively.

M_{11}, M_{12}, M_{21}, and M_{22} are fluid coupling coefficients which depend on the shape of the two bodies, their relative disposition, etc. Fritz (Ref. 9) gives data for M_{ij} for various body shapes and arrangements. It is to be noted that the above equation indicates that the effect of the fluid is to add a certain amount

of mass to the body (M_{11} to body 1), and an external force which is proportional to the acceleration of the adjacent body (mass m_2). Thus, the acceleration of one body affects the force field on another. This force is a strong function of the interbody gap, reaching large values for very small gaps. This inertial coupling is called fluid coupling. It has an important effect in rack dynamics. The lateral motion of a fuel assembly inside the storage location will encounter this effect as will the motion of a rack adjacent to another rack. These effects are included in the equations of motion. For example, the fluid coupling is between node 2* and at the top of the rack in Figure 6.8. Furthermore, the rack equations contain coupling terms which model the effect of fluid in the gaps between adjacent racks. The coupling terms modelling the effects of fluid flowing between adjacent racks are computed assuming that all adjacent racks are vibrating 180^0 out of phase from the rack being analyzed. Therefore, only one rack is considered surrounded by a hydrodynamic mass computed as if there were a plane of symmetry located in the middle of the gap region.

The rack-to-rack hydrodynamic coupling coefficients M_{ij} are inversely proportional to the annular gap between the two bodies. This gap is a function of time as the two bodies vibrate, so that the hydrodynamic masses M_{ij} are functions of time as well. In the previous equations, the notation $O(x_1'^2)$, $O(x_2'^2)$ represent additional nonlinear fluid restoring forces that arise from the development of the interbody fluid coupling effects. These nonlinear restoring forces are only important as the gaps between bodies become small since they are also proportional to the inverse of the square of the current gap. Proper accounting

of the effect of gap size on the hydrodynamic mass M_{ij} and on the fluid restoring forces due to film squeezing can be accounted for at each step in the dynamic simulation, if desired.

Finally, fluid virtual mass is included in the vertical direction vibration equations of the rack; virtual inertia is also added to the governing equation corresponding to the rotational degree-of-freedom, $q_6(t)$ and $q_{22}(t)$.

6.2.4   Damping

In reality, damping of the rack motion arises from material hysteresis (material damping), relative intercomponent motion in structures (structural damping), and fluid viscous effects (fluid damping). In the analysis, a maximum of 2% structural damping is imposed on elements of the rack structure during SSE seismic simulations. This is in accordance with the FSAR and NRC guidelines (Ref. 11). Material and fluid damping due to fluid viscosity are conservatively neglected.

6.2.5   Impact

Any fuel assembly node (e.g., 2*) may impact the adjacent rack structure mass node. To simulate this impact, four compression-only gap elements around each rattling fuel assembly node are provided (see Figure 6.10). The compressive loads developed in these springs provide the necessary data to evaluate the integrity of the cell wall structure and stored array during the seismic event. Figure 6.9 shows the location of the impact springs used to simulate any potential for inter-rack impacts. Section 6.4.2 gives more details on these additional impact springs. Since there are five rattling masses a total of 20 impact springs are used to model fuel assembly-cell wall impact.

6.3   ASSEMBLY OF THE DYNAMIC MODEL

The cartesian coordinate system associated with the rack has the following nomenclature:

o   x =   Horizontal coordinate along the short direction of rack rectangular platform

o   y = Horizontal coordinate along the long direction of the rack rectangular platform

o   z = Vertically upward from the rack base

If the simulation model is restricted to two dimensions (one horizontal motion plus vertical motion, for example) for the purposes of model clarification only, then a descriptive model of the simulated structure which includes gap and friction elements is used as shown in Figure 6-14.

The impacts between fuel assemblies and rack show up in the gap elements, having local stiffness K_I, in Figure 6.14.   In Table 6.2, gap elements 5 through 8 are for the vibrating mass at the top of the rack. The support leg spring rates K_S are modelled by elements 1 through 4 in Table 6.2. Note that the local compliance of the concrete floor is included in K_S. To simulate sliding potential, friction elements 2 plus 8 and 4 plus 6 (Table 6.2) are shown in Figure 6.14. The friction of the support/liner interface is modelled by a piecewise linear spring with a suitably large stiffness K_f up to the limiting lateral load, μN, where N is the current compression load at the interface

between support and liner. At every time step during the transient analysis, the current value of N (either zero for liftoff condition, or a compressive finite value) is computed. Finally, the support rotational friction springs K_R reflect any rotational restraint that may be offered by the foundation. This spring rate is calculated using a modified Bousinesq equation (Ref. 6) and is included to simulate the resistive moment of the support to counteract rotation of the rack leg in a vertical plane. This rotation spring is also nonlinear, with a zero spring constant value assigned after a certain limiting condition of slab moment loading is reached.

The nonlinearity of these springs (friction elements 9, 11, 13, and 15 in Table 6.2) reflects the edging limitation imposed on the base of the rack support legs. If this effect is neglected, any support leg bending, induced by liner/baseplate friction forces, is resisted by the leg acting as a beam cantilevered from the rack baseplate. This leads to higher predicted loads at the support leg - baseplate junction than if the moment resisting capacity at the floor is included in the model.

The spring rate K_S modelling the effective compression stiffness of the structure in the vicinity of the support, is computed from the equation:

$$\frac{1}{K_S} = \frac{1}{K_1} + \frac{1}{K_2} + \frac{1}{K_3}$$

where:

K_1 = spring rate of the support leg treated as a tension-compression member

K_2 = local spring rate of pool slab

K_3 = spring rate of folded plate cell structure above support leg

As described in the preceding section, the rack, along with the base, supports, and stored fuel assemblies, is modelled for the general three-dimensional (3-D) motion simulation by a twenty-two degree-of-freedom model. To simulate the impact and sliding phenomena, up to 64 nonlinear gap elements and 16 nonlinear friction elements are used. Gap and friction elements, with their connectivity and purpose, are presented in Table 6.2. Table 6.3 lists representative values for the racks used in the dynamic simulations.

For the 3-D simulation of a single rack, all support elements (described in Table 6.2) are included in the model.* Coupling between the two horizontal seismic motions is provided both by any offset of the fuel assembly group centroid which causes the rotation of the entire rack and/or by the possibility of liftoff

---

* Since inter-rack impact does not occur in the IP-2 racks, only 8 gap elements are used around the bottom and top edges of the rack instead of the twenty described in Table 6.2. Since their purpose is only to signal if an impact occurs, the exact number utilized has no bearing on the final reported results.

6-13

of one or more support legs. The potential exists for the rack to be supported on one or more support legs during any instant of a complex 3-D seismic event. All of these potential events may be simulated during a 3-D motion and have been observed in the analyses.

6.4   TIME INTEGRATION OF THE EQUATIONS OF MOTION

6.4.1   Time-History Analysis Using Multi-Degree of Freedom Rack Model

Having assembled the structural model, the dynamic equations of motion corresponding to each degree-of-freedom are written by using Lagrange's Formulation. The system kinetic energy can be constructed including contributions from the solid structures and from the trapped and surrounding fluid. A single rack is modelled in detail. The system of equations can be represented in matrix notation as:

$$[M] \{q''\} = \{Q\} + \{G\}$$

where the vector $\{Q\}$ is a function of nodal displacements and velocities, and $\{G\}$ depends on the coupling inertia and the ground acceleration denotes differentiation with time.

Pre-multiplying the above equations by $[M]^{-1}$ renders the resulting equation uncoupled in mass.

We have: $$\{q''\} = [M]^{-1} \{Q\} + [M]^{-1} \{G\}$$

Note that if the mass matrix is updated at every time step because of the time-varying hydrodynamic effects, the

inversion of the equations must be carried out at every increment. The effect of the previously mentioned nonlinear fluid restoring forces is included in the generalized forces Q and accounted for in the analysis when the updating option is used. For the IP-2 analysis, the gaps are not updated.

As noted earlier, in the numerical simulations run to verify structural integrity during a seismic event, the rattling fuel assemblies are assumed to move in phase. This will provide maximum impact force level, and induce additional conservatism in the time-history analysis.

This equation set is mass uncoupled, displacement coupled at each instant in time, and is ideally suited for numerical solution using a central difference scheme. The proprietary, USNRC qualified, computer program "DYNARACK"* is utilized for this purpose.

Stresses in various portions of the structure are computed from known element forces at each instant of time and the maximum value of critical stresses over the entire simulation is reported in summary form at the end of each run.

---

* This code has been previously utilized in licensing of similar racks for Fermi 2 (USNRC Docket No. 50-341), Quad Cities 1 and 2 (USNRC Docket Nos. 50-254 and 265), Rancho Seco (USNRC Docket No. 50-312), Oyster Creek (USNRC Docket No. 50-219), V.C. Summer (USNRC Docket No. 50-395), and Diablo Canyon 1 and 2 (USNRC Docket Nos. 50-275 and 50-323), St. Lucie Unit I (USNRC Docket No. 50-335), Byron Units I and II (USNRC Docket Nos. 50-454, 50-455), Vogtle 2 (USNRC Docket 50-425), and Millstone Unit 1 (USNRC Docket 50-245).

In summary, dynamic analysis of typical multicell racks has shown that the motion of the structure is captured almost completely by the behavior of a twenty-two degree-of-freedom structure; therefore, in this analysis model, the movement of the rack cross-section at any height is described in terms of the rack degrees-of-freedom ($q_1(t),...q_6(t)$ and $q_{17}-q_{22}(t)$). The remaining degrees-of-freedom are associated with horizontal movements of the fuel assembly masses. In this dynamic model, five rattling masses are used to represent fuel assembly movement in the horizontal plane. Therefore, the final dynamic model consists of twelve degrees-of-freedom for the rack plus ten additional mass degrees-of-freedom for the five rattling masses. The totality of fuel mass is included in the simulation and is distributed among the five rattling masses.

6.4.2   <u>Evaluation of Potential for Inter-Rack Impact</u>

Since the racks are closely spaced, the simulation includes impact springs to model the potential for inter-rack impact. To account for this potential, yet still retain the simplicity of simulating only a single rack, gap elements are located on the rack at the top and at the baseplate level. Figure 6.9 shows the location of these gap elements. Impacts between racks or between rack and walls are precluded for the IP-2 pool; however, sixteen impact springs are retained (8 at top and 8 at baseplates) solely to demonstrate that the postulated gaps do not completely close due to rack motion.

6.5   STRUCTURAL ACCEPTANCE CRITERIA

There are two sets of criteria to be satisfied by the rack modules:

a.   Kinematic Criterion

This criterion seeks to ensure that the rack is a physically stable structure. The racks are designed to preclude inter-rack impacts. Therefore, physical stability of the rack is considered along with the criterion that inter-rack impact or rack-to-wall impacts do not occur.

b.   Stress Limits

The stress limits of the ASME Code, Section III, Subsection NF, 1983 Edition are used since this code provides the most appropriate and consistent set of limits for various stress types and various loading conditions. The following loading combinations are applicable (Ref. 1).

Loading Combination	Stress Limit
$D + L$	Level A service limits
$D + L + T_o$	
$D + L + T_o + E$	
$D + L + T_a + E$	Level B service limits
$D + L + T_o + P_f$	
$D + L + T_a + E'$	Level D service limits
$D + L + F_d$	The functional capability of the fuel racks should be demonstrated.

where:

D =   Dead weight-induced stresses (including fuel assembly weight)

L   =   Live Load (0 for the structure, since there are no moving objects in the rack load path).

F_d =   Force caused by the accidental drop of the heaviest load from the maximum possible height.

P_f =   Upward force on the racks caused by postulated stuck fuel assembly

E   =   OBE Earthquake

E'   =   Safe Shutdown Earthquake (SSE)

T_o =   Differential temperature induced loads (normal or upset condition)

T_a =   Differential temperature induced loads (abnormal design conditions)

The conditions T_a and T_o cause local thermal stresses to be produced. The worst situation will be obtained when an isolated storage location has a fuel assembly which is generating heat at the maximum postulated rate. The surrounding storage locations are assumed to contain no fuel. The heated water makes unobstructed contact with the inside of the storage walls, thereby producing the maximum possible temperature difference between the adjacent cells. The secondary stresses thus produced are limited to the body of the rack; that is, the support legs do not experience the secondary (thermal) stresses.

6.6   MATERIALS AND MATERIAL PROPERTIES

The racks will be made from ASME SA240-304 austenitic stainless steel sheet and plate material, SA351 casting material and SA564-630 precipitation hardened stainless steel (to 1100^0F) for supports only. The weld filler material to be used in body welds will be ASME SFA-5.9, classification ER 308L. The neutron absorber material is Boraflex with a minimum B-10 areal density of 0.028 gm/cm^2 for the 269 Region I storage cells and 0.022 gm/cm^2 for the 1105 Region II storage cells. Boraflex is a silicone-based polymer containing fine particles of boron carbide in a homogeneous, stable matrix.

The data on the physical properties of the rack and support materials, obtained from the ASME Boiler & Pressure Vessel Code, Section III, appendices, and supplier's catalog, are listed in Table 6.4. Since the maximum pool bulk temperature is less than 200^0F, this is used as the reference design temperature for evaluation of material properties.

The IP2 spent fuel storage pool is monitored regularly (approximately once per week) for impurities such as chlorides and fluorides. In addition, spent fuel pool water is processed by filtration and demineralization to maintain water purity and clarity. The pool liner, rack lattice structure and fuel storage cells are stainless steel which is compatible with the storage pool environment. The austenitic stainless steel (304) used in the spent fuel storage racks is not susceptible to stress corrosion cracking and thus, corrosion in the spent fuel storage pool environment will be of little significance during the life of

the plant. Dissimilar metal contact corrosion (galvanic attack between the stainless steel rack assemblies and Zircaloy and Inconel in the fuel assemblies) will not be significant because the materials are protected by highly passivating oxide films and are, therefore, at similar galvanic potentials.

The annulus spaces that contain Boraflex in the new high density racks are vented to the spent fuel pool. Venting of the annuli will allow gas generated by the chemical and radiolytic decomposition of the silicone polymer binder, when exposed to the thermal radiation environment, to escape.

6.7 STRESS LIMITS FOR VARIOUS CONDITIONS

The following stress limits are derived from the guidelines of the ASME Code, Section III, Subsection NF, in conjunction with the material properties data of the preceding section (see Section 6.11 for definition of terms).

6.7.1 Normal and Upset Conditions (Level A or Level B)

a. Allowable stress in tension on a net section
= F_t = 0.6 S_y or

F_t = (0.6) (25,000) = 15,000 psi (rack material)

F_t = is equivalent to primary membrane stresses
F_t = (.6) (25,000) = 15,000 psi (upper part of support feet)

= (.6) (106,300) = 63,780 psi (lower part of support feet)

6-20

b.　On the gross section, allowable stress in shear is:

$$F_v = .4\ S_y$$
$$(.4)\ (25,000) = 10,000\ \text{psi (main rack body)}$$

$$F_t = (.4)\ (25,000) = 10,000\ \text{psi (upper part of support feet)}$$

$$= (.4)\ (106,300) = 42,520\ \text{psi (lower part of support feet)}$$

c.　Allowable stress in compression, F_a:

$$F_a = \frac{\left[[1 - \frac{kl^2}{r^2}\ /2C_c^{\ 2}] \right] S_y}{\{(\frac{5}{3}) + [3\ (\frac{kl}{r})\ /8C_c] - [(\frac{kl}{r})^3\ /8C_c^{\ 3}]\}}$$

where:

$$C_c = [\ \frac{(2\pi^2\ E)}{S_y}\ ]^{1/2}$$

kl/r for the main rack body is based on the full height and cross section of the honeycomb region. Substituting numbers, we obtain, for both support leg and honeycomb region:

$$F_a = 15,000\ \text{psi (main rack body)}$$
$$F_a = 15,000\ \text{psi (upper part of support feet)}$$
$$= 63,780\ \text{psi (lower part of support feet)}$$

6-21

d.   Maximum allowable bending stress at the outermost fiber due to flexure about one plane of symmetry:

F_b = 0.60 S_y = 15,000 psi (rack body)
F_b = 15,000 psi (upper part of support feet)
    = 63,780 psi (lower part of support feet)

e.   Combined flexure and compression:

$$\frac{f_a}{F_a} + \frac{C_{mx}\,f_{bx}}{D_x F_{bx}} + \frac{C_{my}f_{by}}{D_y F_{by}} < 1$$

where:

f_a = Direct compressive stress in the section

f_{bx} = Maximum flexural stress along x-axis

f_{by} = Maximum flexural stress along y-axis

C_{mx} = C_{my} = 0.85

$$D_x = 1 - \frac{f_a}{F'_{ex}}$$

$$D_y = 1 - \frac{f_a}{F'_{ey}}$$

where:

$$F'_{ex,ey} = \frac{12\ \pi^2\ E}{23\ \left(\dfrac{kl_{bx,y}}{r_{bx,y}}\right)^2}$$

and the subscripts x,y reflect the particular bending plane of interest.

f. Combined flexure and compression (or tension):

$$\frac{f_a}{0.6S_y} + \frac{f_{bx}}{F_{bx}} + \frac{f_{by}}{F_{by}} < 1.0$$

The above requirement should be met for both the direct tension or compression case.

6.7.2   Level D Service Limits

Section F-1370 (Ref. 12), states that the limits for the Level D condition are the minimum of 1.2 (S_y/F_t) or 0.7 (S_u/F_t) times the corresponding limits for Level A condition. Since 1.2 S_y is greater than 0.7 S_u for the lower part of the support feet, the factor is 1.54 for the lower section under SSE conditions. The factor for the upper portion of the support foot is 2.0. In the above S_y is the yield stress at the design temperature and S_u is the ultimate tensile stress at the design temperature.

Instead of tabulating the results of these six different stresses as dimensioned values, they are presented in a dimensionless form. These stress factors are defined as the ratio

6-23

of the actual developed stress to its specified limiting value.
With this definition, the limiting value of each stress factor is
1.0 for the OBE and 2.0 (or 1.54) for the SSE condition.

6.8   RESULTS FOR THE ANALYSIS OF SPENT FUEL RACKS UNDER
       3-D SEISMIC MOTION

       Figures 6.2, 6.4, and 6.6 show the pool slab motion used
for horizontal x, horizontal y, and vertical directions. This
motion is for the SSE earthquake.

       Results are abstracted here for critical cases.

       A complete synopsis of the analysis of the modules,
subject to the SSE earthquake motions, is presented in a summary
Table 6.5 which gives the bounding values of stress factors R_i (i
= 1,2,3,4,5,6,7). The stress factors are defined as:

R_1 =   Ratio of direct tensile or compressive stress on a
           net section to its allowable value (note support
           feet only support compression)

R_2 =   Ratio of gross shear on a net section in the x-
           direction to its allowable value

R_3 =   Ratio of maximum bending stress due to bending
           about the x-axis to its allowable value for the
           section

R_4 =   Ratio of maximum bending stress due to bending
           about the y-axis to its allowable value

R_5 =   Combined flexure and compressive factor (as defined
           in 6.7.1e above)

R_6 =   Combined flexure and tension (or compression)
           factor (as defined in 6.7.1f above)

6-24

R_7 = Ratio of gross shear on a net section in the y-direction to its allowable value.

As stated before, the allowable value of R_i (i =1,2,3,4,5,6,7) is 1 for the OBE condition and 2 for the SSE (except for the lower section of the support where the factor is 1.54)

The rack modules sit on bearing pads so that the support pressures are further reduced when transmitted to the pool floor. These bearing pads are free to slide. Analysis shows, however, that sliding will occur only between support foot and bearing pad if the coefficient of friction between the support foot and pad is less than the coefficient of friction between bearing pad and liner. Conversely, if the coefficient of friction between bearing pad and liner is less than the coefficient of friction between support foot and bearing pad, no sliding will occur between support foot and pad; rather, all sliding will occur between pad and liner. In the IP-2 plant, both coefficients of friction are essentially the same; it is sufficient to demonstrate that if the pad is assumed not to slide, then the requirement on support foot horizontal motion is met if the support foot does not move over the pad geometry limits, and that liner bearing pressures are within acceptable limits.

The dynamic analysis gives the maximax (maximum in time and in space) values of the stress factors at critical locations in the rack module. Values are also obtained for maximum rack displacements and for critical impact loads. Table 6.5 presents critical results for the stress factors, and rack to fuel impact load. Table 6.6 presents maximum results for horizontal displacements at the top and bottom of the rack in the x and y direction. x is always the short direction of the rack. Also in Table 6.6, for each run, both the maximum value of the sum of all

support foot loadings (4 supports) as well as each individual maximum is reported. The table also gives values for the maximum vertical load and the corresponding net shear force at the liner at the same time instant, and for the maximum net shear load and the corresponding vertical force at a support foot at the same time instant.

The results presented in Tables 6.5 and 6.6 represent all runs carried out. Referring to Section 2, the following racks are considered as critical to evaluate structural integrity:

Rack B   (Region I heaviest rack)
Rack D   (Region II heaviest rack)
Rack G-2   (rack adjacent to cask area)

The critical case for structural integrity calculations is included. Appendix A to this Section 6 contains a partial output from one of the DYNARACK simulation runs of a single rack under 3-D excitation. The initial pages showing input data and model description are given along with the final summary pages giving maximum loads, displacements, and stress factors.

It is noted that the critical load factors reported for the support feet are all for the upper segment of the foot and are to be compared with the limiting value of 2.0. The load factors for the lower portion of the support foot are much lower and therefore are not reported in the tables.

Analyses have been carried out to show that significant margins of safety exist against local deformation of the fuel storage cell due to rattling impact of fuel assemblies.

Results obtained for all rack sizes and shapes are enveloped by the data presented herein. Overturning has also been considered for the cases where racks are adjacent to open areas. This has been done by assuming a multiplier of 1.5 on the SSE horizontal earthquakes (more conservative than the OT Position Paper) and checking predicted displacements if there were no obstacles. It is found that the horizontal displacements do not grow to such an extent as to imply any possibility for overturning.

6.9 IMPACT ANALYSES

6.9.1 Impact Loading Between Fuel Assembly and Cell Wall

The local stress in a cell wall is conservatively estimated from the peak impact loads obtained from the dynamic simulations. Plastic analysis is used to obtain the limiting impact load that can be tolerated. The limit load is calculated as 6602 lbs. per cell. Referring to Table 6.5, we note that the actual impact loads are substantially smaller than this limit load value.

6.9.2 Impacts Between Adjacent Racks

All of the dynamic analyses assume, conservatively, that adjacent racks move completely out of phase. Thus, the highest potential for inter-rack impact is achieved. The displacements obtained from the dynamic analyses are less than 50% of the rack-to-rack spacing or rack-to-wall spacing. Therefore, we conclude that no impacts between racks or between racks and walls occur during the SSE event.

6.10   WELD STRESSES

Critical weld locations under seismic loading are at the bottom of the rack at the baseplate connection and at the welds on the support legs. Results from the dynamic analysis using the simulation codes are surveyed and the maximum loading is used to qualify the welds on these locations.

6.10.1   Baseplate to Rack Welds and Cell-to-Cell Welds

Subsection NF (Ref. 2) permits, for the SSE condition, an allowable weld stress $\tau = .42\ S_u = 29{,}820$ psi. For all cases considered, the maximum weld stress for the baseplate to rack welds is bounded from above by the the value 7700 psi, which is below the limiting value for SSE conditions.

The weld between baseplate and support leg is checked using limit analysis techniques. The structural weld at that location is considered safe if the interaction curve satisfies

$$G\ (F/F_y,\ M/M_y) < 1 \qquad M = M\ (M_1,\ M_2)$$

where F_y, M_y are the limit load and moment under direct load only and direct moment only. F and M are the absolute values of the actual peak force and moments applied to the weld section. The limiting case of all analyses performed gives a factor .367 which is below the 1.0 limit.

The critical area that must be considered for fuel-cell to fuel-cell welds is the weld between the cell tubes. This weld is continuous near the baseplate at the support feet, but is

discontinuous as we proceed along the tube length. Stresses in the fuel cell tube to fuel cell tube welds develop along the length of each fuel tube due to fuel assembly impact with the cell wall. This occurs if fuel assemblies in adjacent tubes are moving out of phase with one another so that impact loads in two adjacent cells are in opposite directions which would tend to separate the channel from the tube at the weld. The maximum load that can be transferred in this weld region for the SSE condition is calculated as 5271 lbs. at every fuel cell connection to adjacent cells. The upper bound to the load required to be transferred is only 1199 lbs. where we have used a bounding maximum cell impact load of 424 lbs., assumed two impact locations are supported by each weld region, and have increased the load by $\sqrt{2}$ to account for 3-D effects. Therefore, there is a large margin of safety between tube-to-tube welds in the rack.

6.10.2   Heating of an Isolated Cell

Weld stresses due to heating of an isolated hot cell are also computed. The assumption used is that a single cell is heated, over its entire length, to a temperature above the value associated with all surrounding cells. No thermal gradient in the vertical direction is assumed so that the results are conservative. Using the temperatures associated with this unit, analysis shows that the welds along the entire cell length do not exceed the allowable value for a thermal loading condition. Section 7 discusses a quantification of this thermal stress.

6.11 TERMINOLOGY USED IN SECTION 6

S1, S2, S3, S4	Support designations
P_i	Absolute degree-of-freedom number i
q_i	Relative degree-of-freedom number i
μ	Coefficient of friction
U_i	Pool floor slab displacement time history in the i-th direction
x,y coordinates	horizontal direction
z coordinate	vertical direction
K_I	Impact spring between fuel assemblies and cell
K_f	Linear component of friction spring
K_S	Axial spring of support leg locations
N	Compression load in a support foot
K_R	Rotational spring provided by the pool slab
Subscript i	When used with U or X indicates direction (i = 1 x-direction, i = 2 y-direction, i = 3 z-direction)
R_i	Stress factors for direct, bending, shear, and combined cases on the specified gross cross section
S_y	Material yield stress

6.12 REFERENCES

1. USNRC Standard Review Plan, NUREG-0800, Chapter 3.

2. ASME Boiler & Pressure Vessel Code, Section III, Subsection NF (1983).

3. USNRC Regulatory Guide 1.29, "Seismic Design Classification," Rev. 3, 1978.

4. "Friction Coefficients of Water Lubricated Stainless Steels for a Spent Fuel Rack Facility," Prof. Ernest Rabinowicz, MIT, a report for Boston Edison Company, 1976.

5. USNRC Regulatory Guide 1.92, "Combining Modal Responses and Spatial Components in Seismic Response Analysis," Rev. 1, February, 1976.

6. "The Component Element Method in Dynamics with Application to Earthquake and Vehicle Engineering," S. Levy and J.P.D. Wilkinson, McGraw Hill, 1976.

7. "Dynamics of Structures," R.W. Clough and J. Penzien, McGraw Hill (1975).

8. "Mechanical Design of Heat Exchangers and Pressure Vessel Components," Chapter 16, K.P. Singh and A.I. Soler, Arcturus Publishers, Inc., 1984.

9. R.J. Fritz, "The Effects of Liquids on the Dynamic Motions of Immersed Solids," Journal of Engineering for Industry, Trans. of the ASME, February 1972, pp 167-172.

10. "Dynamic Coupling in a Closely Spaced Two-Body System Vibrating in Liquid Medium: The Case of Fuel Racks," K.P. Singh and A.I. Soler, 3rd International Conference on Nuclear Power Safety, Keswick, England, May 1982.

11. USNRC Regulatory Guide 1.61, "Damping Values for Seismic Design of Nuclear Power Plants," 1973.

12. ASME Boiler and Pressure Vessel Code, Section III, Appendix F (1983).

Table 6.1

DEGREES OF FREEDOM

Location (Node)	Displacement			Rotation		
	U_x	U_y	U_z	θ_x	θ_y	θ_z
1	P1	P2	P3	q4	q5	q6
2	P17	P18	P19	P20	P21	P22

Point 2 is assumed attached to rigid rack at the top most point.

Location (Node)	U_x	U_y
2*	P7	P8
3*	P9	P10
4*	P11	P12
5*	P13	P14
1*	P15	P16

where:

$$P_i = q_i(t) + U_1(t) \qquad i = 1,7,9,11,13,15,17$$

$$= q_i(t) + U_2(t) \qquad i = 2,8,10,12,14,16,18$$

$$= q_i(t) + U_3(t) \qquad i = 3,19$$

$U_i(t)$ are the 3 known earthquake displacements.

Table 6.2
NUMBERING SYSTEM FOR GAP ELEMENTS AND FRICTION ELEMENTS

I. <u>Nonlinear Springs (Gap Elements)</u> (64 Total)

Number	Node Location	Description
1	Support S1	Z compression only element
2	Support S2	Z compression only element
3	Support S3	Z compression only element
4	Support S4	Z compression only element
5	$2,2^*$	X rack/fuel assembly impact element
6	$2,2^*$	X rack/fuel assembly impact element
7	$2,2^*$	Y rack/fuel assembly impact element
8	$2,2^*$	Y rack/fuel assembly impact element
9-24	Other rattling masses for nodes 1^*, 3^*, 4^* and 5^*	
25	Bottom cross-section of rack (around edge)	Inter-rack impact elements
.		Inter-rack impact elements
.		Inter-rack impact elements
.		Inter-rack impact elements
.		Inter-rack impact elements
.		Inter-rack impact elements
.		Inter-rack impact elements
44		Inter-rack impact elements
45	Top cross-section of rack (around edge)	Inter-rack impact elements
.		Inter-rack impact elements
.		Inter-rack impact elements
.		Inter-rack impact elements
.		Inter-rack impact elements
.		Inter-rack impact elements
.		Inter-rack impact elements
64		Inter-rack impact elements

Table 6.2
(continued)

NUMBERING SYSTEM FOR GAP ELEMENTS AND FRICTION ELEMENTS

II. Friction Elements (16 total)

Number	Node Location	Description
1	Support S1	X direction friction
2	Support S1	Y direction friction
3	Support S2	X direction friction
4	Support S2	Y direction friction
5	Support S3	X direction friction
6	Support S3	Y direction friction
7	Support S4	X direction friction
8	Support S4	Y direction friction
9	S1	X Slab moment
10	S1	Y Slab moment
11	S2	X Slab moment
12	S2	Y Slab moment
13	S3	X Slab moment
14	S3	Y Slab moment
15	S4	X Slab moment
16	S4	Y Slab moment

Table 6.3

TYPICAL INPUT DATA FOR RACK ANALYSES

ITEM	VALUE
Rack ID	D 11x13 (Region II)
Support Foot Spring Constant K_s (lb/in.)	4.96×10^6
Frictional Spring Constant K_f (lb/in.)	1.938×10^9
Rack to Fuel Assembly Impact Spring Constant (lb/in.)	1.26×10^6 (x direction) 1.76×10^6 (y direction)
Elastic Shear Spring for Rack (lb/in.)	1.804×10^5 (x-z shear) 3.451×10^5 (y-z shear)
Elastic Bending Spring Rack (lb/in/in.)	2.689×10^{10} (x-z bending) 3.736×10^{10} (y-z bending)
Elastic Extensional Spring (lb/in.)	3.20×10^7
Elastic Torsional Spring (lb/in/in.)	9.17×10^8
Foundation Rotational Resistance Springs K_R (lb/in/in.)	5.67×10^7
Gaps (in.) for hydrodynamic effect (h_1, h_3 are -,x faces; and h_2, h_4 are -,+ y faces, respectively)	$h_1 = .6875$ $h_2 = 1.75$ $h_3 = .6875$ $h_4 = .625$

Table 6.4

RACK MATERIAL DATA

Material	Young's Modulus E (psi)	Yield Strength S_y (psi)	Ultimate Strength S_u (psi)
304 S.S.	27.6×10^6	25000	71000
Section III Reference	Table I-6.0	Table I-2.2	Table I-3.2

SUPPORT MATERIAL DATA

	Material	Young's Modulus E (psi)	Yield Strength S_y (psi)	Ultimate Strength S_u (psi)
1	ASTM-240, Type 304 (upper part of support feet)	27.6×10^6 psi	25,000 psi	71,000 psi
2	ASTM 564-630	27.6×10^6 psi	106,300 psi	140,000 psi
	Section III References		Table I-2.1	Table I-3.1

Table 6.5
STRESS FACTORS AND RACK TO FUEL IMPACT LOAD

Run	Remarks	Rack/Fuel Impact Load (lb) (Per Cell)		STRESS FACTORS		
-----	---------	---------------------------------------	---	R_1	R_2	R_3
D0b	Rack D Cof = .8, SSE Filled with Regular Fuel	219.0	* **	.013 ___ .165	.013 ___ .016	.120 ___ .057
D0d	Rack D Cof = .2, SSE Full Load, Regular Fuel	219.0		.013 ___ .165	.013 ___ .025	.120 ___ .091
G2a	Rack G2 (11x12) Cof = .8, SSE Full Load Regular Fuel	242.0		.013 ___ .141	.013 ___ .014	.091 ___ .038

---

*   Upper values are for rack baseplate section.

**   Lower values are for support foot cross section (upper part).
     See last page of Table 6.5 for stress factors R_4-R_7.

Table 6.5
(continued)

Run	Remarks	Rack/Fuel Impact Load (lb) (Per Cell)		STRESS FACTORS		
				R_1	R_2	R_3
B02	Rack B (9x12) Cof = .8, SSE Full Load Regular Fuel	291.0	* **	.008 ——— .154	.008 ——— .022	.061 ——— .082
B03	Rack B Cof = .2, SSE Full Load Regular Fuel	291.0		.008 ——— .154	.008 ——— .025	.061 ——— .091
B04	Rack B Cof = .2, SSE 12 Cells Filled with Regular Fuel	57.0		.005 ——— .036	.002 ——— .006	. ——— .023

---

*   Upper values are for rack baseplate section.

**   Lower values are for support foot cross section (upper part). See last page of Table 6.5 for stress factors R_4-R_7.

Table 6.5
(continued)

| | STRESS FACTORS | | | |
Run	R_4	R_5	R_6	R_7
D0b	.077	.152	.177	.019
	.038	.211	.219	.024
D0d	.077	.152	.177	.019
	.062	.246	.260	.036
G2a	.076	.128	.150	.015
	.033	.175	.181	.016
B02	.060	.089	.103	.011
	.05	.226	.239	.034
B03	.060	.089	.103	.011
	.06	.245	.262	.037
B04	.014	.058	.062	.009
	.011	.024	.028	.003

Table 6.6

RACK DISPLACEMENTS AND SUPPORT LOADS
(all loads are in lbs.)

RUN	FLOOR LOAD (sum of all support feet)	MAXIMUM SUPPORT LOAD		VERTICAL LOAD[*]	SHEAR LOAD[**]	DX[***] (in.)	DY (in.)
D0c	2.466×10^5	1	104100.	104100.	9652.	.1525	.1441
		2	97450.	77447.	10244.	.0006	.0007
		3	90990.				
		4	98370.				
D0d	2.466×10^5	1	104100.	104100.	16133.	.1525	.1441
		2	97440.	96655.	16297.	.0006	.0007
		3	90990.				
		4	98370.				
G2a	2.277×10^5	1	83100.	88960.	6626.	.1241	.1194
		2	88960.	41133.	7686.	.0005	.0006
		3	88570.				
		4	88890.				

---

[*]   The first line in any set of data is the maximum vertical load and the second line reported is the vertical load when the net horizontal shear at the liner is maximum.

[**] The first line is the net horizontal liner shear when the vertical load is maximum; the second line is the maximum value of the net horizontal shear on any single support foot.

[***] The first line reports results at the top of the rack; the second line reports results at the baseplate. The times at which these maximums occur may be different.

Table 6.6
(continued)

RACK DISPLACEMENTS AND SUPPORT LOADS
(all loads are in lbs.)

RUN	FLOOR LOAD (sum of all support feet)	MAXIMUM SUPPORT LOAD		VERTICAL LOAD[*]	SHEAR LOAD[**]	DX[***] (in.)	DY (in.)
B02	1.95×10^5	1	96750.	96750.	14692.	.1463	.0803
		2	82210.	64719.	15620.	.0009	.0007
		3	73410.				
		4	93690.				
B03	1.95×10^5	1	96760.	96760.	18191.	.1463	.0803
		2	82200.	96340.	18616.	.0009	.0007
		3	73410.				
		4	93710.				
B04	4.926×10^4	1	22590.	22590.	4518.	.0272	.0180
		2	17510.	22590.	4518.	.0006	.0009
		3	16400.				
		4	21480.				

---

[*] The first line in any set of data is the maximum vertical load and the second line reported is the vertical load when the net horizontal shear at the liner is maximum.

[**] The first line is the net horizontal liner shear when the vertical load is maximum; the second line is the maximum value of the net horizontal shear on any single support foot.

[***] The first line reports results at the top of the rack; the second line reports results at the baseplate. The times at which these maximums occur may be different.

FIGURE 6.1

6-42

CONSOLIDATED EDISON CO.
INDIAN POINT UNIT 2

Fifteen Percent of Gravity
Response Spectra

INDIAN POINT H1 SSE

Accel. (G's)

Time Steps (.01 sec./step)
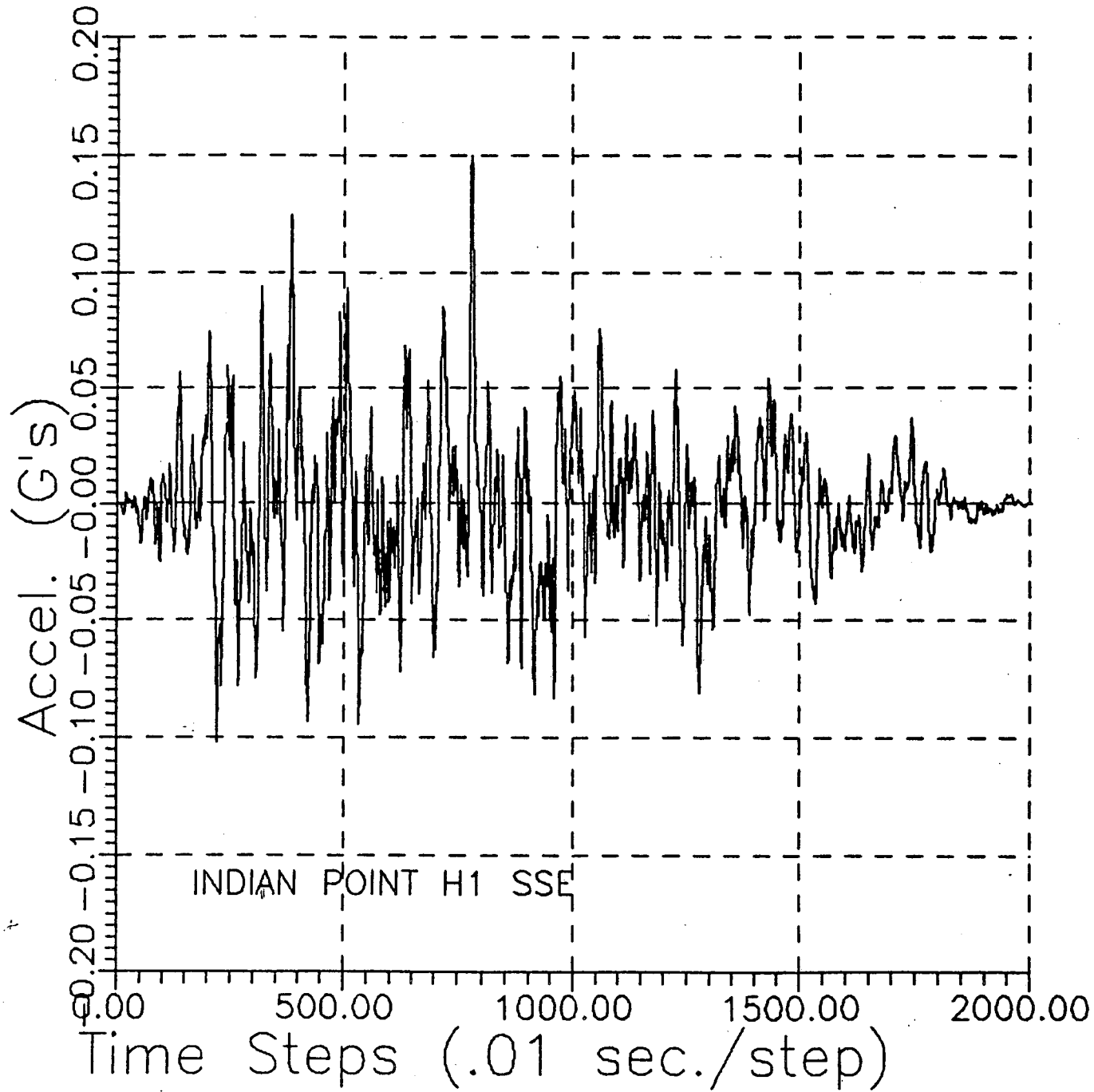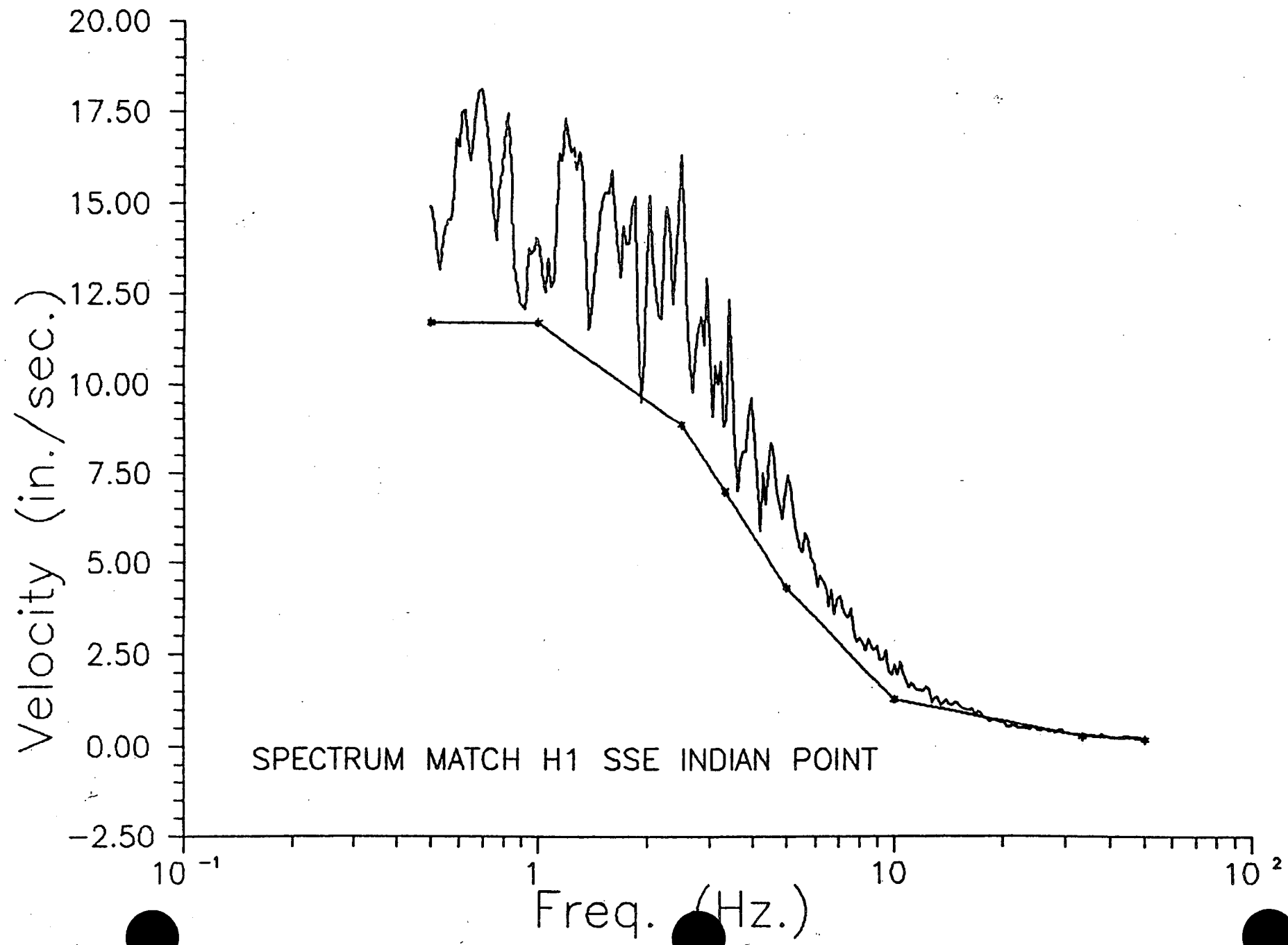
FIGURE 6.2

SPECTRUM MATCH H1 SSE INDIAN POINT

FIGURE 6.3

6-44

INDIAN POINT H2 SSE

FIGURE 6.4

FIGURE 8.5

Figure axes:
- Y-axis: Velocity (in./sec.) ranging from −2.50 to 22.50
- X-axis: Freq. (Hz.) ranging from 10^{-1} to 10^{2}

SPECTRUM MATCH H2 SSE INDIAN POINT

8-46

INDIAN POINT VERTICAL SSE

Accel. (G's) vs Time Steps (.01 sec./step)

6-47

FIGURE 6.6

SPECTRUM MATCH VERTICAL SSE INDIAN POINT

6-48
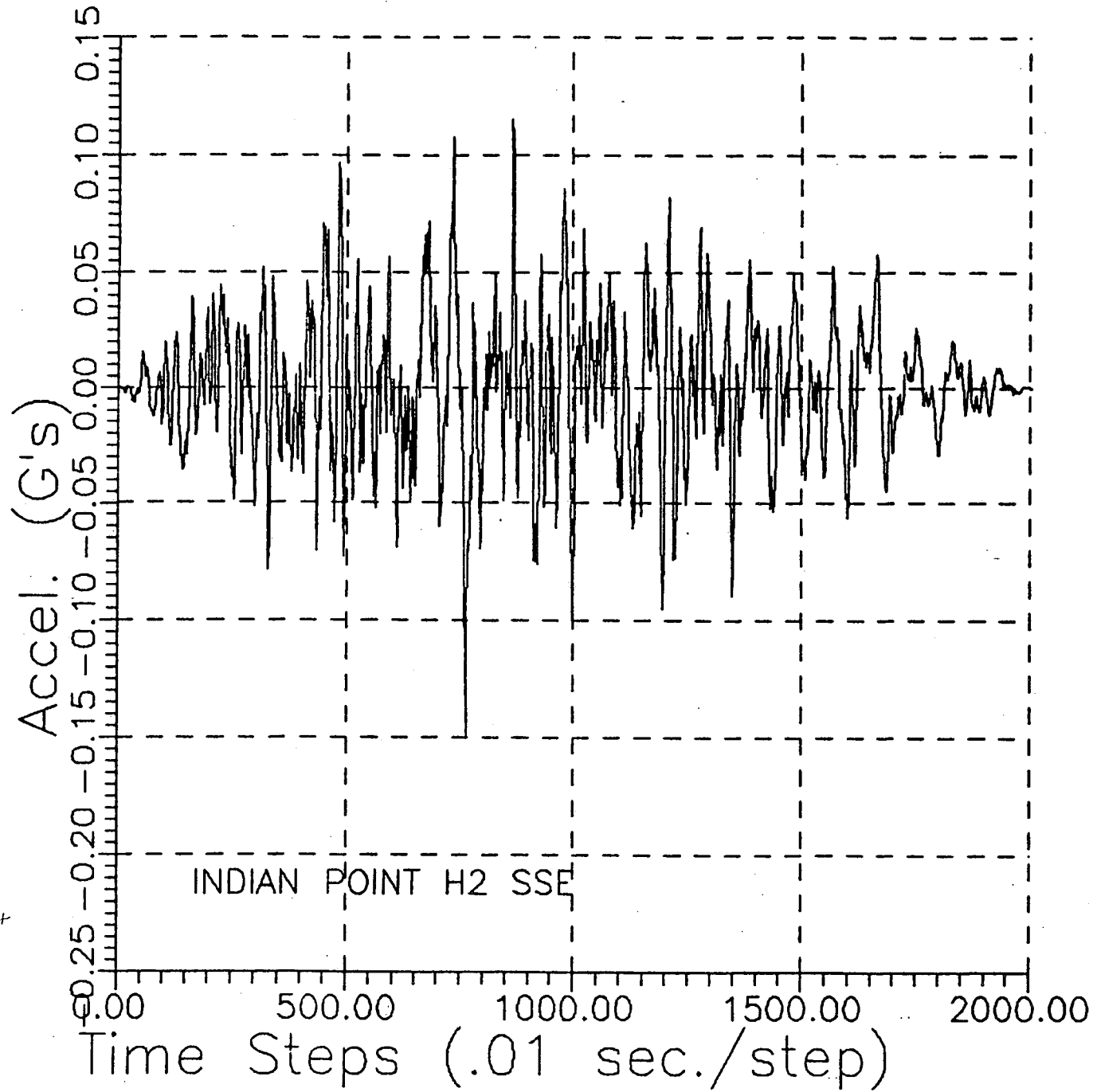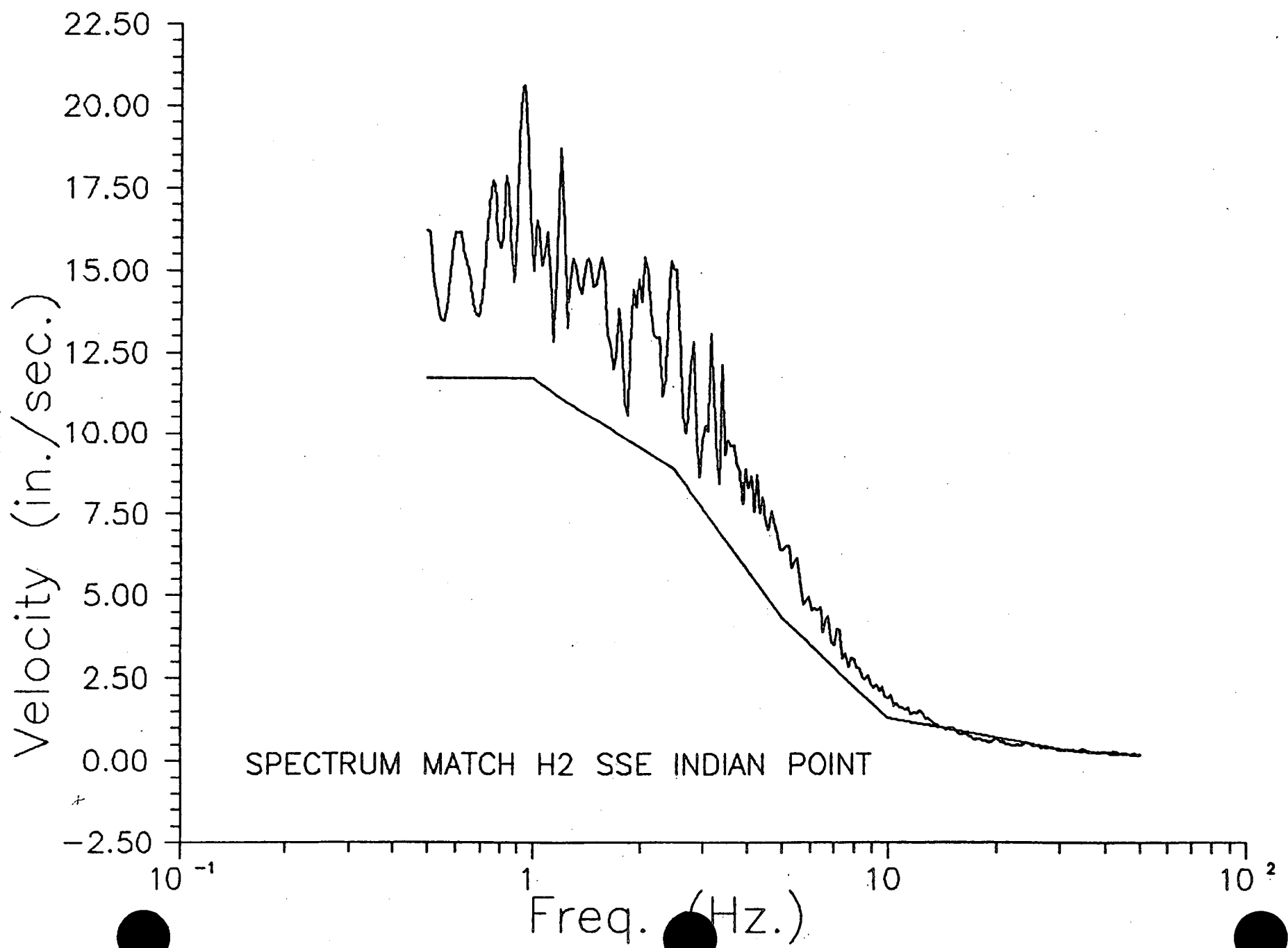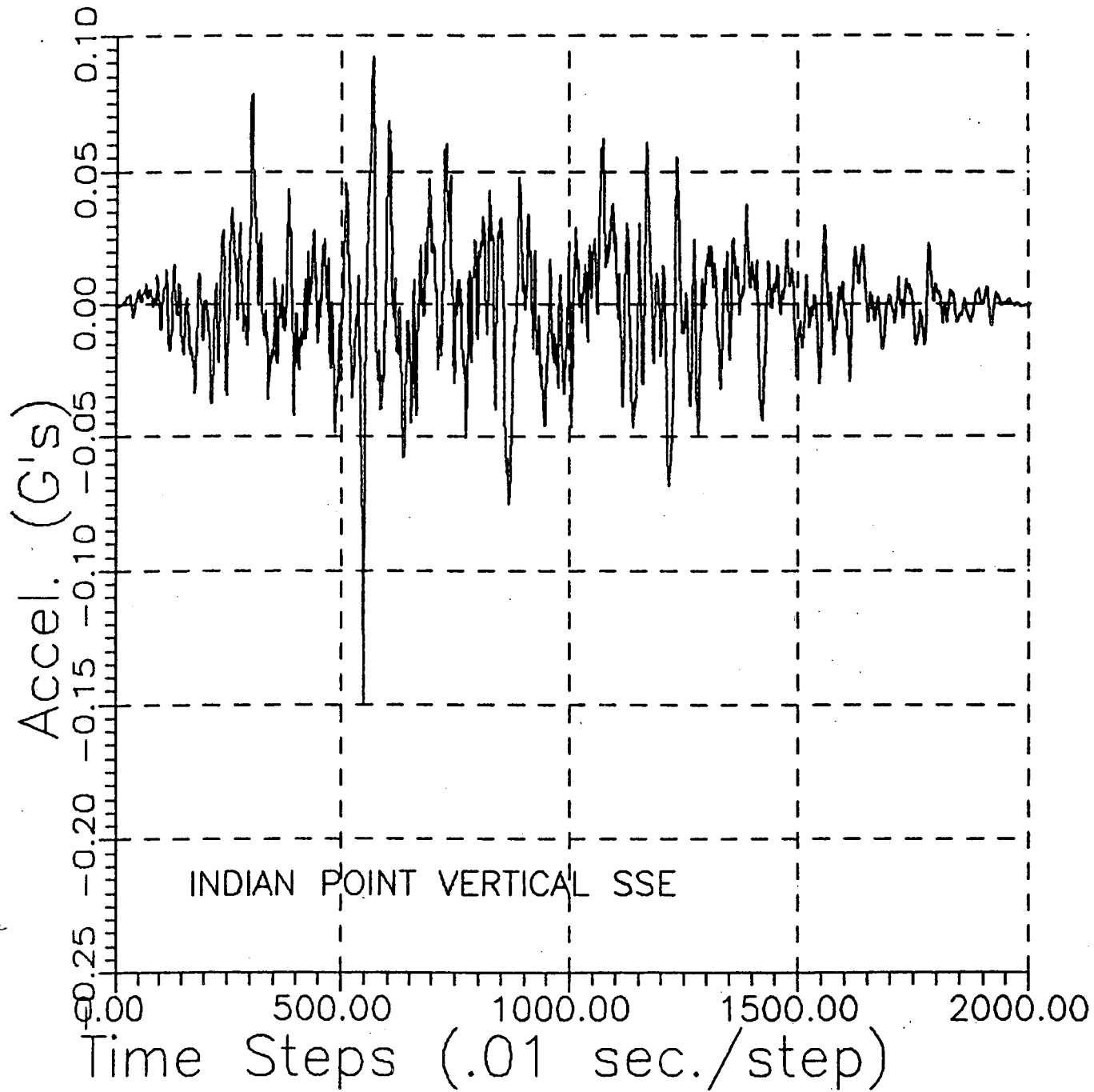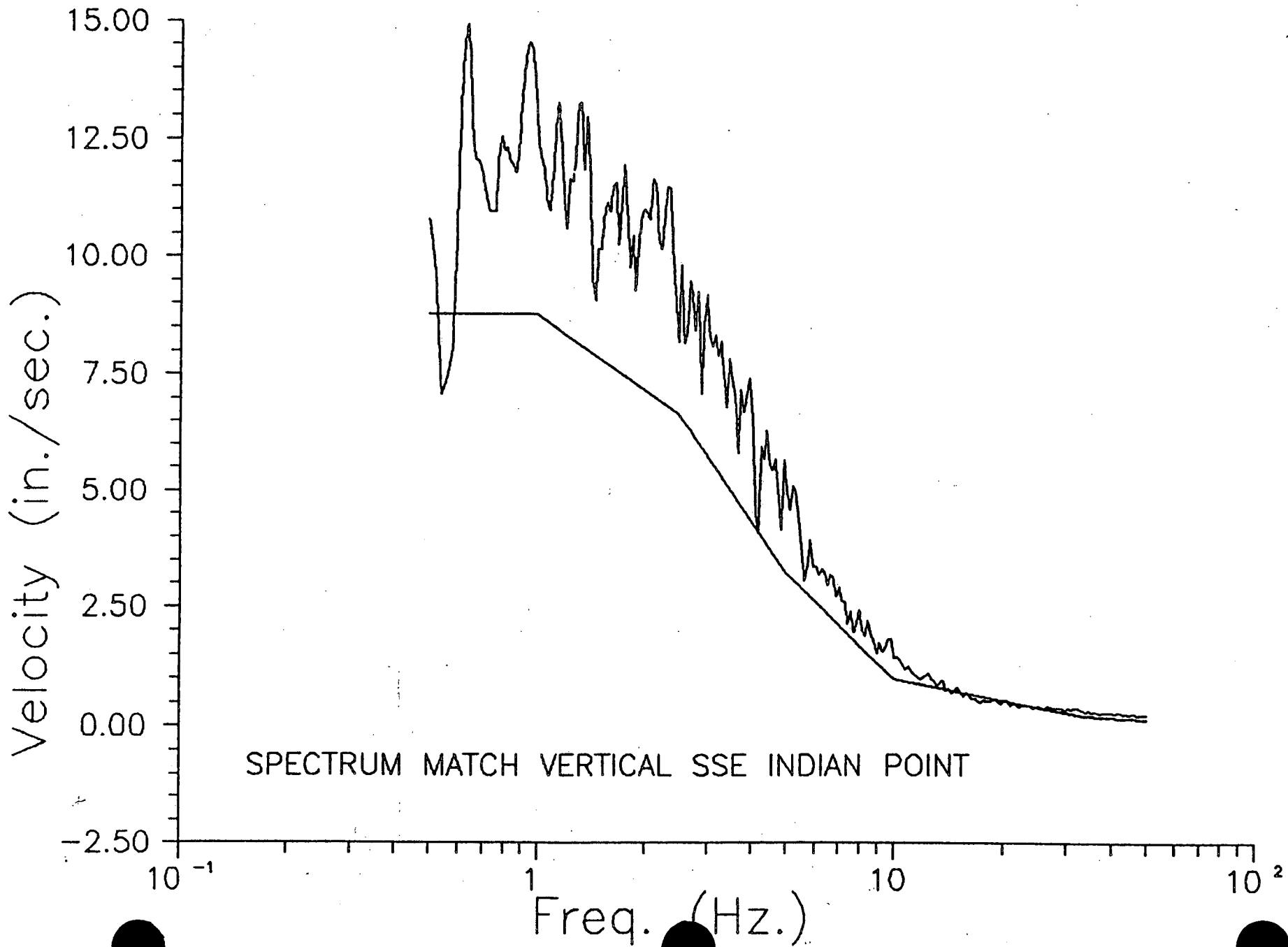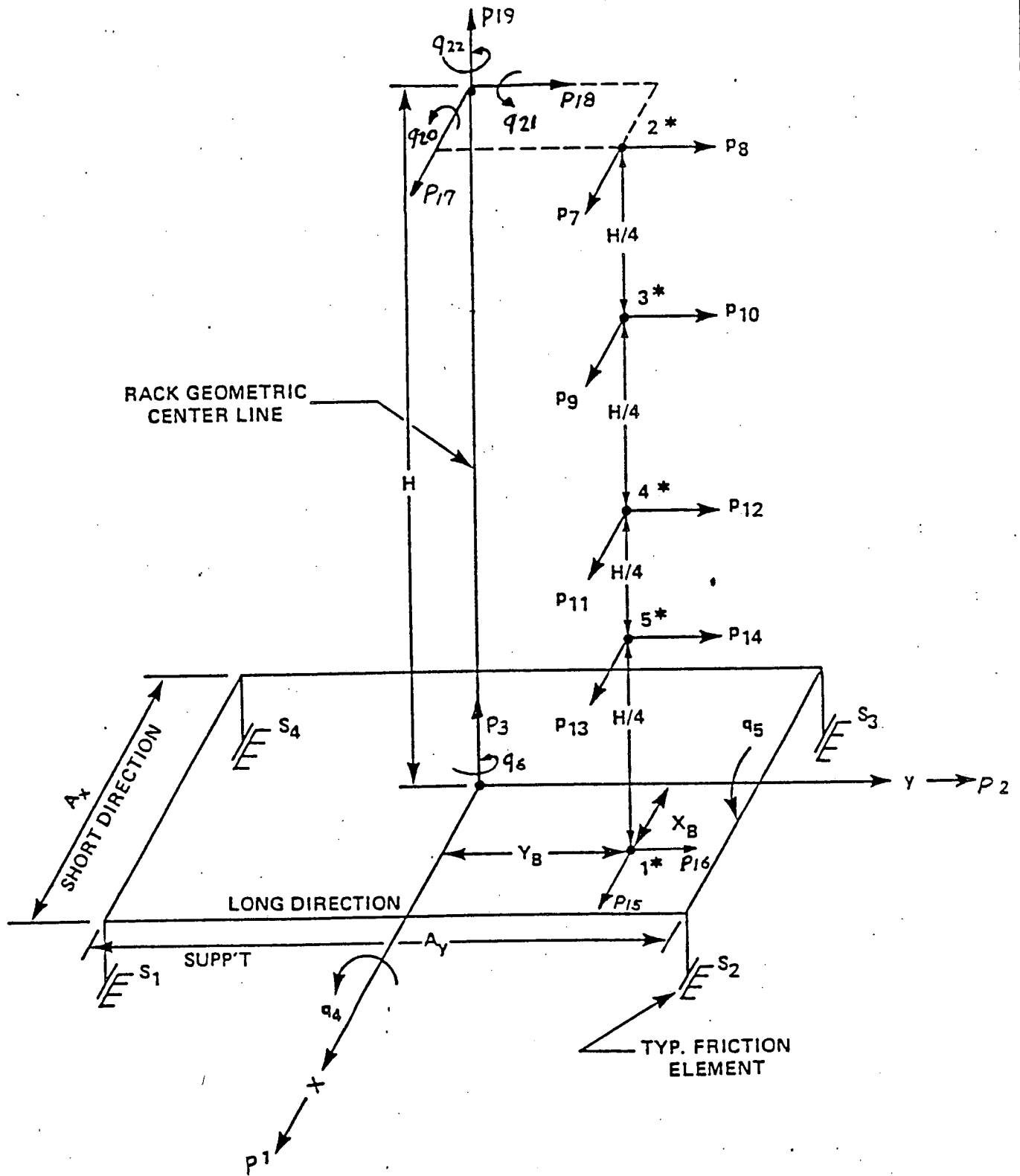
FIGURE 6.7

SCHEMATIC MODEL OF DYNARACK

Figure 6.8

TYPICAL TOP IMPACT ELEMENT

RACK STRUCTURE

TYP. BOTTOM IMPACT ELEMENT

6-50
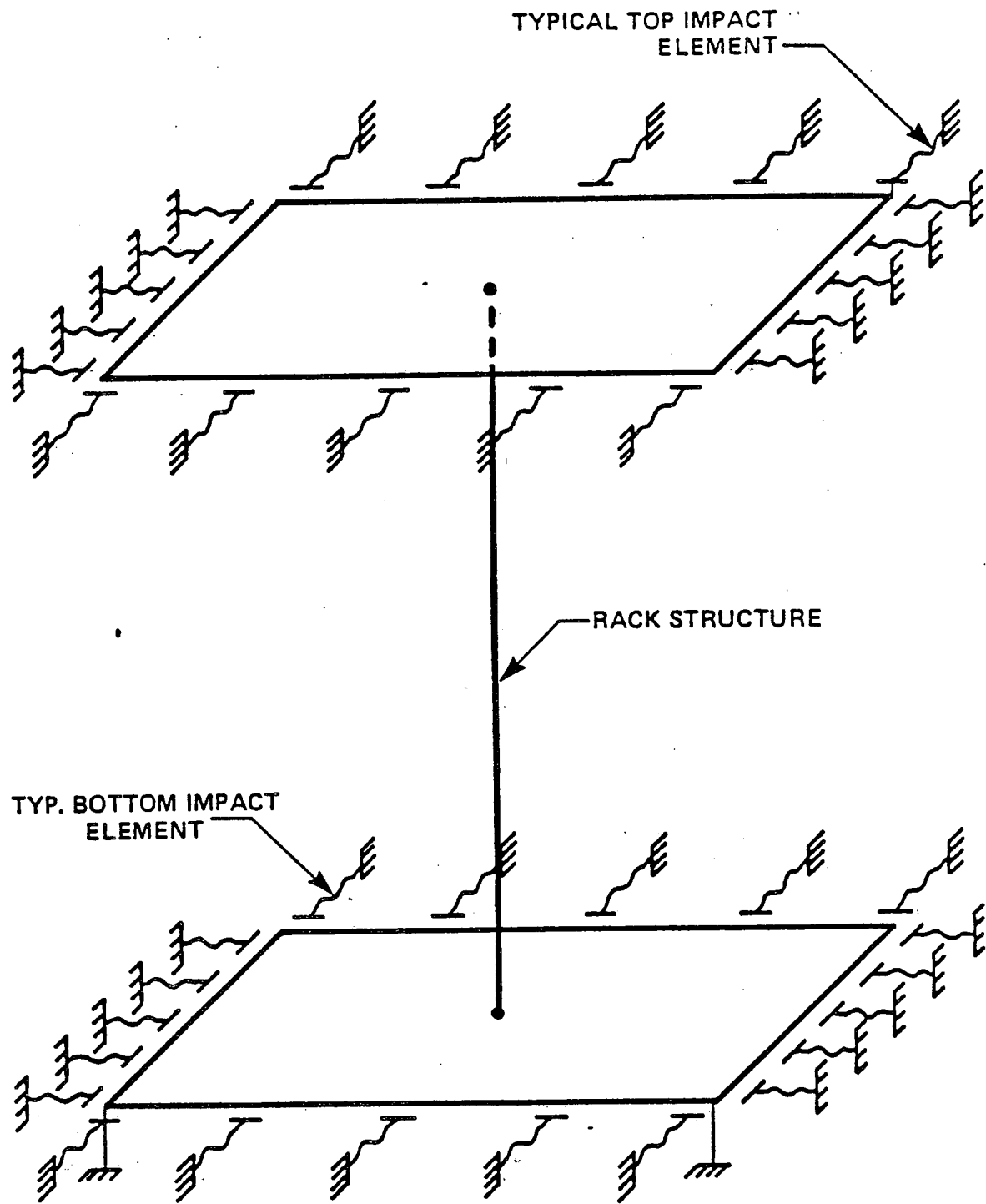
RACK-TO-RACK IMPACT SPRINGS

FIGURE   6.9

CELL WALL

MASS i

FUEL ASSEMBLY/CELL
IMPACT SPRING

X_B

Y_B

i*

Y

X
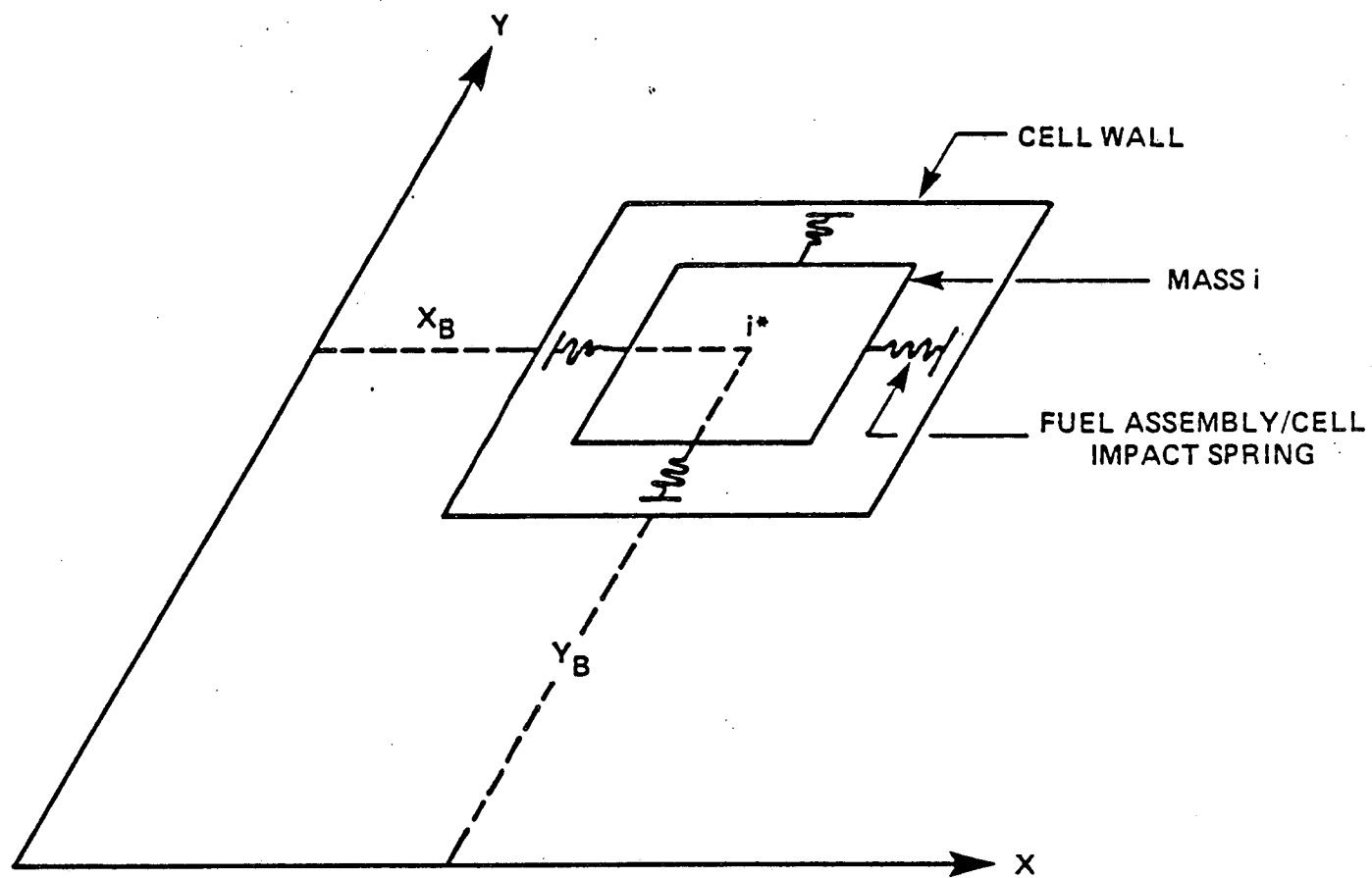
IMPACT SPRING ARRANGEMENT
AT NODE i
FIGURE 6.10
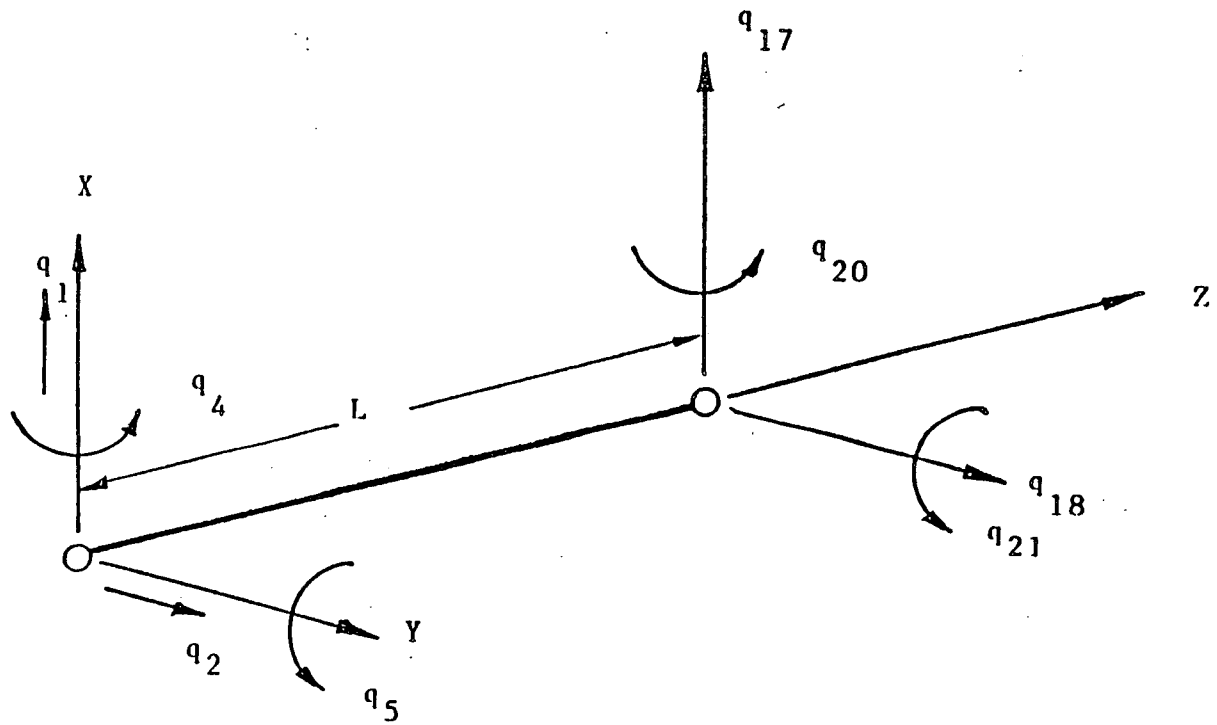
FIGURE 6.11   BEAM NODE MODEL
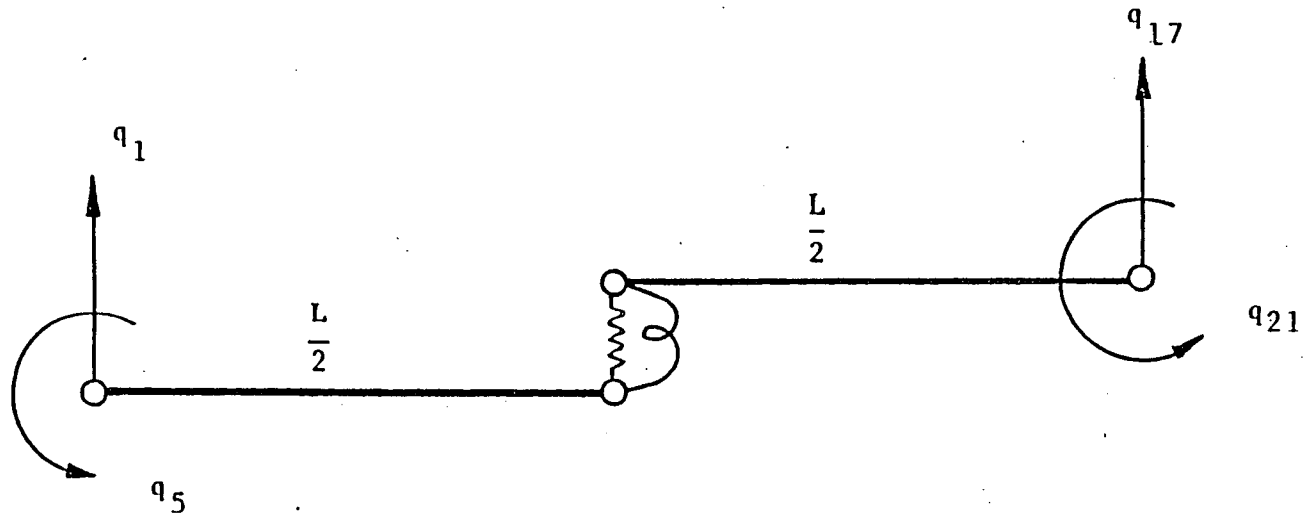
FIGURE 6.12   BEAM SHEAR AND BENDING SPRING
X-Z PLANE
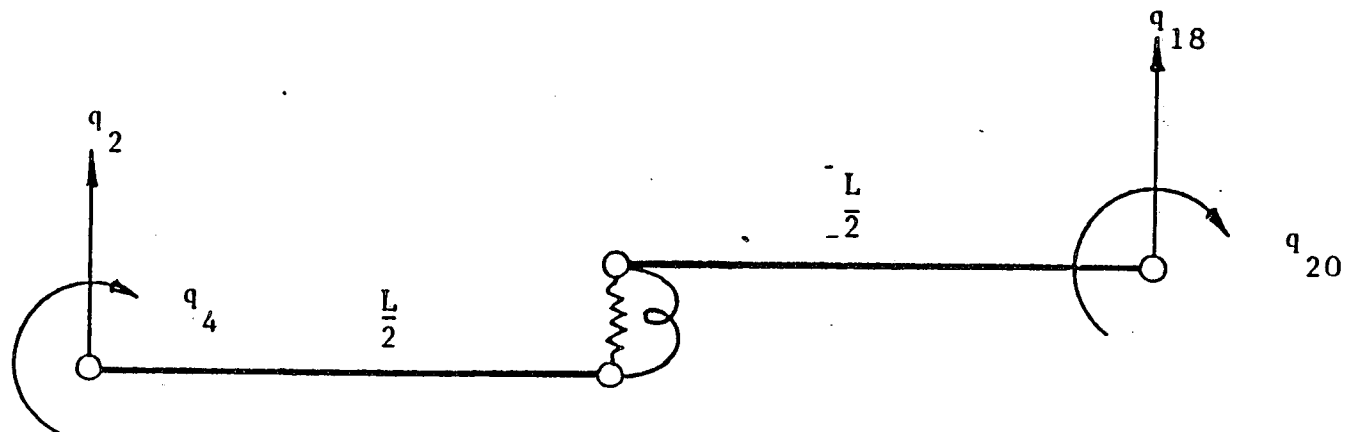
FIGURE 6.13   BEAM SHEAR AND BENDING SPRING
Y-Z PLANE

FUEL ASSY/CELL
IMPACT SPRING , K_I

0.25H

H/2

0.25H

RACK
C.G.

0.25H

H/2

0.25H

TYPICAL
RATTLING MASS

SUPPORT LEG
SPRING, K_S

FRICTION
INTERFACE
SPRING, K_f

FOUNDATION
ROTATIONAL COMPLIANCE
SPRING, K_R
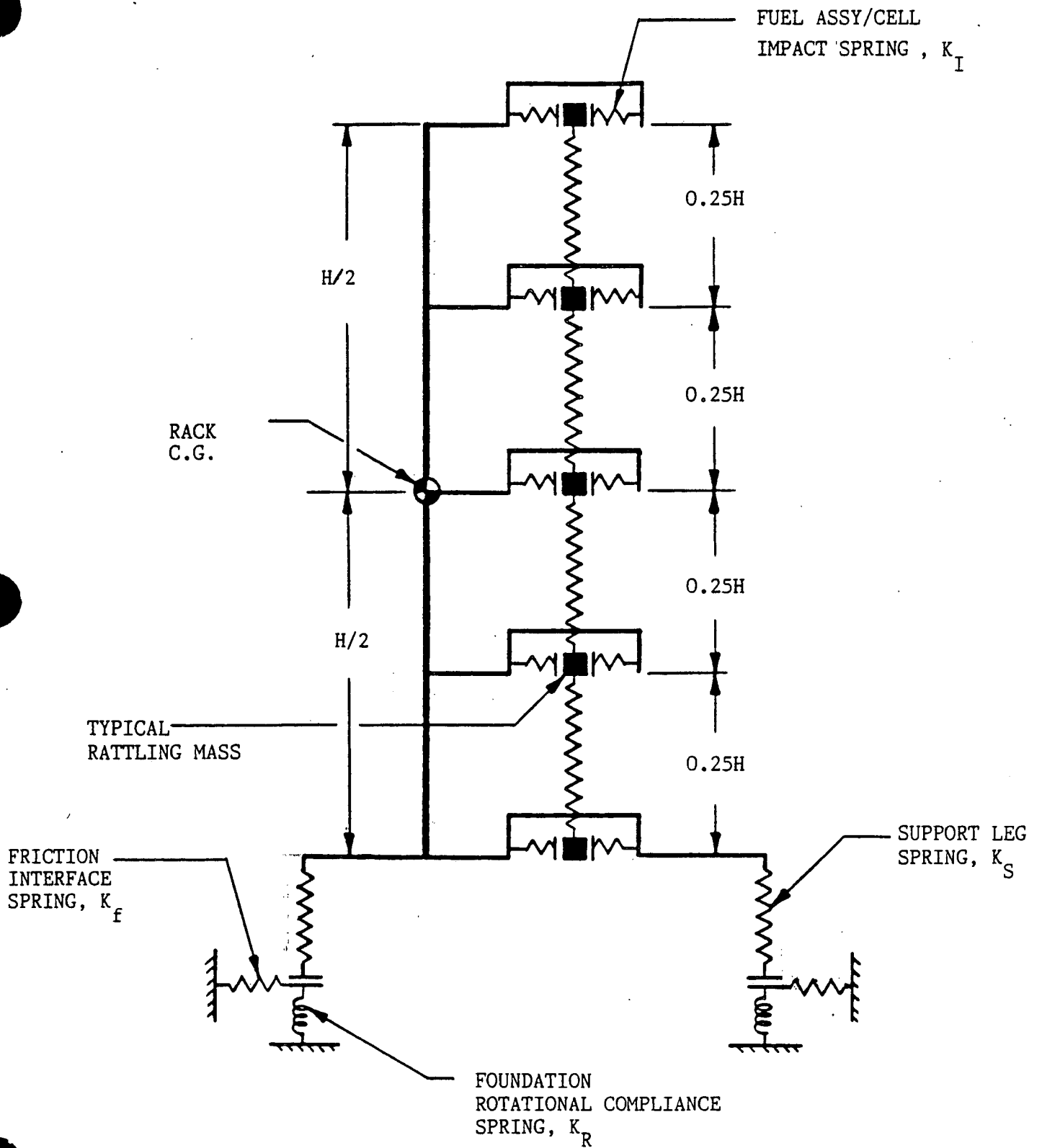
FIGURE 6.14 TWO DIMENSIONAL VIEW OF THE
SPRING-MASS SIMULATION

```
@(#)dynam0.f 1.12    @(#)
@(#)dynas1.f  1.2    12/12/88    @(#)
@(#)dynas2.f  1.16    @(#) 3.14    $
****************************************************
****************************************************
```

THIS PROGRAM HAS BEEN DEVELOPED TO SIMULATE THE
BEHAVIOR OF LUMPED MASS SYSTEMS UNDER TRANSIENT
LOADS. THIS VERSION OF THE CODE IS SUPPORTED BY
   HOLTEC   INC.
THE CODE HAS BEEN VERIFIED TO GIVE GOOD RESULTS
WHEN COMPARED AGAINST ANALYTICAL SOLUTIONS, BUT
THE USER BEARS THE SOLE RESPONSIBILITY FOR THE
CORRECTNESS OF HIS RESULTS AND THE WORK SHOULD
BE CHECKED ACCORDINGLY
O**

Ind. Pt. D 11x13 (Reg.2) df=dindpt.d0a,ccf=.8,cons.fuel,sse

       PROGRAM DYNARACK   --   HOLTEC INT. *****
O***

O   NRE =   30   NWR =   61   IWR =   5

      NTST=   O   IPLOT=   O   NTST1 =   O   NTST2=   O

      NTST3=   O

       FUELRACK DYNAMIC AND STRESS ANALYSIS
              ^@^@^@^@^@^@^@^@
O   NWR1=   61   NWR2=   62   NR1=   21   NR2=   22
NR3=   23

 RACK ELASTICITY IN RUN
O   STRESS COEFFICIENTS FOR RACK:
       CFX = 5.157E-03   CFY= 5.157E-03   CFZ = 5.157E-03
       CMX = 2.607E-04   CMY = 3.069E-04   CTX = 8.813E-04
CTY = 9.395E-04

O   STRESS COEFFICIENTS FOR SUPPORT TOP:
       CFX2 = 2.383E-02   CFY2 = 2.383E-02   CFZ2 = 2.383E-02
       CMX2 = 1.597E-02   CMY2 = 1.597E-02

1

O   STRESS COEFFICIENTS FOR SUPPORT BOTTOM
O   STRESS COEFFICIENTS FOR SUPPORT TOP:
         CFX2 = 4.850E-02   CFY2 = 4.850E-02   CFZ2 = 4.850E-02
         CMX2 = 6.230E-02   CMY2 = 6.230E-02

 STRESS COEFFICIENTS FOR FIXED FOOT 10
 5.56000000000000E-002   5.56000000000000E-002
 1.85000000000000E-002
 7.00700000000000E-003 7.00700000000000E-003
 ALLOWABLE STRESS VALUES FOR RACK
                          FOR SUPPORT TOP
                          FOR SUPPORT BOTTOM
                          FOR FIXED FOOT
 FTR,FAR,FVR,FBR=   15000.00   15000.00   10000.00   15000.00
 FTO,FAO,FVO,FBO=   15000.00   15000.00   10000.00   15000.00
 FTB,FAB,FVB,FBB=   63780.00   63780.00   42520.00   63780.00
 FTF,FAF,FVF,FBF=   15000.00   15000.00   10000.00   15000.00
 factors cd,cb for top,bottom,and rack
 these factors allow reduction for reduced geometry
 1.0 1.0 1.0 1.0 1.0 1.0 1.0 1.0
O   NZ = 22   NEWLDS= 0   NFV= 22

      MFV   =   7   NSV= 0   MSV   = 0   NIC= 0
 NSINF= 0

 NSINS= 0
O
O
O   H(HT. OF FUEL RACK,Z-DIRECTION FROM BASE)...... =   169.
      AX(WIDTH OF FUEL RACK, X-DIRECTION)........... =   100.
      AY(WIDTH OF FUEL RACK, Y-DIRECTION)........... =   118.
      DEL(TIME STEP FOR INTEGRATION)................. =   .500E-04
      TSTP(PRINT TIME INTERVAL)...................... =   5.00
      TTL(TOTAL ELAPSED RUN TIME)................... =   15.0
      EFF. X GAP IN X DIR. (Fluid mass calc.)....... =   .344
      EFFECTIVE DYNAMIC GAP FOR CALCULATING
          INTERNAL HYDRODYNAMIC COUPLING BETWEEN
          FUEL ASSEMBLIES AND CELL WALLS............. =   .187
      EFF. Y GAP IN Y DIR. (Fluid mass calc.)....... =   .461

O   DENW(MASS DENSITY OF WATER).................... =   .959E-04
      DRY WEIGHT OF RACK............................. =   .200E+05

2

```
WGTFUEL(          THE DRY WEIGHT OF A SINGLE
          LOADED FUEL ASSEMBLY)................... =  .300E+04
     Inside span of fuel cell..................... =  8.80
     Outside span of fuel assembly cluster......... =  8.43
     XBR(X COORD. OF FUEL ASSEMBLY GROUP).......... =  .000E+00
     YBR(Y COORD. OF FUEL ASSEMBLY GROUP).......... =  .000E+00



O     FAN(NO. OF FUEL ASSEMBLIES CONSIDERED IN GROUP)=  143.
      BA(COEF. K IN CASE 6 OF FRITZ S PAPER)........ =  .543
      FRA(EFFECTIVE METAL X-SECT AREA:FUEL RACK).... =  408.
      FRIZ..RACK POLAR MOMENT OF INERTIA............ =  .142E+05



   NU = 0 - no hydro mass update..NU=   0.00000000000000E+000
   Fuel Array file number =  1.0
   Area of individual cell = 1.356000000000000
    Inertia of individual cell= 18.469000000000001
   Radius of gyration of individual cell=  3.690557000000000


O     BETAD(STRUCTURAL DAMPING FACTOR MULTIPLYING
           SPRING STIFFNESSES)...................... =  .200E-02
      WSUP(WEIGHT OF ONE SUPPORT LEG)............... =  71.3
      ST8(TIME SPAN ENCOMPASSED BY ONE LINE OF INPUT
         DATA FROM FILES NR1,NR2,NR3).............. =  .600E-01
      ST9(AMPLICATION FACTOR FOR FORCE DATA ON NR1). =  1.00
      ST10(                     FORCE DATA ON NR2). =  1.00
      ST11(                     FORCE DATA ON NR3). =  1.00
      ST12(TIME INCREMENT FOR FORCE TIME FILES)..... =  .100E-01



O     NX   NO. OF CELLS IN X DIRECTION          =          11
      NY   NO. OF CELLS IN Y DIRECTION          =          13
      NFM IS NUMBER OF FUEL ASSEMBLY MASSES......... =           5
      FAN1(NO. OF CELLS IN FUEL RACK)............... =        143.
      EO(THICKNESS OF FUEL RACK SIDE PLATES)........ =  .380E-01
      E1(LENGTH OF FUEL RACK SUPPORT LEGS).......... =  6.00
      E2........................................... =  .500



   PARAMETER SETTINGS FOR EXTERNAL HYDRO MASS
     hydro z rotation coeff.= 1.0 1.0 1.0 1.0

                              3
```

hydro gaps.............= .687500000000000 1.750000000000000
.68750000000000 .525000000000000
hydro side gap coeff.....= .408000000000000 1.0 .408000000000000
.408000000000000
coeff. alfa1,alfa2,alfa3,alf4.....= 1.0 1.0 1.0 1.0
NSUP= 1XS= 45.479999999999997 YS= -54.479999999999997
NSUP= 2XS= 45.479999999999997 YS= 54.479999999999997
NSUP= 3XS= -45.479999999999997 YS= 54.479999999999997
NSUP= 4XS= -45.479999999999997 YS= -54.479999999999997
QUAD,XQ,YQ= 1   .00   .00
LEVEL,MQ =   1.100   2.200   3.200   4.200
5.300
QUAD,NQ=   11.00
 NUMBER OF SUPPORTS   4
 FUEL ASSEMBLY ARRAY IN RACK

   1 1 1 1 1 1 1 1 1 1 1 1 1
   1 1 1 1 1 1 1 1 1 1 1 1 1
   1 1 1 1 1 1 1 1 1 1 1 1 1
   1 1 1 1 1 1 1 1 1 1 1 1 1
   1 1 1 1 1 1 1 1 1 1 1 1 1
   1 1 1 1 1 1 1 1 1 1 1 1 1
   1 1 1 1 1 1 1 1 1 1 1 1 1
   1 1 1 1 1 1 1 1 1 1 1 1 1
   1 1 1 1 1 1 1 1 1 1 1 1 1
   1 1 1 1 1 1 1 1 1 1 1 1 1
   1 1 1 1 1 1 1 1 1 1 1 1 1

    positive X direction down, positive Y to right
   in prop thru double sum
O   *****DATA ABOVE : STOP ELEMENTS*****

ONON-LINEAR SPRING   1   C1=   .000D+00 C2= .496D+07 C3=
.992D+04
NC/CC= 3 .10D+01 4 -.54D+02 5 -.45D+02
   INITIAL FORCE =   .000E+00
O   *****DATA ABOVE : STOP ELEMENTS*****

ONON-LINEAR SPRING   2   C1=   .000D+00   C2=   .496D+07   C3=
.992D+04
NC/CC= 3 .10D+01 4 .54D+02 5 -.45D+02
   INITIAL FORCE =   .000E+00
O   *****DATA ABOVE : STOP ELEMENTS*****

ONON-LINEAR SPRING   3   C1=   .000D+00 C2= .496D+07 C3=
.992D+04

4

```
NC/CC= 3  .10D+01  4  .54D+02  5  .45D+02
   INITIAL FORCE =   .000E+00
O      *****DATA ABOVE : STOP ELEMENTS*****

ONON-LINEAR SPRING   4   C1=      .000D+00      C2=      .496D+07   C3=
.992D+04
NC/CC= 3  .10D+01  4 -.54D+02  5  .45D+02
   INITIAL FORCE =   .000E+00
O      *****DATA ABOVE : STOP ELEMENTS*****

ONON-LINEAR  SPRING     5   C1=      .374D+00  C2=  .126D+06   C3=
.251D+03
NC/CC= 7  .10D+01  1  .00D+00 17 -.10D+01  5  .00D+00 21  .00D+00
6  .00D+00 22  .00D+00
   INITIAL FORCE =   .000E+00
O      *****DATA ABOVE : STOP ELEMENTS*****

ONON-LINEAR  SPRING     6   C1=      .000D+00  C2=  .126D+06   C3=
.251D+03
NC/CC= 7 -.10D+01  1  .00D+00 17  .10D+01  5  .00D+00 21  .00D+00
6  .00D+00 22  .00D+00
   INITIAL FORCE =   .000E+00
O      *****DATA ABOVE : STOP ELEMENTS*****

ONON-LINEAR  SPRING     7   C1=      .374D+00  C2=  .176D+06   C3=
.352D+03
NC/CC= 8  .10D+01  2  .00D+00 18 -.10D+01  4  .00D+00 20  .00D+00
6  .00D+00 22  .00D+00
   INITIAL FORCE =   .000E+00
O      *****DATA ABOVE : STOP ELEMENTS*****

ONON-LINEAR  SPRING     8   C1=      .000D+00  C2=  .176D+06   C3=
.352D+03
NC/CC= 8 -.10D+01  2  .00D+00 18  .10D+01  4  .00D+00 20  .00D+00
6  .00D+00 22  .00D+00
   INITIAL FORCE =   .000E+00
O      *****DATA ABOVE : STOP ELEMENTS*****

ONON-LINEAR  SPRING     9   C1=      .327D+00  C2=  .126D+06   C3=
.251D+03
NC/CC= 9  .10D+01  1 -.16D+00 17 -.84D+00  5  .79D+01 21 -.24D+02
6  .00D+00 22  .00D+00
   INITIAL FORCE =   .000E+00
O      *****DATA ABOVE : STOP ELEMENTS*****

ONON-LINEAR  SPRING     10   C1=      .468D-01  C2=  .126D+06   C3=
```

```
.251D+03
NC/CC= 9 -.10D+01  1  .16D+00 17  .84D+00  5 -.79D+01 21  .24D+02
6  .00D+00 22  .00D+00
    INITIAL FORCE =   .000E+00
O       *****DATA ABOVE : STOP ELEMENTS*****


ONON-LINEAR  SPRING     11    C1=    .327D+00   C2=  .176D+06  C3=
.352D+03
NC/CC=10  .10D+01  2 -.16D+00 18 -.84D+00  4 -.79D+01 20  .24D+02
6  .00D+00 22  .00D+00
    INITIAL FORCE =   .000E+00
O       *****DATA ABOVE : STOP ELEMENTS*****


ONON-LINEAR  SPRING     12    C1=    .468D-01   C2=  .176D+06  C3=
.352D+03
NC/CC=10 -.10D+01  2  .16D+00 18  .84D+00  4  .79D+01 20 -.24D+02
6  .00D+00 22  .00D+00
    INITIAL FORCE =   .000E+00
O       *****DATA ABOVE : STOP ELEMENTS*****


ONON-LINEAR  SPRING     13    C1=    .281D+00   C2=  .126D+06  C3=
.251D+03
NC/CC=11  .10D+01  1 -.50D+00 17 -.50D+00  5  .21D+02 21 -.21D+02
6  .00D+00 22  .00D+00
    INITIAL FORCE =   .000E+00
O       *****DATA ABOVE : STOP ELEMENTS*****


ONON-LINEAR  SPRING     14    C1=    .935D-01   C2=  .126D+06  C3=
.251D+03
NC/CC=11 -.10D+01  1  .50D+00 17  .50D+00  5 -.21D+02 21  .21D+02
6  .00D+00 22  .00D+00
    INITIAL FORCE =   .000E+00
O       *****DATA ABOVE : STOP ELEMENTS*****


ONON-LINEAR  SPRING     15    C1=    .281D+00   C2=  .176D+06  C3=
.352D+03
NC/CC=12  .10D+01  2 -.50D+00 18 -.50D+00  4 -.21D+02 20  .21D+02
6  .00D+00 22  .00D+00
    INITIAL FORCE =   .000E+00
O       *****DATA ABOVE : STOP ELEMENTS*****


ONON-LINEAR  SPRING     16    C1=    .935D-01   C2=  .176D+06  C3=
.352D+03
NC/CC=12 -.10D+01  2  .50D+00 18  .50D+00  4  .21D+02 20 -.21D+02
6  .00D+00 22  .00D+00
    INITIAL FORCE =   .000E+00
```

6

O   *****DATA ABOVE : STOP ELEMENTS*****

ONON-LINEAR   SPRING   17   C1=   .234D+00   C2= .126D+06 C3=
.251D+03
NC/CC=13 .10D+01   1 -.84D+00 17 -.16D+00   5 .24D+02 21 -.79D+01
6 .00D+00 22 .00D+00
   INITIAL FORCE =   .000E+00
O   *****DATA ABOVE : STOP ELEMENTS*****

ONON-LINEAR   SPRING   18   C1=   .140D+00   C2= .126D+06 C3=
.251D+03
NC/CC=13 -.10D+01   1 .84D+00 17 .16D+00   5 -.24D+02 21 .79D+01
6 .00D+00 22 .00D+00
   INITIAL FORCE =   .000E+00
O   *****DATA ABOVE : STOP ELEMENTS*****

ONON-LINEAR   SPRING   19   C1=   .234D+00   C2= .176D+06 C3=
.352D+03
NC/CC=14 .10D+01   2 -.84D+00 18 -.16D+00   4 -.24D+02 20 .79D+01
6 .00D+00 22 .00D+00
   INITIAL FORCE =   .000E+00
O   *****DATA ABOVE : STOP ELEMENTS*****

ONON-LINEAR   SPRING   20   C1=   .140D+00   C2= .176D+06 C3=
.352D+03
NC/CC=14 -.10D+01   2 .84D+00 18 .16D+00   4 .24D+02 20 -.79D+01
6 .00D+00 22 .00D+00
   INITIAL FORCE =   .000E+00
O   *****DATA ABOVE : STOP ELEMENTS*****

ONON-LINEAR   SPRING   21   C1=   .187D+00   C2= .126D+06 C3=
.251D+03
NC/CC=15 .10D+01   1 -.10D+01 17 .00D+00   5 .00D+00 21 .00D+00
6 .00D+00 22 .00D+00
   INITIAL FORCE =   .000E+00
O   *****DATA ABOVE : STOP ELEMENTS*****

ONON-LINEAR   SPRING   22   C1=   .187D+00   C2= .126D+06 C3=
.251D+03
NC/CC=15 -.10D+01   1 .10D+01 17 .00D+00   5 .00D+00 21 .00D+00
6 .00D+00 22 .00D+00
   INITIAL FORCE =   .000E+00
O   *****DATA ABOVE : STOP ELEMENTS*****

ONON-LINEAR   SPRING   23   C1=   .187D+00   C2= .176D+06 C3=
.352D+03

7

```
NC/CC=16  .10D+01  2 -.10D+01 18  .00D+00  4  .00D+00 20  .00D+00
6  .00D+00 22  .00D+00
    INITIAL FORCE =  .000E+00
O      *****DATA ABOVE : STOP ELEMENTS*****

ONON-LINEAR   SPRING     24    C1=     .187D+00   C2=  .176D+06  C3=
.352D+03
NC/CC=16 -.10D+01  2  .10D+01 18  .00D+00  4  .00D+00 20  .00D+00
6  .00D+00 22  .00D+00
    INITIAL FORCE =  .000E+00
O      *****DATA ABOVE : STOP ELEMENTS*****

ONON-LINEAR   SPRING     25    C1=     .688D+00   C2=  .100D+03  C3=
.200D+00
NC/CC= 1  .10D+01  6  .59D+02
    INITIAL FORCE =  .000E+00
O      *****DATA ABOVE : STOP ELEMENTS*****

ONON-LINEAR SPRING  26   C1=     .688D+00    C2=    .100D+03   C3=
.200D+00
NC/CC= 1  .10D+01  6 -.59D+02
    INITIAL FORCE =  .000E+00
O      *****DATA ABOVE : STOP ELEMENTS*****

ONON-LINEAR   SPRING     27    C1=     .688D+00    C2= .100D+03  C3=
.200D+00
NC/CC= 1 -.10D+01  6 -.59D+02
    INITIAL FORCE =  .000E+00
O      *****DATA ABOVE : STOP ELEMENTS*****

ONON-LINEAR SPRING  28   C1=     .688D+00    C2=    .100D+03   C3=
.200D+00
NC/CC= 1 -.10D+01  6  .59D+02
    INITIAL FORCE =  .000E+00
O      *****DATA ABOVE : STOP ELEMENTS*****

ONON-LINEAR   SPRING     29    C1=     .175D+01   C2=  .100D+03  C3=
.200D+00
NC/CC= 2  .10D+01  6  .50D+02
    INITIAL FORCE =  .000E+00
O      *****DATA ABOVE : STOP ELEMENTS*****

ONON-LINEAR SPRING  30   C1=     .175D+01    C2=    .100D+03   C3=
.200D+00
NC/CC= 2  .10D+01  6 -.50D+02
    INITIAL FORCE =  .000E+00
```

8

O   *****DATA ABOVE : STOP ELEMENTS*****

ONON-LINEAR   SPRING   31   C1=   .625D+00   C2=   .100D+03   C3=
.200D+00
NC/CC= 2 -.10D+01   6 -.50D+02
   INITIAL FORCE =   .000E+00
O   *****DATA ABOVE : STOP ELEMENTS*****

ONON-LINEAR SPRING   32   C1=   .625D+00   C2=   .100D+03   C3=
.200D+00
NC/CC= 2 -.10D+01   6 .50D+02
   INITIAL FORCE =   .000E+00
O   *****DATA ABOVE : STOP ELEMENTS*****

ONON-LINEAR   SPRING   33   C1=   .688D+00   C2=   .100D+02   C3=
.200D-01
NC/CC=17 .10D+01   6 .59D+02
   INITIAL FORCE =   .000E+00
O   *****DATA ABOVE : STOP ELEMENTS*****

ONON-LINEAR SPRING   34   C1=   .688D+00   C2=   .100D+02   C3=
.200D-01
NC/CC=17 .10D+01   6 -.59D+02
   INITIAL FORCE =   .000E+00
O   *****DATA ABOVE : STOP ELEMENTS*****

ONON-LINEAR   SPRING   35   C1=   .688D+00   C2=   .100D+02   C3=
.200D-01
NC/CC=17 -.10D+01   6 -.59D+02
   INITIAL FORCE =   .000E+00
O   *****DATA ABOVE : STOP ELEMENTS*****

ONON-LINEAR SPRING   36   C1=   .688D+00   C2=   .100D+02   C3=
.200D-01
NC/CC=17 -.10D+01   6 .59D+02
   INITIAL FORCE =   .000E+00
O   *****DATA ABOVE : STOP ELEMENTS*****

ONON-LINEAR   SPRING   37   C1=   .175D+01   C2=   .100D+02   C3=
.200D-01
NC/CC=18 .10D+01   6 .50D+02
   INITIAL FORCE =   .000E+00
O   *****DATA ABOVE : STOP ELEMENTS*****

ONON-LINEAR SPRING   38   C1=   .175D+01   C2=   .100D+02   C3=
.200D-01

9

```
NC/CC=18  .10D+01  6 -.50D+02
   INITIAL FORCE =   .000E+00
O      *****DATA ABOVE : STOP ELEMENTS*****

ONON-LINEAR  SPRING    39   C1=    .625D+00   C2= .100D+02  C3=
.200D-01
NC/CC=18 -.10D+01  6 -.50D+02
   INITIAL FORCE =   .000E+00
O      *****DATA ABOVE : STOP ELEMENTS*****

ONON-LINEAR SPRING   40   C1=    .625D+00    C2=    .100D+02   C3=
.200D-01
NC/CC=18 -.10D+01  6  .50D+02
   INITIAL FORCE =   .000E+00
OFRICTION ELEMENT    1  N1=-101  C1=  .800D+00  C2=  .193781D+10
NC/CC= 1  .10D+01  6  .54D+02  5 -.60D+01
OFRICTION ELEMENT    2  N1=   0  C1=  .800D+00  C2=  .193781D+10
NC/CC= 2  .10D+01  6  .45D+02  4  .60D+01
OFRICTION ELEMENT    3  N1=-102  C1=  .800D+00  C2=  .193781D+10
NC/CC= 1  .10D+01  6 -.54D+02  5 -.60D+01
OFRICTION ELEMENT    4  N1=   0  C1=  .800D+00  C2=  .193781D+10
NC/CC= 2  .10D+01  6  .45D+02  4  .60D+01
OFRICTION ELEMENT    5  N1=-103  C1=  .800D+00  C2=  .193781D+10
NC/CC= 1  .10D+01  6 -.54D+02  5 -.60D+01
OFRICTION ELEMENT    6  N1=   0  C1=  .800D+00  C2=  .193781D+10
NC/CC= 2  .10D+01  6 -.45D+02  4  .60D+01
OFRICTION ELEMENT    7  N1=-104  C1=  .800D+00  C2=  .193781D+10
NC/CC= 1  .10D+01  6  .54D+02  5 -.60D+01
OFRICTION ELEMENT    8  N1=   0  C1=  .800D+00  C2=  .193781D+10
NC/CC= 2  .10D+01  6 -.45D+02  4  .60D+01
OFRICTION ELEMENT    9  N1=-101  C1=  .275D+01  C2=  .566772D+08
NC/CC= 4  .10D+01
OFRICTION ELEMENT   10  N1=   0  C1=  .275D+01  C2=  .566772D+08
NC/CC= 5  .10D+01
OFRICTION ELEMENT   11  N1=-102  C1=  .275D+01  C2=  .566772D+08
NC/CC= 4  .10D+01
OFRICTION ELEMENT   12  N1=   0  C1=  .275D+01  C2=  .566772D+08
NC/CC= 5  .10D+01
OFRICTION ELEMENT   13  N1=-103  C1=  .275D+01  C2=  .566772D+08
NC/CC= 4  .10D+01
OFRICTION ELEMENT   14  N1=   0  C1=  .275D+01  C2=  .566772D+08
NC/CC= 5  .10D+01
OFRICTION ELEMENT   15  N1=-104  C1=  .275D+01  C2=  .566772D+08
NC/CC= 4  .10D+01
OFRICTION ELEMENT   16  N1=   0  C1=  .275D+01  C2=  .566772D+08
NC/CC= 5  .10D+01
```

10

O   ****UNMODIFIED INPUT ABOVE :SPRING-DAMPER ELEMENTS ****

 spring element 1 is for v**2 fluid effects
OSPRING ELEMENT   1 C1= .000D+00 C2=   .000000D+00
NC/CC= 1 .10D+01
    NON LINEAR DAMPING COEF=-1.10953D+03
    INITIAL FORCE =   .000E+00
O   ****UNMODIFIED INPUT ABOVE :SPRING-DAMPER ELEMENTS ****

 spring element 2 is for v**2 fluid effects
OSPRING ELEMENT   2 C1= .000D+00 C2=   .000000D+00
NC/CC= 2 .10D+01
    NON LINEAR DAMPING COEF=-6.75296D+02
    INITIAL FORCE =   .000E+00
O   ****UNMODIFIED INPUT ABOVE :SPRING-DAMPER ELEMENTS ****

 spring element 3 is for v**2 fluid effects
OSPRING ELEMENT   3 C1= .000D+00 C2=   .000000D+00
NC/CC=17 .10D+01
    NON LINEAR DAMPING COEF=-1.10953D+03
    INITIAL FORCE =   .000E+00
O   ****UNMODIFIED INPUT ABOVE :SPRING-DAMPER ELEMENTS ****

 spring element 4 is for v**2 fluid effects
OSPRING ELEMENT   4 C1= .000D+00 C2=   .000000D+00
NC/CC=18 .10D+01
    NON LINEAR DAMPING COEF=-6.75296D+02
    INITIAL FORCE =   .000E+00
O   ****UNMODIFIED INPUT ABOVE :SPRING-DAMPER ELEMENTS ****

OSPRING ELEMENT   5 C1= .538D+08 C2=   .268922D+11
NC/CC=21 .10D+01 5 -.10D+01
    INITIAL FORCE =   .000E+00
O   ****UNMODIFIED INPUT ABOVE :SPRING-DAMPER ELEMENTS ****

OSPRING ELEMENT   6 C1= .361D+03 C2=   .180392D+06
NC/CC=17 .10D+01 21 -.85D+02 1 -.10D+01 5 -.85D+02
    INITIAL FORCE =   .000E+00
O   ****UNMODIFIED INPUT ABOVE :SPRING-DAMPER ELEMENTS ****

11

OSPRING ELEMENT   7 C1= .747D+08 C2= .373609D+11
NC/CC=20 -.10D+01   4 .10D+01
    INITIAL FORCE =   .000E+00
O   ****UNMODIFIED INPUT ABOVE :SPRING-DAMPER ELEMENTS ****

OSPRING ELEMENT   8 C1= .690D+03 C2= .345129D+06
NC/CC=18 .10D+01 20 .85D+02 2 -.10D+01   4 .85D+02
    INITIAL FORCE =   .000E+00
O   ****UNMODIFIED INPUT ABOVE :SPRING-DAMPER ELEMENTS ****

OSPRING ELEMENT   9 C1= .640D+05 C2= .320121D+08
NC/CC=19 .10D+01   3 -.10D+01
    INITIAL FORCE =   .000E+00
O   ****UNMODIFIED INPUT ABOVE :SPRING-DAMPER ELEMENTS ****

OSPRING ELEMENT   10 C1= .183D+07 C2= .917154D+09
NC/CC=22 .10D+01   6 -.10D+01
    INITIAL FORCE =   .000E+00
O   ****UNMODIFIED INPUT ABOVE :SPRING-DAMPER ELEMENTS ****

OSPRING ELEMENT   11 C1= .000D+00 C2= .000000D+00
NC/CC= 7 .42D+02   9 -.85D+02 11 .42D+02
    INITIAL FORCE =   .000E+00
O   ****UNMODIFIED INPUT ABOVE :SPRING-DAMPER ELEMENTS ****

OSPRING ELEMENT   12 C1= .000D+00 C2= .000000D+00
NC/CC= 9 .42D+02 11 -.85D+02 13 .42D+02
    INITIAL FORCE =   .000E+00
O   ****UNMODIFIED INPUT ABOVE :SPRING-DAMPER ELEMENTS ****

OSPRING ELEMENT   13 C1= .000D+00 C2= .000000D+00
NC/CC=11 .42D+02 13 -.85D+02 15 .42D+02
    INITIAL FORCE =   .000E+00
O   ****UNMODIFIED INPUT ABOVE :SPRING-DAMPER ELEMENTS ****

OSPRING ELEMENT   14 C1= .000D+00 C2= .000000D+00
NC/CC= 8 .42D+02 10 -.85D+02 12 .42D+02
    INITIAL FORCE =   .000E+00

O   ****UNMODIFIED INPUT ABOVE :SPRING-DAMPER ELEMENTS ****

OSPRING ELEMENT 15 C1= .000D+00 C2= .000000D+00
NC/CC=10 .42D+02 12 -.85D+02 14 .42D+02
    INITIAL FORCE = .000E+00
O   ****UNMODIFIED INPUT ABOVE :SPRING-DAMPER ELEMENTS ****

OSPRING ELEMENT 16 C1= .000D+00 C2= .000000D+00
NC/CC=12 .42D+02 14 -.85D+02 16 .42D+02
    INITIAL FORCE = .000E+00
    Pstat,jsup,xcen,ycen=   446444.370454884370000   4
0.00000000000000E+000
  0.00000000000000E+000
    Z30,R40,R50= -.2250E-01 .0000E+00 .0000E+00
    parameter xinc= -1.0
    fluid coupling v**2 terms included
                    FREQ=   168.06690772
        DT=   .00094745
                    FREQ=   223.65314613
        DT=   .00071198
                    FREQ=   26.29693338
        DT=   .00605529
                    FREQ=   51.91679691
        DT=   .00306713
                    FREQ=   62.11657330
        DT=   .00256350
                    FREQ=   36.76367486
        DT=   .00433133
                    FREQ=   1.86061121
        DT=   .08558245
                    FREQ=   2.15698359
        DT=   .07382331
                    FREQ=   2.30170534
        DT=   .06918160
                    FREQ=   2.69530391
        DT=   .05907893
                    FREQ=   2.30925525
        DT=   .06895542
                    FREQ=   2.71371658
        DT=   .05867807
                    FREQ=   2.30419129
        DT=   .06910696
                    FREQ=   2.70554937
        DT=   .05885521

13

```
                         FREQ=        3.26836380
        DT=        .04872030
                         FREQ=        3.84838953
        DT=        .04137722
                         FREQ=        1.01834996
        DT=        .15636635
                         FREQ=        1.85771824
        DT=        .08571572
                         FREQ=      166.60059776
        DT=        .00095579
                         FREQ=       23.94275300
        DT=        .00665068
                         FREQ=       28.69782979
        DT=        .00554870
                         FREQ=         .17819212
        DT=        .89361788
**********,DEL1=        .00005000 NODE=    0
  nz= 22 mx= 16 my= 16 mw= 40
  max value,nz,mx,my,mw= 40
    0.0000E+00  -6.8972E-02    2.7808E-02     7.3752E-02    5.4799E-02
-3.2466E-02 -1.3655E-01
    0.0000E+00   1.3659E-01    1.2944E-01     6.7176E-02    1.3699E-02
-9.5228E-02 -1.0548E-01
    0.0000E+00  -9.5217E-02   -1.9940E-01    -2.6637E-01   -2.7115E-01
-2.5261E-01 -2.0500E-01
    0.0000E+00   1.0000E-02    2.0000E-02     3.0000E-02    4.0000E-02
 5.0000E-02   6.0000E-02
O              **********          TIME =       .00000D+00
**********
O                    DISPLACEMENT OF SPRING ELEMENTS
OX=      .000000D+00      .000000D+00      .000000D+00      .000000D+00
.000000D+00  .000000D+00  .000000D+00   .000000D+00
      .000000D+00      .000000D+00      .000000D+00      .000000D+00
.000000D+00  .000000D+00  .000000D+00   .000000D+00
O                    SPRING DAMPER ELEMENT FORCES
OFX=  -.00000D+00 -.00000D+00 -.00000D+00 -.00000D+00 -.00000D+00
-.00000D+00 -.00000D+00 -.00000D+00 -.00000D+00
      -.00000D+00 -.00000D+00 -.00000D+00 -.00000D+00 -.00000D+00
-.00000D+00 -.00000D+00
O                    DISPLACEMENT OF FRICTION CONTACTS
OY=      .000000D+00      .000000D+00      .000000D+00      .000000D+00
.000000D+00  .000000D+00  .000000D+00   .000000D+00
      .000000D+00      .000000D+00      .000000D+00      .000000D+00
.000000D+00  .000000D+00  .000000D+00   .000000D+00
O                    FRICTION CONTACTS FORCES
OFY=   .00000D+00  .00000D+00  .00000D+00  .00000D+00  .00000D+00
```

```
.00000D+00   .00000D+00   .00000D+00   .00000D+00
        .00000D+00   .00000D+00   .00000D+00   .00000D+00   .00000D+00
.00000D+00   .00000D+00
0                    DISPLACEMENT OF NON-LINEAR SPRINGS
OW=      -.225009D-01   -.225009D-01   -.225009D-01   -.225009D-01
.000000D+00   .000000D+00   .000000D+00   .000000D+00
        .000000D+00       .000000D+00       .000000D+00       .000000D+00
.000000D+00   .000000D+00   .000000D+00   .000000D+00
        .000000D+00       .000000D+00       .000000D+00       .000000D+00
.000000D+00   .000000D+00   .000000D+00   .000000D+00
        .000000D+00       .000000D+00       .000000D+00       .000000D+00
.000000D+00   .000000D+00   .000000D+00   .000000D+00
        .000000D+00       .000000D+00       .000000D+00       .000000D+00
.000000D+00   .000000D+00   .000000D+00   .000000D+00
0                    NON-LINEAR SPRING FORCES
OFW=    .11161D+06   .11161D+06   .11161D+06   .11161D+06   .00000D+00
.00000D+00   .00000D+00   .00000D+00   .00000D+00
        .00000D+00   .00000D+00   .00000D+00   .00000D+00   .00000D+00
.00000D+00   .00000D+00   .00000D+00   .00000D+00
        .00000D+00   .00000D+00   .00000D+00   .00000D+00   .00000D+00
.00000D+00   .00000D+00   .00000D+00   .00000D+00
        .00000D+00   .00000D+00   .00000D+00   .00000D+00   .00000D+00
.00000D+00   .00000D+00   .00000D+00   .00000D+00
        .00000D+00   .00000D+00   .00000D+00   .00000D+00
0                    GENERALIZED DISPLACEMENTS
OZ=        .000000D+00       .000000D+00   -.225009D-01       .000000D+00
.000000D+00   .000000D+00   .000000D+00   .000000D+00
        .000000D+00       .000000D+00       .000000D+00       .000000D+00
.000000D+00   .000000D+00   .000000D+00   .000000D+00
        .000000D+00       .000000D+00   -.225009D-01       .000000D+00
.000000D+00   .000000D+00


    FINAL SUMMARY FOR THIS RUN
Ind.Pt.  D   11x13 (Reg.2)  df=dindpt.d0a,ccf=.8,cons.fuel,sse

    MAX.FLOOR LOAD= 4.933D+05
     MAX.IMPACT FORCES
        GAP ELEMENT         MAX.FORCE           TIME
                1           1.818D+05           6.588D+00
                2           1.818D+05           9.416D+00
                3           1.838D+05           1.016D+01
                4           1.802D+05           7.299D+00
                5           4.341D+04           9.997D+00
                6           3.879D+04           9.469D+00
                7           2.961D+04           1.384D+01
                8           2.671D+04           1.434D+01
```

15

9	3.460D+04	1.500D+01
10	3.180D+04	1.458D+01
11	5.524D+04	8.157D+00
12	5.618D+04	8.507D+00
13	3.181D+04	1.278D+01
14	3.160D+04	1.232D+01
15	5.006D+04	1.071D+01
16	4.746D+04	1.107D+01
17	2.132D+04	7.147D+00
18	2.234D+04	1.476D+01
19	4.625D+04	1.078D+01
20	4.370D+04	1.116D+01
21	1.295D+04	1.178D+01
22	1.503D+04	9.287D+00
23	2.180D+04	7.492D+00
24	2.414D+04	9.387D+00
25	0.000D+00	0.000D+00
26	0.000D+00	0.000D+00
27	0.000D+00	0.000D+00
28	0.000D+00	0.000D+00
29	0.000D+00	0.000D+00
30	0.000D+00	0.000D+00
31	0.000D+00	0.000D+00
32	0.000D+00	0.000D+00
33	0.000D+00	0.000D+00
34	0.000D+00	0.000D+00
35	0.000D+00	0.000D+00
36	0.000D+00	0.000D+00
37	0.000D+00	0.000D+00
38	0.000D+00	0.000D+00
39	0.000D+00	0.000D+00
40	0.000D+00	0.000D+00

FLUID DAMPER	MAX. FORCE
1	2.077D-04
2	4.194D-04
3	3.943D+03
4	3.674D+03
5	4.340D+06
6	5.272D+04
7	6.031D+06
8	6.939D+04
9	1.330D+03
10	4.345D+02
11	0.000D+00
12	0.000D+00
13	0.000D+00

```
           14              0.000D+00
           15             '0.000D+00
           16              0.000D+00
PAD MOVEMENTS IF ANY
            1              0.000D+00
            2              0.000D+00
            3              0.000D+00
            4              0.000D+00
            5              0.000D+00
            6              0.000D+00
            7              0.000D+00
            8              0.000D+00
                  NODE     XTIME  UXMAX      YTIME        UYMAX
            1              1190     .3442      440          .2501
            2              1190     .0013      440          .0012
  RTIME=   1190 ROTMAX = .4737E-06
 VZ=    .00000D+00 at time=      0  VFOOT=  .00000D+00   at time    0
 max.thetax,thetay(radians)=   .2029E-03 .2235E-03
  MAX.LINER SHEAR FORCE=        17434.  VERT.FORCE=      158665.
  MAX.LINER VERT. FORCE=       183735.  SHEAR FORCE=      12391.
  max movements at rack top
 rotx,roty, at top= 3.63989319157717E-004 3.77570469393786E-004
  max. total fuel impact load over height
 pxx,pyy= 73661.639837163733000 119978.31556294651000


   STRESS COEFFICIENTS AT TOP OF RACK
   fzedge,fz0,xvs,yvs,xmm,ymm for k=1,6
 1      .134D-01       .111D-04      .434D-06       .277D-06       .359D-04
.227D-04
 2         .744D-02    .410D-04      .278D-06       .120D-06       .231D-04
.979D-05
 3      .102D-01       .536D-05      .727D-06       .976D-07       .605D-04
.799D-05
 4         .983D-02    .122D-04      .115D-07       .500D-06       .101D-05
.413D-04
 5      .102D-01       .536D-05      .727D-06       .976D-07       .605D-04
.799D-05
 6         .983D-02    .122D-04      .115D-07       .500D-06       .101D-05
.413D-04


        STRUCTURAL ACCEPTANCE-ASME NF
             SECTION NUMBER      1
 R 1=  .138AT TIME   660  R2=  .018AT TIME 1195  R3=    .011AT TIME
440
 R 4=    .012AT TIME 1190  R5=  .148AT TIME   660  R6=  .149AT TIME
660
```

17

```
R 7=   .020AT TIME   444   R8=   .011AT TIME   440   R9=   .012AT TIME
1190
   R10=   .148AT TIME   660   R*=   .149AT TIME   660   R
             SECTION NUMBER    2
   R 1=   .289AT TIME   660   R2=   .037AT TIME 1195   R3=   .100AT TIME
444
   R 4=   .085AT TIME 1195   R5=   .355AT TIME   661   R6=   .366AT TIME
661
   R 7=   .042AT TIME   444   R8=   .100AT TIME   444   R9=   .085AT TIME
1195
   R10=   .355AT TIME   661   R*=   .366AT TIME   661   R
             SECTION NUMBER    3
   R 1=   .138AT TIME   943   R2=   .018AT TIME 1195   R3=   .011AT TIME
440
   R 4=   .012AT TIME 1190   R5=   .148AT TIME   943   R6=   .150AT TIME
943
   R 7=   .020AT TIME   444   R8=   .011AT TIME   440   R9=   .012AT TIME
1190
   R10=   .148AT TIME   943   R*=   .150AT TIME   943   R
             SECTION NUMBER    4
   R 1=   .289AT TIME   943   R2=   .037AT TIME 1195   R3=   .100AT TIME
444
   R 4=   .085AT TIME 1195   R5=   .360AT TIME   943   R6=   .373AT TIME
943
   R 7=   .042AT TIME   444   R8=   .100AT TIME   444   R9=   .085AT TIME
1195
   R10=   .360AT TIME   943   R*=   .373AT TIME   943   R
             SECTION NUMBER    5
   R 1=   .140AT TIME 1017   R2=   .018AT TIME 1195   R3=   .011AT TIME
440
   R 4=   .012AT TIME 1190   R5=   .149AT TIME 1017   R6=   .151AT TIME
1017
   R 7=   .020AT TIME   444   R8=   .011AT TIME   440   R9=   .012AT TIME
1190
   R10=   .149AT TIME 1017   R*=   .151AT TIME 1017   R
             SECTION NUMBER    6
   R 1=   .292AT TIME 1017   R2=   .037AT TIME 1195   R3=   .100AT TIME
444
   R 4=   .085AT TIME 1195   R5=   .351AT TIME 1015   R6=   .362AT TIME
440
   R 7=   .042AT TIME   444   R8=   .100AT TIME   444   R9=   .085AT TIME
1195
   R10=   .351AT TIME 1015   R*=   .362AT TIME   440   R
             SECTION NUMBER    7
   R 1=   .137AT TIME   731   R2=   .018AT TIME 1195   R3=   .011AT TIME
440
```

18

```
R 4=   .012AT TIME 1190   R5=   .145AT TIME   731   R6=   .147AT TIME
731
R 7=   .020AT TIME   444   R8=   .011AT TIME   440   R9=   .012AT TIME
1190
R10=   .145AT TIME   731   R*=   .147AT TIME   731   R
           SECTION NUMBER     8
R 1=   .286AT TIME   731   R2=   .037AT TIME 1195   R3=   .100AT TIME
444
R 4=   .085AT TIME 1195   R5=   .351AT TIME   730   R6=   .363AT TIME
730
R 7=   .042AT TIME   444   R8=   .100AT TIME   444   R9=   .085AT TIME
1195
R10=   .351AT TIME   730   R*=   .363AT TIME   730   R
           SECTION NUMBER     9
R 1=   .021AT TIME   567   R2=   .032AT TIME 1195   R3=   .202AT TIME
439
R 4=   .182AT TIME 1189   R5=   .232AT TIME   945   R6=   .272AT TIME
945
R 7=   .036AT TIME   444   R8=   .202AT TIME   439   R9=   .182AT TIME
1189
R10=   .232AT TIME   945   R*=   .272AT TIME   945   R
```

19

7.0   ACCIDENT CONSIDERATIONS AND THERMAL (SECONDARY) STRESS

7.1   ACCIDENT CONSIDERATIONS

The following accidents have been considered:

o   Dropped Fuel Assembly

o   Cask Drop

o   Rack Drop

o   Abnormal Location of a Fuel Assembly

o   Consequences of a Seismic Event

o   Loss of Cooling

7.1.1   Dropped Fuel Assembly

The consequences of dropping a new or spent fuel assembly as it is being moved over stored fuel is discussed below.

a.   Dropped Fuel Accident I

A fuel assembly and its' associated handling tool (weight approximately 2000 pounds) is dropped from 36" above a storage location and impacts the base of the module. Local failure of the baseplate is acceptable; however, the rack design should ensure that gross structural failure does not occur and the subcriticality of the adjacent fuel assemblies is not violated. Calculated results show that the baseplate is not pierced and the rack loading on the liner is well below that caused by seismic loads. Thus the structural integrity of the rack, and subcriticality of the stored fuel array is assured.

b.   Dropped Fuel Accident II

One fuel assembly dropping from 36" above the rack and

hitting the top of the rack. Permanent deformation of the rack is acceptable, but is required to be limited to the top region such that the rack cross-sectional geometry at the level of the top of the active fuel (and below) is not altered. Analysis demonstrates that the maximum local stress at the top of the rack is less than material yield point. Thus, the functionality of the rack is not affected.

The results of the radiological evaluation of a dropped fuel assembly show that the doses are well within the limits of 10CFR Part 100. This evaluation is presented in Section 8.

The results of the criticality evaluation shows that the dropped fuel accident II will not result in a significant increase in reactivity due to the separation distance. This evaluation is presented in Section 4.7.2.

7.1.2   Cask Drop

Current Technical Specifications for IP2 require that a spent fuel cask shall not be moved over any region of the spent fuel pool. This restriction effectively precludes a cask being handled over the spent fuel pool, and consequently, a cask drop analysis is not necessary.

7.1.3   Rack Drop

The IP2 Technical Specifications allow movement of a rack and its associated handling tool over the spent fuel pool but prohibit movement of a rack over fuel. All work in the spent fuel pool area will be controlled and performed in strict accordance with specific written procedures. Administrative controls will preclude the movement of a rack directly over any fuel. The maximum weight of a rack and its associated handling tool, as evaluated for purposes of applying Technical Specification

3.8.C.1, was 20 tons. The maximum weight of a rack and its associated handling tool to be carried over the spent fuel pool in connections with this proposed modification will be 19.4 tons. Therefore the movement of racks over the spent fuel pool (but not over fuel) for the proposed reracking is acceptable with the existing IP2 Technical Specifications.

Sections 5.1.1, 5.1.2 and 5.1.6 of NUREG-0612, entitled "Control of Heavy Loads at Nuclear Power Plants", provide guidance for heavy load handling operations. Section 5.1.2 provides four alternatives for assuring the safe handling of heavy loads during a fuel storage rack replacement. Alternative (1) of Section 5.1.2 provides guidelines that the control of heavy loads can be satisfied by establishing that the potential for a heavy load drop is extremely small, as demonstrated by satisfaction of the single-failure-proof crane criteria. The provisions of Alternative (1) will be met during implementation of the subject application.

NUREG-0554, entitled "Single-Failure-Proof Cranes for Nuclear Power Plants", provides guidance for the design, fabrication, installation and testing of new cranes that are of a high reliability design. For operating plants, NUREG-0612, Appendix C, entitled "Modification of Existing Cranes", provides guidelines on the implementation of NUREG-0554 at operating plants. An evaluation of storage rack movements which will be accomplished by the IP2 Fuel Storage Building crane to determine conformance with the NUREG-0612, Appendix C guidelines demonstrated that alternative (1) above is satisfied. The Fuel Storage Building crane has a rated capacity of 40 tons, which incorporates a design safety factor of five. The maximum weight of any existing or replacement storage rack and its associated

handling tool is 19.4 tons. Therefore, there is ample safety factor margin for movements of the storage racks by the Fuel Storage Building crane. This applies to non-redundant load-bearing components. Redundant special lifting devices, which have a rated capacity sufficient to maintain sufficient safety factors, will be utilized in the movements of the storage racks. As per NUREG-0612, Appendix B, this ensures that the probability of a load drop is extremely low.

The existing mechanical stops will be removed so that the Fuel Storage Building crane will have access to any location over the spent fuel pool. However, administrative controls, which incorporate predetermined safe load pathways, will ensure that at no time will any storage rack be moved directly over an irradiated fuel assembly. In addition, no heavy loads will be carried in the spent fuel pool area until all fuel in the pool has decayed for a minimum of 6 months. This provides sufficient time for decay of gaseous radionuclides in the fuel (gap activity) such that accidental release of all these gases would result in potential offsite doses less than 10 percent of 10CFR 100 limits.

7.1.4   Abnormal Location of a Fuel Assembly

The abnormal location of a fresh unirradiated fuel assembly of 5.0% enrichment could, in the absence of soluble poison, result in exceeding the design reactivity limitation (k_{eff} of 0.95). This could occur if a fresh fuel assembly of the highest permissible enrichment were to be either positioned outside and adjacent to a storage rack module or inadvertently loaded into a Region II storage cell, with the latter condition producing the larger positive reactivity increment. Although criticality would not be attained even in the absence of soluble

poison (maximum k_{eff} of 0.978, including uncertainties), soluble boron actually present in the spent fuel pool water, for which credit is permitted under these conditions, would assure that the reactivity is maintained substantially less than the design limitation. Calculations show that a soluble poison concentration of 350 ppm boron is sufficient to maintain a k_{eff} less than 0.946 (including uncertainties) under the maximum postulated accident condition. This evaluation is discussed in Section 4.7.

7.1.5   Consequences of a Seismic Event

The free-standing rack modules were analyzed for the seismic events postulated in the IP2 FSAR. The maximum kinematic displacement of a rack module was found to be less than 50% of the inter-module spacings. The modules were also demonstrated to be kinematically stable for amplified seismic loadings as required by the OT position paper. The maximum fuel assembly to storage cell impact load at any impact point is less than 400 lbs. which is a small fraction of the limit load for the storage cell wall. The maximum rack welding stress is less than 50% of the ASME Code (Section III, Subsection NF) allowables at all locations in the rack module. Detailed data may be found in Section 6 of this report.

The displacement of the rack modules resulting from a postulated seismic event has been included in the criticality analyses for the new racks. With the potential alteration of the spacing between rack modules considered, k_{eff} remains below 0.95. This evaluation is discussed in Section 4.7.3.

7.1.6   Loss of Cooling

In the event of a complete failure of the IP2 spent fuel heat removal system the maximum heat-up rate for the full core discharge case assuming the minimum required discharge time (see Figure 5-1) is 17.8^{0}F/hr. Assuming a maximum bulk pool temperature of 180^{0}F results in a minimum time of approximately 1.8 hours to bulk pool boiling. The required makeup capacity, to prevent decreasing level, is 62 gpm (see section 5.1.4). Three principal methods are available for providing makeup water in sufficient quantities to prevent a decrease in spent fuel pool level. These are:

o   Demineralized water (unborated) from the Primary Water Storage Tank.

o   Borated water from the Refueling Water Storage Tank.

o   Non-demineralized water from the fire protection system.

Therefore, even in the unlikely combined occurence of 95^{0}F river water temperature and a full core discharge, sufficient time and water makeup sources are available to prevent decrease in the spent fuel pool level.

The temperature and level indicators for the spent fuel pool would warn the operator of a loss of cooling. Thus, there is sufficient time to take any necessary action to provide adequate cooling and makeup while the cooling capability of the spent fuel pool cooling system is being restored.

7.2   Thermal (Secondary Stress)
7.2.1   Local Buckling of Fuel Cell Walls

This sub-section and the next one presents details on the secondary stresses produced by temperature effects.

The allowable local buckling stresses in the fuel cell walls are obtained by using classical plate buckling analysis. The following formula for the critical stress has been used.

$$\sigma_{cr} = \frac{\beta \pi^2 E t^2}{12 b^2 (1 - \mu^2)}$$

where $E = 28 \times 10^6$ psi, μ is Poisson's ratio, $t = .075"$, $b = 8.8"$. The factor β is suggested in [1] to be 4.0 for a long panel loaded as shown in Figure 7.1.

For the given data
$$\sigma_{cr} < 7352 \text{ psi}$$

It should be noted that this calculation is based on the applied stress being uniform along the entire length of the cell wall. In the actual fuel rack, the compressive stress comes from consideration of overall bending of the rack structures during a seismic event and as such is negligible at the rack top and maximum at the rack bottom. It is conservative to apply the above equation to the rack cell wall if we compare σ_{cr} with the maximum compressive stress anywhere in the cell wall. As shown in Section 6, this local buckling stress limit is not violated anywhere in the body of the rack modules.

7.2.2   Analysis of Welded Joints in Rack

In-rack welded joints are examined under the loading conditions arising from thermal effects due to an isolated hot cell, in this sub-section. Under both sets of load conditions, the weld stresses are found to be below the allowable value of 24000 psi in shear that is given in Table NF3291.1-1 of ASME Section III, Division 1, Subsection NF, 1983.

A thermal gradient between cells will develop when an isolated storage location contains a fuel assembly emitting maximum postulated heat, while the surrounding locations are empty. We can obtain a conservative estimate of weld stresses along the length of an isolated hot cell by considering a beam strip uniformly heated by 60^0F, and restrained from growth along one long edge. The configuration is shown in Figure 7.1.

Using a shear beam theory, and subjecting the strip to a uniform temperature rise $\Delta T = 60^0F$, we can calculate an estimate of the maximum value of the average shear stress in the strip. The strip is subjected to the following boundary conditions (Figure 7.2).

   a.   Displacement U_x $(x,y) = 0$ at $x = 0$, at $y = w/2$, all x.

   b.   Average force M_x, acting on the cross section Ht = 0 at
         $x = L$, all y.

The final result for wall shear stress, maximum at $x = 1$, is found to be given as

$$\tau_{max} = \frac{E \ \alpha \ \Delta \ T}{.931}$$

where $E = 28 \times 10^6$ psi, $\alpha = 9.5 \times 10^{-6}$ in/in ^0F and $\Delta T = 60^0F$.

Therefore, we obtain an estimate of maximum weld shear stress in an isolated hot cell, due to thermal gradient, as

$$\tau_{max} = 17143 \text{ psi}$$

Since this is a secondary thermal stress, we use the allowable shear stress criteria for faulted conditions as a guide ($\tau < .42S_u$).
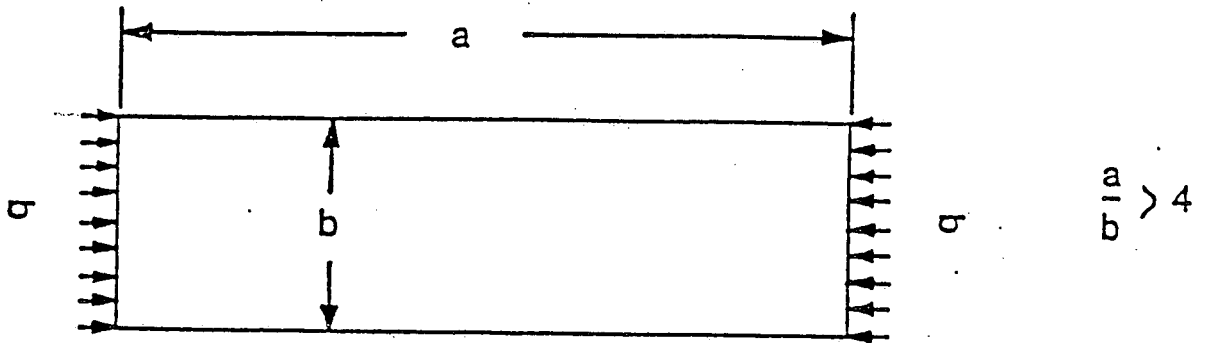
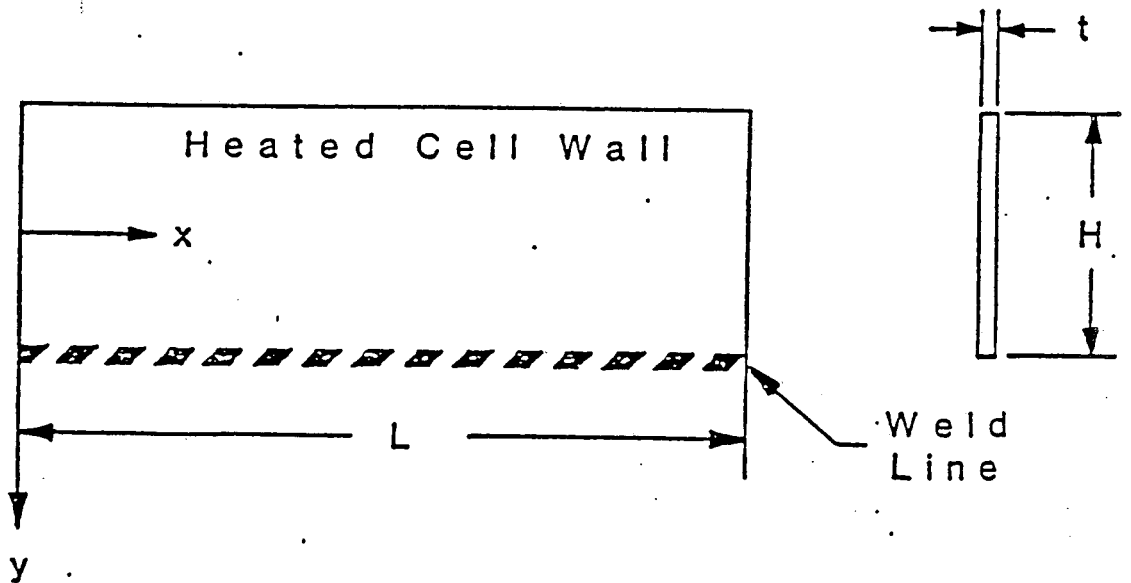# FIG. 7.1
LOADING ON RACK WALL

FIG. 7.2
WELDED JOINT IN RACK

8.0   RADIOLOGICAL EVALUATION

8.1   FUEL HANDLING ACCIDENT

8.1.1   Assumptions and Source Term Calculations

An evaluation of the consequences of a fuel handling accident has been made for fuel of 5 wt% initial enrichment burned to 60,000 MWD/MTU, with the reactor assumed to have been operating at 3216 MW thermal power (consistent with FSAR radiological analysis) immediately prior to the postulated accident. As in previous evaluations, a fuel handling accident is assumed to result in the release of all gaseous fission products contained in the fuel-rod gaps of a single assembly at the time of the accident. Guidelines and assumptions specified in Regulatory Guide 1.25[*] were used as the basis for the evaluation.

Most of the gaseous fission products having a significant impact on the off-site doses are the short lived nuclides of Iodine and Xenon. The exception is Kr-85 with a 10.73 year half-life. Since the off-site radiological consequences are dominated by the short-lived nuclides, the calculated doses will not differ appreciably from those of previous evaluations. The

---

[*]   "Assumptions Used For Evaluating the Potential Radiological Consequences of a Fuel Handling Accident in the Fuel Handling and Storage Facility for Boiling and Pressurized Water Reactors".

present evaluation used ORIGEN-2 (an improved version of the ORNL
Isotope Generation code) as a means of calculating the reactor
core saturation inventories of radionuclides, and included yields
from fission of the Plutonium produced at the higher burnup.

Calculations were made for five different time intervals
following shutdown, to illustrate the effect of post-shutdown
cooling time (prior to fuel movement) on the gap inventory. The
Xenon gap inventories shown in Table 1 include the contribution
from the decay of the Iodine precursors that existed in the gap at
the time of reactor shutdown.

The following equation, from Reg Guide 1.25, was used to
calculate the thyroid dose (D) from the inhalation of radioiodine,

$$D = \sum_i \frac{F_g \; I_i \; F \; P \; B \; R_i \; (x/Q)}{DF_p \; DF_f} \quad \text{Rads}$$

summed over all iodine radionuclides.

F_g = fraction of fuel rod
Iodine inventory in gap
space (0.1)

I_i = core Iodine radio-
nuclide inventory at
time of the accident
(curies)

F = Fraction of core
damaged so as to
release Iodine in the
rod gap (1/193)

B = Breathing rate =
3.47×10^{-4} cubic
meters per second

R_i = Dose conversion
factor (rads/curie)
from Reg. Guide 1.25

(x/Q) = atmospheric
diffusion factor
(7.5×10^{-4}
sec/m^3)

P = Core peaking factor
(1.65)

DF_p = effective Iodine decontamination factor for pool water (= 100)

DF_f = effective Iodine decontamination factor for filters (= 6.67).

The function used to calculate the external whole body dose from beta (D_β) or gamma (D_γ) radiation in the cloud uses many of the terms defined above and is given by:

$$D_\beta = \sum_i 0.23 \, (x/Q) \, F \, P \, F_g \, G_i \, E_{\beta_i} \quad \text{and}$$

$$D_\gamma = \sum_i 0.25 \, (x/Q) \, F \, P \, F_g \, G_i \, E_{\gamma_i}$$

G_i is the core inventory of the gaseous radionuclides of Xe and Kr and the functions above are summed over all the noble gases. These functions assume the noble gas decontamination factors in water and the filters are 1.0. As specified in Reg. Guide 1.25, the fraction, F_g, of the noble gases released to the fuel rod gaps is 0.1 for Xe and 0.3 for Kr-85. The gap inventories of radioiodines make a negligible contribution to the whole body doses, D_β or D_γ, because of the large decontamination factors appropriate to the iodines.

8.1.2   Results

A summary of the assumptions used to evaluate the fuel handling accident is given in Table 8-2. The minimum time after shutdown when fuel assemblies would be moved was conservatively

8-3

assumed to be 90 hours (actual time to discharge is a little more than 7 days). At 90 hours, the consequences at the site boundary of a fuel handling accident releasing all of the gaseous fission product radioactivity in the gaps of all rods in one failed assembly over the entire course of the accident are:

$$\text{Inhalation thyroid dose} = 31.7 \text{ Rads}$$
$$\text{Whole body beta dose, } D_\beta = 2.22 \text{ Rads}$$
$$\text{Whole body gamma dose, } D_\gamma = 1.88 \text{ Rads}$$

As expected, these doses are not significantly changed from those from the earlier evaluation, the difference being due to differences in source term calculations (TID-14844 vs. ORIGEN-2) and in use of a more conservative (x/Q) value. These doses are, however, well within the limits of 10 CFR Part 100 in conformance with the acceptance criteria of SRP 15.7.4. (Rev.1, July 1981).

Calculated consequences for the fuel handling accident assumed to occur at the various time intervals following shutdown are listed below:

	TIME AFTER SHUTDOWN				
	90 hrs	130 hrs	7 days	10 days	90 days
D = Thyroid Dose	31.7	26.8	23.2	17.8	0.018
D_β = Whole body β	2.22	1.67	1.39	0.99	0.156
D_γ = Whole body γ	1.88	1.36	1.09	0.73	0.0014

8.2   SOLID RADWASTE

Currently, resins are generated by the spent fuel pool purification system. Current frequency of resin change out is approximately once every 1.5 years. No significant increase in volume of solid radioactive wastes is expected due to the new racks based on operating plant experience with high density fuel storage. It is estimated that a minimal amount of additional resins will be generated by the spent fuel pool cleanup system during reracking.

8.3   GASEOUS RELEASES

Gaseous releases from the Fuel Storage Building (FSB) are combined with other plant ventilation systems prior to sampling. The plant gaseous releases are reported semi-annually per NRC Regulatory Guide 1.21. The gaseous releases from the FSB comprise less than one percent of the total radioactivity released through the plant vent. No significant increases are expected as a result of the reracking.

8.4   PERSONNEL EXPOSURE

a. The range of values for recent isotopic analyses of spent fuel pool water is shown on Table 8.3.

b. Operating experience shows dose rates of less than 2.5 mrem/hour either at the edge or above the center of the spent fuel pool regardless of the quantity of fuel stored. This is not expected to change with the proposed reracking because radiation levels above the pool are due primarily to

radioactivity in the water, which experience shows to return to a level of equilibrium. Stored spent fuel is so well shielded by the water above the fuel that dose rates at the top of the pool from this source are negligible.

c. There have been negligible concentrations of airborne radioactivity from the spent fuel pool. Operating plant experience with high density fuel storage has shown no noticeable increases in airborne radioactivity above the spent fuel pool or at the site boundary. Recent air samples taken above the spent fuel pool have shown less than detectable levels of airborne radioactivity. No significant increases are expected from the more dense storage of spent fuel.

d. As stated in Section 8.2, reracking and utilization of the new racks will result in no significant increase in the radwaste generated by the spent fuel pool cleanup system. This is because operating experience has shown that with high density storage racks, there is no significant increase in the radioactivity levels in the spent fuel pool water, and no significant increase in the annual person-rem due to the increase fuel storage, including the changing of spent fuel pool cleaning system resins and filters.

e. A small amount of primary coolant corrosion product (crud) deposited on the fuel assembly surface may spall off during emplacement in the spent fuel pool from the reactor. Once fuel is placed into a pool storage position, additional crud spalling is minimal.

The highest possible water level is maintained in the spent fuel pool to keep exposure as low as reasonably achievable. Should crud buildup ever be detected on the spent fuel pool walls around the pool edge, it could easily be washed down.

f.   There is no access underneath the spent fuel pool.
     Therefore during normal operation, the radiation
     dose rate around the outside of the pool should
     not effectively increase should freshly discharged
     fuel be located in the cells adjacent to the pool
     liner. The depth of the water above the fuel is
     sufficient so there will be no measurable increase
     in dose rates above the pool due to radiation
     emitted directly from the fuel.

Operating experience has shown a negligible increase in person-rem due to the increased fuel storage with high density racks. Therefore, a negligible increase in the annual person-rem is expected at Indian Point 2 as a result of the increase storage capacity of the spent fuel pool with the higher density storage racks.

The existing Indian Point 2 health physics program did not have to be modified as a result of the previous increase in storage of spent fuel. It is not anticipated that the health physics program will need to be modified for this increase in storage capability.

8.5   RADIATION PROTECTION DURING RERACK ACTIVITIES

8.5.1   General Description of Protective Measures

Gamma radiation levels in the pool area are constantly monitored by the station Area Radiation Monitoring System, which has a high level alarm feature. Additionally, periodic radiation and contamination surveys are conducted in work areas as necessary. Where there is a potential for significant airborne radionuclide concentrations, continuous air samplers are used in

addition to periodic grab sampling. Personnel working in radiologically controlled areas will wear protective clothing, and when required by work area conditions, respiratory protective equipment, as required by the applicable Radiation Work Permit (RWP). Personnel monitoring equipment is assigned to and worn by all personnel in the work area. At a minimum, this equipment consists of a thermoluminescent dosimeter (TLD) and self-reading pocket dosimeter. Additional personnel monitoring equipment, such as extremity badges, are utilized as required.

Contamination control measures are used to protect persons from internal exposures to radioactive material and to prevent the spread of contamination. Work, personnel traffic, and the movement of material and equipment in and out of the area are controlled so as to minimize contamination problems. Material and equipment will be monitored and appropriately decontaminated and/or wrapped prior to removal from the spent fuel pool area. The plant radiation protection staff will closely monitor and control all aspects of the work so that personnel exposures, both internal and external, are maintained as low as reasonably achievable (ALARA).

Water levels in the spent fuel pool will be maintained to provide adequate shielding from the direct radiation of the spent fuel. Prior to rack replacement, the spent fuel pool cleanup system will be operated to reduce the activity of the pool water to as low a level as can be practically achieved.

8.5.2   Anticipated Exposure During Reracking

Total occupational exposure for the reracking operation is estimated to be between 5 and 10 person-rem, as indicated in Table 8.4. At the present time, the use of divers is not anticipated. Prior to beginning the reracking, detailed operating procedures will be prepared, with full consideration of ALARA principles. Similar operations have been performed in a number of facilities in the past and there is every reason to believe that reracking can be safely and efficiently accomplished at Indian Point 2, with minimum radiation exposure to personnel.

8.6   RACK DISPOSAL

The spent fuel storage rack modules that will be removed from the spent fuel pool weigh up to 36,000 pounds each. The total weight of these racks is approximately 180 tons. They will be cleaned (e.g. washing and wipe down) of most loose contamination, packaged and shipped to a licensed radioactive waste processing facility.

Shipping containers will meet the requirements of DOT regulations pertaining to radioactive waste shipments, including limitations with respect to the waste surface dose and radioclide activity distribution. Shipping containers will be certified to meet all requirements for a strong tight package. The maximum weight of a loaded shipping container will be in accordance with the American Association of State Highway and Transportation Officials (AASHTO). Trucks and drivers used for rack and waste transportation will have all permits and qualifi-

8-9

cations required by the Federal DOT and the DOT for each State through which the truck will pass.

At the waste processing facility, the racks will be decontaminated to the maximum extent possible. Remaining portions of the racks and contaminated waste generated from decontamination will be buried at a licensed radioactive waste burial site. In preparing non-decontaminatable waste for shipment and subsequent burial, volume reduction methodologies will be employed such as compaction, combining metallic materials with "soft waste" to minimize void space, and super compaction where feasible.

TABLE 8.1   RADIONUCLIDE INVENTORIES AND CONSTANTS

NUCLIDE	SHUTDOWN CORE INVENTORY CURIES	DECAY CONST. λ, 1/HRS	GAP INVENTORY, CURIES					DOSE CONVERSION RI	E_β (MEV)	E_γ (MEV)
			90 hrs	130 hrs	7 days	10 days	90 days			
I-131	8.555E+7	3.593E-3	6.192E+6	5.363E+6	4.679E+6	3.613E+6	3.653E+3	1.48E+6	0.186	0.389
I-132	1.223E+8	3.028E-1	0	0	0	0	0	5.35E+4	–	–
I-133	1.683E+8	3.334E-2	8.374E+5	2.208E+5	6.217E+4	5.637E+3	0	4.0 E+5	0.419	0.597
I-134	1.842E+8	7.920E-1	0	0	0	0	0	2.5 E+4	–	–
I-135	1.584E+8	1.048E-1	1.269E+3	1.918E+1	0	0	0	1.24E+5	0.394	1.456
Kr-85M	1.810E+6	1.548E-1	0	0	0	0	0		–	–
Kr-85	1.422E+8	7.374E-6	4.263E+5	4.263E+5	4.260E+5	4.257E+5	4.200E+5		0.251	0.002
Kr-87	3.377E+7	5.436E-1	0	0	0	0	0		–	–
Kr-88	4.724E+7	2.441E-1	0	0	0	0	0		–	–
Xe-133M	5.352E+6	1.289E-2	2.462E+5	1.505E+5	9.258E+4	3.618E+4	0		–	0.233
Xe-133	1.688E+8	5.508E-3	1.229E+7	9.986E+6	8.148E+6	5.507E+6	1.418E+2		0.102	0.081
Xe-135	3.307E+7	7.632E-2	4.456E+5	2.218E+4	1.242E+3	0	0		0.309	0.262
Xe-135M	3.426E+7	2.736	2.026E+2	0	0	0	0		–	0.527

NOTES: (1) Xenon gap inventories include contribution from iodine precursors accumulated in the gap
(2) Gap inventory of 0 means less than one Curie

Table 8.2   DATA AND ASSUMPTIONS FOR THE EVALUATION OF THE FUEL HANDLING ACCIDENT

1. **Source Term Assumptions** | **VALUES**

   Core power level, MWT | 3216

   Fuel burnup, MWD/MTU | 60,000

   Analytical method | ORIGEN-2

2. **Release Assumptions**

   Number of failed assemblies | 1 of 193

   Fraction of core inventory released to gap

% of the Iodines	10
% of the Xenons	10
% of Kr-85	30

   Assumed power peaking factor | 1.65

   Inventory in gap available for release | Table 8.1

   Pool decontamination factors

   | For Iodines | 100 |
   | For Noble gases | 1 |

   Filter decontamination factors

   | For Iodines | 6.67 |
   | For noble gases | 1 |

   Atmospheric Dispersion, (x/Q) | 7.5×10^{-4} sec/m^3

   Breathing rate | 3.47×10^{-4} m^3/sec

Table 8.3   TYPICAL SPENT FUEL POOL RADIONUCLIDE CONCENTRATIONS[*]

NUCLIDE	CONCENTRATION (μc/cc)
CO-57	< 2.74 x 10^{-6}
CO-58	1.23 x 10^{-4}
CO-60	1.12 x 10^{-3}
CS-134	6.82 x 10^{-5}
CS-137	2.78 x 10^{-4}

---

*   These concentrations are indicative of concentrations expected to be seen at the time the rerack installation work is being done.

Table 8.4   PRELIMINARY ESTIMATE OF PERSON-REM
EXPOSURES DURING RERACKING

Step	Number of Personnel	Hours	Estimated Exposure [1]
Remove empty racks	5	40	0.5 to 1.0
Wash and Decon racks	3	10	0.08 to 0.2
Clean and Vacuum Pool	3	25	0.3 to 0.6
Partial installation of new rack modules	5	20	0.25 to 0.5
Move fuel to new racks	2	150	0.8 to 1.5
Remove remaining racks	5	120	1.5 to 3.0
Wash and Decon racks	3	30	0.2 to 0.4
Install remaining new rack modules	5	35	0.4 to 0.8
Prepare old racks for shipment	4	80	1.0 to 2.0 [2]
Total Exposure, person-rem			5 to 10

[1]   Assumes minimum dose rate of 2 1/2 mR/hr (expected) to a maximum
of 5 mR/hr, except for pool vacuuming operations which assumes 4
to 8 mR/hr.

[2]   Maximum expected exposure, although details of preparation and
packaging of old racks for shipment have not yet been determined.

9.0   IN-SERVICE SURVEILLANCE PROGRAM

9.1.   Background and Summary

Boraflex, the neutron absorbing material incorporated in the rack design, consists of finely divided particles of boron carbide (B_4C) uniformly distributed in a silicone type polymeric base. Based upon results of test programs, it is concluded that Boraflex is a satisfactory material for reactivity control in spent fuel storage racks. Nevertheless, it is prudent to establish a surveillance program to monitor the integrity and performance of Boraflex on a continuing basis. The EPRI "Guidelines for a Standard Boraflex Coupon Surveillance Program"[1] were used in development of the Indian Point 2 Boraflex surveillance program.

9.2   Fabrication Surveillance

The fabrication Quality Assurance program and the use of qualified Boraflex neutron absorbing material, satisfies an initial verification test to assure that the proper quantity and placement of material is achieved during fabrication of the racks.

9.3   In-Service Surveillance

A surveillance program to verify the Boraflex material long term stability and mechanical integrity is provided in compliance with the "OT Position for Review and Acceptance of Spent Fuel Storage and Handling Applications".[2]

The Boraflex in-service surveillance program presented in this section uses representative coupon samples to monitor performance without disrupting the integrity of the storage system.

9.3.1   Coupon Description

The coupons used in the surveillance program will be taken from the Boraflex production lot. The program will use a total of 40 test coupons each mounted in a stainless steel jacket, simulating as nearly as possible, the actual in-service geometry, physical mounting, materials, and flow conditions of the Boraflex in the storage racks. Two "trees" of 20 coupons each (10 representing each of the two regions of the rack) will be mounted in designated storage cells. One of the two trees will be used for accelerated testing and the other tree for normal long-term testing. The Boraflex coupons will be approximately 7 inches wide and 15 inches long.

Each coupon will be carefully pre-characterized prior to insertion in the pool to provide reference initial values for comparison with measurements made after irradiation. Archive samples of the Boraflex will also be retained for later comparison with the irradiated coupons. A unique identification number will be engraved on one side of the coupon holder. The coupon holders will be fastened with screws to facilitate easy opening without contributing to mechanical damage to the Boraflex specimen contained within.

The two coupon trees will be installed in two separate areas in Region II of the racks. The one tree designated for accelerated testing will be located such that the freshly discharged fuel will be in the surrounding cells. The other tree, designated for normal long-term testing, will be located such that the surrounding cells will be filled with freshly discharged fuel once and remain there.

9.3.2 Testing

Initial surveillance will be performed after a pre-determined interval of exposure in the pool environment which depends on the placement of irradiated fuel assemblies along-side the test coupons. The initial surveillance will be implemented after an exposure interval approximately corresponding to two fuel cycles. Based on results of the initial surveillance measurements, determination will then be made for future scheduling.

The pre-characterization and in-service characterization of the coupons will involve the same testing. As a minimum, this testing will include:

o   Mechanical and Geometrical Properties
     (Shore A hardness and coupon dimensions),

o   Neutron Absorption, and

o   Visual examination and photography.

Acceptance criteria for the irradiated coupons will be

- o   Hardness remaining above a Shore A of 90,

- o   Shrinkage in length and width less than or equal to 2 1/2 percent, and

- o   No measurable loss in Boron-10 content within the accuracy of the neutron absorption measurements.

In the event these criterion are exceeded, an engineering evaluation will be initiated to determine the significance of the deviation and to identify corrective action, if any, that may be necessary or desirable.

9.4   References

1.   K. Lindquist and D. Kline, "An Assessment of Boraflex
      Performance in Spent-Nuclear-Fuel Storage Racks, EPRI
      Report NP-6159, December 1988.

2.   Nuclear Regulatory Commission, Letter to all Power
      Reactor Licensees, from B.K. Grimes, April 14, 1978,
      transmitting the "OT Position for Review and Accep-
      tance of Spent Fuel Storage and Handling Applica-
      tions," as amended by the NRC letter dated January
      18, 1979.

10.0   COST/BENEFIT ASSESSMENT

The cost/benefit of the reracking modification is demonstrated in the following sections.

10.1   HISTORY

By letter dated March 4, 1975 and supplements dated May 9, 1975, July 23, 1975, August 19, 1975, September 11, 1975, October 1, 1975 and October 10, 1975, Consolidated Edison requested, from the NRC, authorization to increase the storage capacity of the Indian Point 2 spent fuel pool from 264 to 482 storage locations. On December 16, 1975 the NRC issued Amendment No. 14 to Facility Operating License No. DPR-26 for Indian Point 2, authorizing such modifications.

A second increase in spent fuel storage capacity was requested by Consolidated Edison from the NRC by letter dated September 7, 1979 and supplements May 6, 1980, February 10, 1981 and July 28, 1981. This request was for an increase in storage capacity of the Indian Point 2 spent fuel pool from 482 to 980 storage locations. On January 11, 1982 the NRC issued Amendment No. 75 to Facility Operating License No. DPR-26 for Indian Point 2, authorizing such modifications.

10.2   NEED FOR INCREASED STORAGE CAPACITY

a. Consolidated Edison currently has no contractual arrangements with any fuel reprocessing facility. There are no operating or planned fuel reprocessing facilities available in the U.S.

Consolidated Edison has executed contracts with the U.S. Department of Energy (DOE) pursuant to the Nuclear Waste Policy Act of 1982. However, the disposal facilities are not expected to be available for spent fuel any earlier than 1998 if a monitored retrieval storage (MRS) facility is constructed, or 2003 for construction of a permanent repository (Reference 1).

b. Table 10-1 includes a projected refueling schedule for Indian Point 2 and the expected number of fuel assemblies that will be transferred into the spent fuel pool at each refueling until the ability to maintain a full core discharge capability is lost in 1995. At present the licensed capacity is 980 storage cells. All calculations in the table for loss of full core discharge (FCD) capability are based on the number of licensed total cells in the pool. The table is then continued assuming the installation of 1374 replacement cells which lengthens the time of loss of FCD to the year 2007.

c. The Indian Point 2 spent fuel pool will contain 604 fuel assemblies at the time of reracking. It is best to minimize the inventory of spent fuel in the pool at the time of reracking in order to minimize fuel handling and radiation exposure.

d. Adoption of this proposed spent fuel storage expansion would not necessarily extend the time period that spent fuel assemblies would be stored on site. Spent fuel will be removed from the site for disposal under the provisions of the Nuclear Waste Policy Act of 1982, but a government facility is not expected to be available to accept full reload quantities of spent fuel from Indian Point 2 before 2003 [2].

10.3   ESTIMATED COSTS

Total construction cost associated with the proposed modification is estimated to be approximately 4.4 million dollars. This figure includes the cost of designing and fabricating the spent fuel racks; engineering costs; installation and support costs at the site; and removal and offsite disposal of the existing racks.

10.4   CONSIDERATION OF ALTERNATIVES

a.   There are no operational commercial reprocessing facilities available for Consolidated Edison's needs in the United States, nor are there expected to be any in the foreseeable future.

b.   While plans are being formulated by DOE for construction of spent fuel disposal facilities per the Nuclear Waste Policy Act of 1982, a facility is not expected to be available to accept spent fuel any earlier than the 1998 to 2003 time frame.[1]

c.   Consolidated Edison does not own or control any facility where it could transfer spent fuel from Indian Point 2. The Indian Point 1 nuclear plant, owned by Consolidated Edison, does not contain facilities capable of storing Indian Point 2 spent fuel, nor is such storage permitted under the Indian Point 1 license.

d.   There are no existing available independent spent fuel storage facilities. Transfer of Indian Point 2 spent fuel to other utility facilities would only compound storage problems there and is not a viable option.

e. Licensed at-reactor spent fuel storage alternatives involving dry cask/vault storage were evaluated and excluded from consideration at this time due to technical and overall economic reasons. The existing crane capacity plus the limited land space available at the Indian Point 2 site were key considerations in favor of expanding at-reactor storage through reracking over the alternatives of dry cask/vault storage.

f. If Indian Point 2 were forced to shutdown for lack of spent fuel storage space, there would be a significant loss of economic benefit to our customers. The present estimated cost of replacement power (averaged for the period 1988-91) is approximately $500,000 per nuclear full-power day.

10.5   RESOURCES COMMITTED

Reracking of the spent fuel pools will not result in any irreversible and irretrievable commitments of water, land and air resources. The land area now used for the spent fuel pool will be used more efficiently by safely increasing the density of fuel storage.

The materials used for new rack fabrication are discussed in Section 3.0. These materials are not expected to significantly foreclose alternatives available with respect to any other licensing actions designed to improve the capacity for storage of spent fuel.

10.6 THERMAL IMPACT ON THE ENVIRONMENT

Section 5.0 considered the following: the additional heat load and the anticipated maximum temperature of water in the spent fuel pool that would result from the proposed expansion, the resulting increase in evaporation rates, the additional heat load on component and/or plant cooling water systems, and whether there will be any significant increase in the amount of heat released to the environment. As discussed in Section 5.0, the proposed increase in storage capacity will result in an insignificant impact on the environment.

10.7 REFERENCES

1. U.S. Department of Energy, "OCRWM Mission Plan Amendment," June 1987.

2. U.S. Department of Energy, "Annual Capacity Report," June 1987.

Table 10.1

FUEL ASSEMBLY DISCHARGE DATA

Batch	No. of Assemblies Discharged	Equivalent Operating Time (yrs)	Discharge[1] Date	Shutdown Time (yrs)	No. of Assemblies in Pool After Outage
1	72	1.50	3/30/76	37.78	72
2	60	2.50	2/13/78	35.90	132
3	61	3.50	6/16/79	34.57	
	2	2.00			195
4	49	3.00	10/17/80	33.23	
	4	2.00			
	1	1.00			
5	16	4.20	9/18/82	31.31	
	43	3.20			
	16	2.20			324
6	10	4.40	6/2/84	29.60	
	10	3.40			
	8	3.20			
	7	2.40			
	7	2.20			396
7	61	3.60	1/13/86	27.98	
	3	2.30			
	4	2.00			464
8	57	3.50	9/1/87	26.35	
	11	2.30			
9	57	3.31	3/18/89	24.81	
	15	2.22			604

(1) All dates from 1991 on are estimated dates.

(2) Loss of full core discharge (FCD) capability at 787 cells with current racks; rerack required to regain FCD capability.

(3) Loss of FCD capability with rerack (1374 available storage locations).

Table 10.1
(continued)

FUEL ASSEMBLY DISCHARGE DATA

Batch	No. of Assemblies Discharged	Equivalent Operating Time (yrs)	Discharge[1] Date	Shutdown Time (yrs)	No. of Assemblies in Pool After Outage	
10	72	4.00	1/1/91	23.01	676	
11	72	4.75	1/1/93	21.01	748	
12	72	4.75	1/1/95	19.01	820	(2)
13	72	4.75	1/1/97	17.01	892	
14	72	4.75	1/1/99	15.01	964	
15	72	4.75	1/1/01	13.00	1036	
16	72	4.75	1/1/03	11.00	1108	
17	72	4.75	1/1/05	9.00	1180	
18	72	4.75	1/1/07	7.00	1252	(3)
19	72	4.75	1/1/09	5.00	1324	
20	72	4.75	1/1/11	3.00	1396	
21	72	4.75	1/1/13	1.00	1468	
22A	72	1.00	12/31/13	174 hr	1540	
22B	72	2.60	12/31/13	174 hr.	1612	
22C	49	4.20	12/31/13	174 hr.	1661	

(1) All dates from 1991 on are estimated dates.

(2) Loss of full core discharge (FCD) capability at 787 cells with current racks; rerack required to regain FCD capability.

(3) Loss of FCD capability with rerack (1374 available storage locations).